AD-A094 480 TEXAS A AND M UNIV COLLEGE STATION DEPT OF METEOROLOGY F/G 4/1
ATMOSPHERIC STRUCTURE DETERMINED FROM SATELLITE DATA.(U)
JAN 81 K S KNIGHT, J R SCOGGINS DAAG29-76-G-0078
UNCLASSIFIED NASA-RP-1071 NL

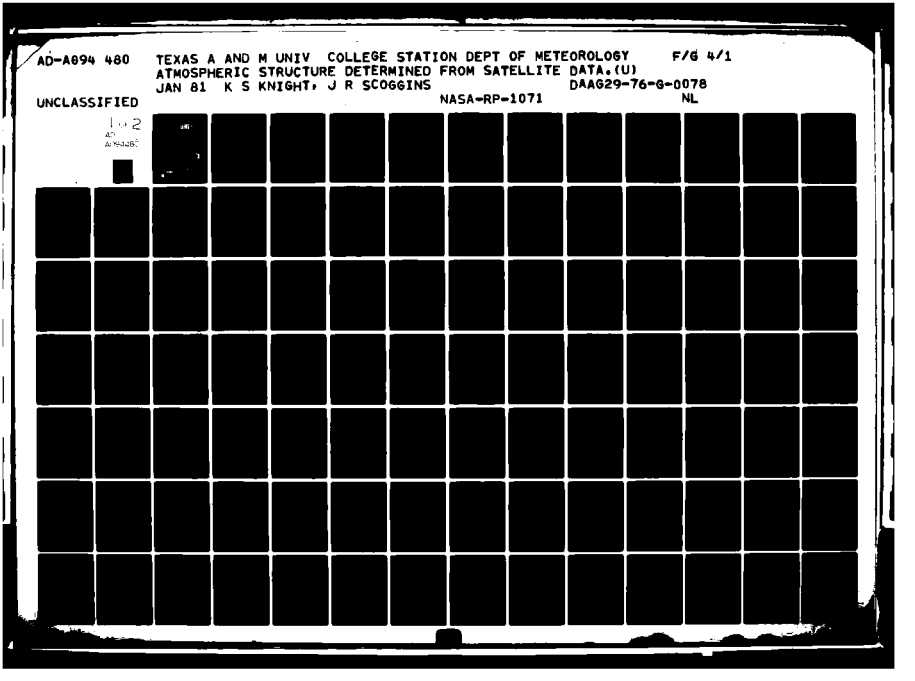

NASA Reference Publication

1082

Atmospheric Structure Determined From Satellite Data

Keith Shelburne Knight and James R. Scoggins

JANUARY 1981

(19) RP-1071

(9)

(18) NASA Reference Publication 1071

(15) DAAG29-76-G-0078

(6) Atmospheric Structure Determined From Satellite Data.

(10) Keith Shelburne Knight and James R. Scoggins
Texas A&M University
College Station, Texas

(11) Jan 81

(12) 108

NASA
National Aeronautics
and Space Administration

**Scientific and Technical
Information Branch**

1981

400161

ACKNOWLEDGMENTS

The authors thank Dr. Aylmer H. Thompson, Dr. Glen N. Williams, Dr. Kenneth C. Brundidge, and Dr. Vance E. Moyer for their comments and suggestions during the preparation of this report, Miss Karen Cobbs for the typing of the manuscript, and Miss Betty Seymour and Miss Doreen Westwood for their help with the figures.

This research was supported by the U. S. Army Research Office, under Grant No. DAAG 29-76-G-0078 to the Department of Meteorology, Texas A&M University.

This report is published with the permission of the U. S. Army Research Office for use in connection with studies utilizing space technology for weather-related programs in progress in the Atmospheric Sciences Division, Space Sciences Laboratory, NASA, Marshall Space Flight Center.

TABLE OF CONTENTS

TABLE OF CONTENTS (Continued)

LIST OF TABLES

LIST OF FIGURES

LIST OF FIGURES (Cont'd)

LIST OF FIGURES (Cont'd)

LIST OF FIGURES (Cont'd)

LIST OF FIGURES (Cont'd)

ATMOSPHERIC STRUCTURE DETERMINED FROM SATELLITE DATA*

Keith Shelburne Knight and James R. Scoggins
Department of Meteorology, Texas A&M University

1. INTRODUCTION

The availability of atmospheric soundings using measurements made from a satellite platform represents a recent development in making meteorological observations. This new form of data could potentially allow substantial improvement in our knowledge of the structure and state of the atmosphere because: 1) satellite soundings can be made on a global scale with more uniformity and better resolution than with balloon launches from the present rawinsonde network; 2) all measurements would be made by the same instrument so that any errors resulting from the variability between rawinsonde instruments would be eliminated; and 3) the satellite measures the entire vertical extent of the sounding at one time so that errors resulting from downstream drift and subsequent deviation of the balloon from a vertical path would be eliminated.

Since the satellite measurements do not represent point values as do rawinsonde measurements, studies must be done to determine the applications and suitability of satellite sounding data in meteorology. In this research, Nimbus-6 satellite data are used to perform analyses of several geographic regions, and these analyses are compared to rawinsonde analyses for the same areas. In this way, the capabilities and limitations of satellite data can be determined. Emphasis is placed on vertical profiles of quantitative differences between satellite and rawinsonde values for the several geographic regions, and explanations for differences between the regions are presented in terms of the differing synoptic conditions present. The ability of the satellite to detect and depict atmospheric structural features is evaluated on the basis of the differences between rawinsonde and satellite constant-pressure charts and cross sections.

---

* Research supported by U. S. Army Research Office, Research Triangle Park, North Carolina, under Grant DAAG 29-76-G-0078 to the Department of Meteorology, Texas A&M University.

2. BACKGROUND AND STATEMENT OF PROBLEM

a. Statement of problem

The introduction and implementation of the technology for taking atmospheric soundings from a satellite platform has created a new type of meteorological data and raised some questions as to the usefulness and capabilities of the new data. Until the middle 1970's there was a deficiency in our knowledge of the specific capabilities of satellite soundings in the detection of structural features of the atmosphere. Several studies of satellite soundings have been done during recent years for specific geographical areas, but no studies have been done concerning broad-scale evaluation of the quality of satellite soundings over several geographic regions and in areas of differing synoptic conditions.

In this study, satellite sounding data have been chosen for analysis for a wide swath between the equator and the north pole at a time when varied synoptic conditions in that swath were present. These conditions enable an evaluation of the capabilities of satellite data in terms of atmospheric structural features, ground conditions, moisture content, and weather.

b. Previous studies

A method for deriving quantitative profiles of temperature and water vapor content is given by Smith et al. (1972). The first investigations into the quality of these quantitative satellite data emphasized the similarity of patterns between profiles of satellite and radiosonde measurements (Wark and Hilleary, 1969; Hanel and Conrath, 1969). Temperature and humidity profiles showed the same general features in satellite data--Nimbus-3 at that time--as in rawinsonde data. In an early experiment, measurements of the lower troposphere were made from a satellite sensor flown in an airplane (Rosenkranz et al., 1972). These measurements were checked against direct measurements made by flying the airplane through the layers in question shortly after the satellite observations were made. Results

indicated that layer thicknesses for the 1000-500- and 500-250-mb layers could be computed to within 15 m of the directly-measured value, and that water content could be measured only to within a large experimental error. Other similar experiments have been done using ground-based sensors (Snider, 1972).

Staelin, Barrett, and Waters (1973) found temperature differences between satellite and radiosonde profiles ranging between 1 and 4 K over an altitude range of 1 to 20 km, with the largest discrepancies found at the tropopause and near the surface. The region of relatively large differences near the tropopause is a recurring phenomenon and is usually attributed to vertical smoothing in the satellite data. Layer-mean temperature differences between satellite and radiosonde data for 13 pressure levels (1000, 850, 700, 500, 400, 300, 250, 200, 150, 100, 70, 50, and 30 mb) were found by Waters et al. (1975) to be 2.1 K in December and 1.6 K in June. This was done with Nimbus-5 data.

A study by Smith (1969) indicated that satellite data could theoretically show agreement with radiosonde geopotential height fields on constant-pressure surfaces, although with somewhat weaker gradients. Studies of cross sections differ as to approach and results. Shen et al. (1974) compared rawinsonde and satellite cross sections of temperature and geostrophic wind over the Air Mass Transformation Experiment (AMTEX) area over the East China Sea near Okinawa, and found good agreement in both parameters between cross sections of the two types of data. They compared 1200 GMT radiosonde data with Nimbus-5 satellite data taken at approximately 1530 GMT, but did not present cross sections of quantitative differences.

Kapela and Horn (1975) compared isentropic cross sections from 1200 GMT radiosonde data with those from Nimbus-5 Infrared Temperature Profile Radiometer (ITPR) and Nimbus-E Microwave Spectrometer (NEMS) soundings, and found agreement with regard to patterns of isolines, but considerably less detail in the satellite cross section than in the radiosonde cross section. The same was true in cross sections of geostrophic and gradient wind.

Arnold et al. (1976) compared cross sections of rawinsonde and Nimbus-5 Temperature-Humidity Infrared Radiometer (THIR) and ITPR

temperatures and derived winds, and again agreement was found as to general patterns but significant differences in cross sections of derived wind were present due to differences in horizontal temperature gradients obtained from the two types of data. Quantitative differences were presented in cross-section form in this study, with largest values located near the tropopause and in local areas near the surface. In one case a secondary jet maximum was found in a satellite-derived cross section of wind where none existed in the rawinsonde data. A similar discrepancy appeared in the study by Shen et al. (1974), but in that case the additional jet maximum was verified by cloud photographs. Horn et al. (1976) compared cross sections of Nimbus-5 temperatures and derived winds from 1700 GMT satellite data with 1200 and 0000 GMT radiosonde data to determine whether the satellite patterns were consistent with the changing synoptic situation at the time of the observations. They found the satellite patterns to be consistent, but again with loss of detail.

In summary, the satellite cross sections obtained and analyzed in these studies showed similarity to radiosonde data, but with less detail and with local areas of differences significant enough to cause fairly large errors in fields of derived variables.

Since spatial separation between satellite and rawinsonde sounding points could account for much of the difference found between the two types of soundings, a study was done on the horizontal variability of temperature to determine the extent of the spatial origin of differences (Bruce et al., 1977). These results indicated that 1 K of difference could be attributed to spatial separation effects due to the fact that the rawinsonde measured a point value and the satellite measured an area average. If separation approaches 200 km, the difference expected could be up to 2 K. This could account for a significant portion of the difference found in some of the above studies.

c. Objectives

The primary objective of this research is the determination of how well quantitative satellite data can be used to interpret the synoptic structure of the atmosphere. This evaluation is made over a wide range

of synoptic and surface conditions by comparing the satellite data with rawinsonde data in several geographic regions. Atmospheric parameters including ambient and dew-point temperature, potential and equivalent potential temperature, geopotential height, and geostrophic wind are examined.

3. DATA UTILIZED

a. Satellite data

Satellite data used in this study were obtained from the National Environmental Satellite Service (NESS). These data consist of temperature and dew-point temperature at 21 pre-selected pressure levels from 1000 to 100 mb (1000, 950, 920, 850, 780, 700, 670, 620, 570, 500, 475, 430, 400, 350, 300, 250, 200, 150, 135, 115, and 100 mb), along with an approximate surface elevation, the latitude and longitude of the sounding point, and the date and time of the sounding. The same pressure levels are used in all regions, since these levels are derived from the characteristics of the weighting function for each wavelength band sensed by the satellite radiometers. A temperature is determined from the energy emitted in each wavelength band, and applied to a particular level in the atmosphere depending on the characteristics of the weighting function for that wavelength band. The temperature so obtained, although applied at a single pressure level, actually represents energy emitted from all levels in the atmosphere, so that vertical smoothing is present in the soundings.

The horizontal spacing of satellite soundings is approximately the same as that for rawinsonde stations over the continental United States, and this spacing remains nearly constant for all locations including oceanic and mountainous areas.

An important characteristic of these satellite soundings is that they do not include surface parameters. A surface brightness temperature is given, but it represents the radiative temperature of the surface itself, rather than the shelter air temperature (Arnold et al., 1976). Values of surface pressure are not included. Thus, for the purposes of calculating geopotential height, surface parameters other than elevation must be obtained from some other source.

In order to obtain the surface parameters for the satellite sounding points, surface hourly data were obtained from the Texas A&M University archives of National Weather Service teletype and facsimile data, and from the National Climatic Center. Surface values of temperature, dew-point temperature, and altimeter setting were plotted

and analyzed for the time closest to that of the satellite pass for the region under consideration. Interpolation was done as needed to arrive at the best estimate of the surface conditions for that time. The three parameters were then spatially interpolated to obtain values at the satellite sounding points. This yields surface values of temperature and dew-point temperature, but does not give values of surface pressure, which must be derived from the interpolated altimeter settings.

In conventional surface observations, station pressures are converted to altimeter settings by applying a standard atmosphere correction according to:

$$ALT = P + \Delta P$$

where ALT is the altimeter setting, P is the station pressure, and ΔP is pressure thickness in the standard atmosphere between station and standard sea level pressure which is 1013.25 mb. This value is used so that calculations of altimeter setting will be uniform for all stations, and therefore is not intended to represent actual sea level pressure.

For calculation of ΔP in the standard atmosphere, hydrostatic equilibrium is assumed, so that

$$\frac{dP}{dZ} = -\frac{gP}{RT} .$$

With lapse rate β, and a surface temperature of T_0, the relation between pressure and elevation is found by substituting the expression for temperature into the hydrostatic relation and integrating. This gives

$$P_1 = P_0\left(1 - \frac{\beta Z}{T_0}\right)$$

where Z (in meters) is the elevation of the satellite sounding point, i.e., the height above the standard sea level where temperature and pressure are T_0 and P_0, respectively.

Since P_1 is the pressure at satellite surface points in the standard atmosphere, and β is the standard atmosphere lapse rate (6.5 K/km), we have

$$P_1 = 1013.25\left(1 - \frac{0.0065\ Z}{288}\right)^{5.26}$$

where ΔP can now be defined as

$$\Delta P = P_0 - P_1 = 1013.25\left(1 - \left(1 - \frac{0.0065\ Z}{288}\right)^{5.26}\right).$$

P is unknown so we convert the spatially estimated altimeter settings of the satellite points to station pressure by

$$P = ALT - \Delta P$$

where the values of P are the values of surface pressures at the satellite points.

This station pressure, the surface temperature, and dew point from interpolated hourly observations, and the surface elevation which was supplied with each satellite sounding, complete the set of surface parameters needed for the satellite sounding data.

b. Rawinsonde data

Rawinsonde data for this study were obtained in part from the Texas A&M University meteorological archives of National Weather Service teletype and facsimile data, and in part from the National Climatic Center. Quantities used include the temperature and dew-point temperature at mandatory and significant levels and geopotential height and wind direction and speed at mandatory levels. In rawinsonde soundings, surface parameters, including elevation, are given as the first significant level, so that independent height calculations do not require any additional data.

4. AREAS SELECTED FOR ANALYSIS AND SYNOPTIC CONDITIONS

The areas chosen for analysis in this study were selected on the basis of synoptic conditions and data availability. Since the satellite scans a wide path between the equator and the pole, a day was desired on which a variety of synoptic conditions occurred in a single satellite swath, and August 25, 1975 was selected. On that day, there was a fairly strong low-pressure region centered over the western border of Hudson Bay associated with an upper-level trough which extended into the central portion of the United States. A cold front extended from the low-pressure center at the surface southward through the extreme east end of Lake Superior, then along the western coast of Lake Michigan, through eastern Iowa, eastern Kansas, and the Texas Panhandle. A warm front extended from a short occlusion into southeastern Canada and the northeastern part of the United States. There was a high-pressure area over the southeastern United States and western Atlantic Ocean that dominated the flow in the Southern States and in the Gulf of Mexico, where there was some convective activity off the coast of Mexico but little other significant weather. Horizontal gradients of atmospheric parameters in this area were small.

From the satellite swath on this day were chosen three of the four regions analyzed in this study. Synoptic charts for the three regions for the surface as well as the 700-, 500-, and 200-mb levels are shown in Figs. 1 through 3. Also shown in these figures are the locations of the satellite and rawinsonde soundings, and the locations of the grid points and cross section for each region. Fig. 1 shows the first region, designated the Caribbean, and Figs. 2 and 3 show the central United States region and the Canada region, respectively. These figures illustrate the low-pressure center in Canada, connected to the front which extends through the central United States, and the region of anticyclonic flow in the Gulf of Mexico.

The fourth region considered in this study, illustrated in Fig. 4, was an area of the western United States including the Rocky Mountains on September 3, 1975. At this time, approximately a week

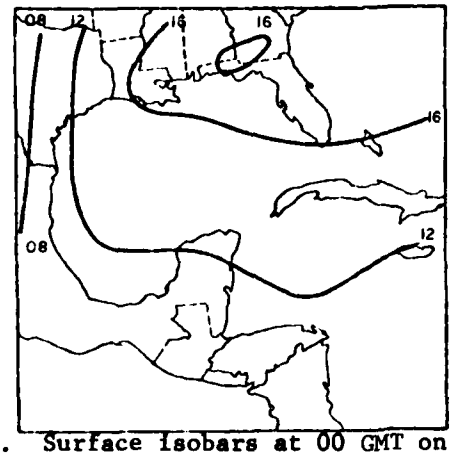

a. Surface isobars at 00 GMT on 26 August 1975.

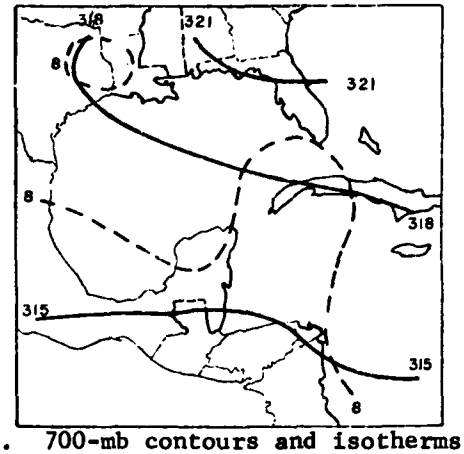

d. 700-mb contours and isotherms at 12 GMT on 25 August 1975.

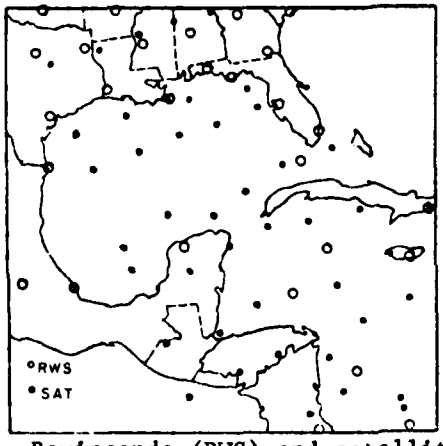

b. Rawinsonde (RWS) and satellite (SAT) sounding locations.

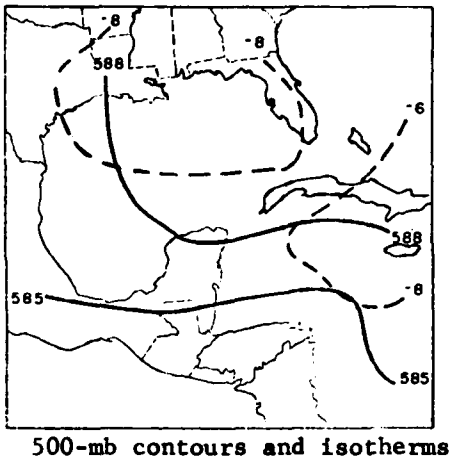

e. 500-mb contours and isotherms at 12 GMT on 25 August 1975.

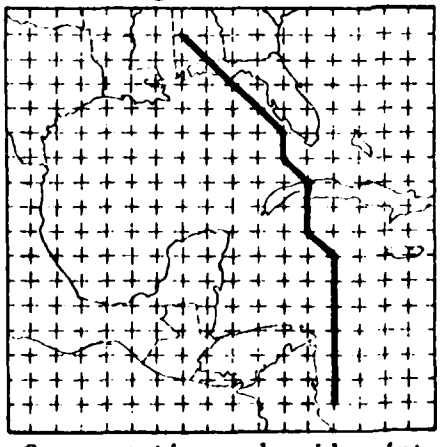

c. Cross section and grid point locations.

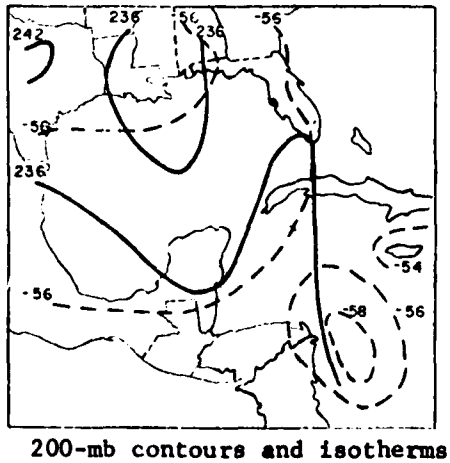

f. 200-mb contours and isotherms at 12 GMT on 25 August 1975.

Fig. 1. Synoptic conditions and locations of grid points, soundings, and the cross section over the Caribbean region.

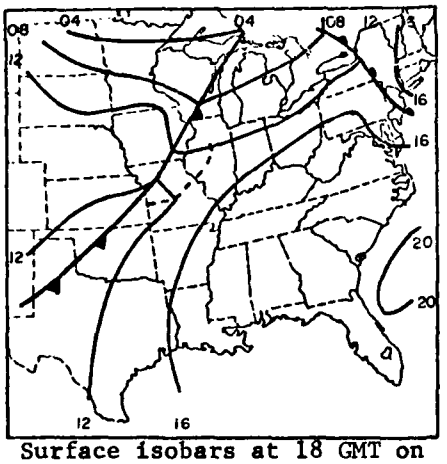

a. Surface isobars at 18 GMT on 25 August 1975.

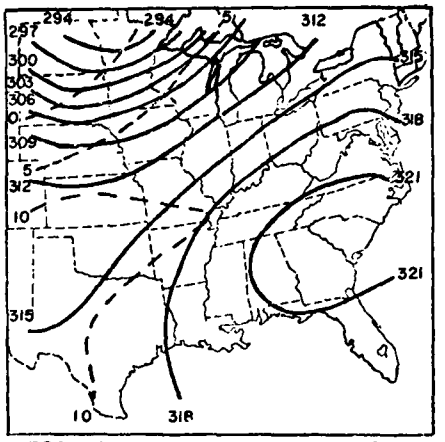

d. 700-mb contours and isotherms at 12 GMT on 25 August 1975.

b. Rawinsonde (RWS) and satellite (SAT) sounding locations.

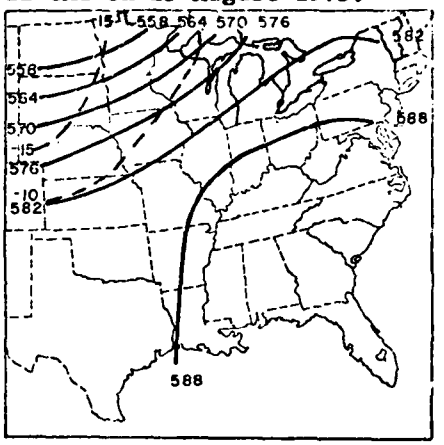

e. 500-mb contours and isotherms at 12 GMT on 25 August 1975.

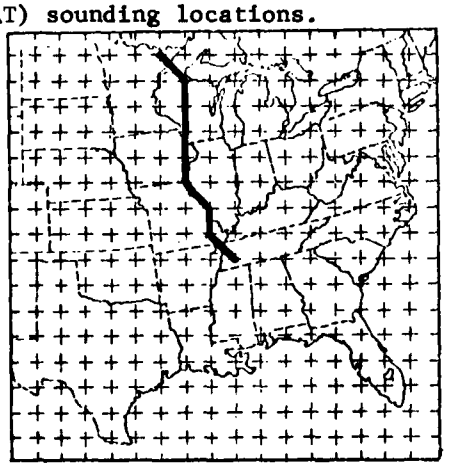

c. Cross section and grid point locations.

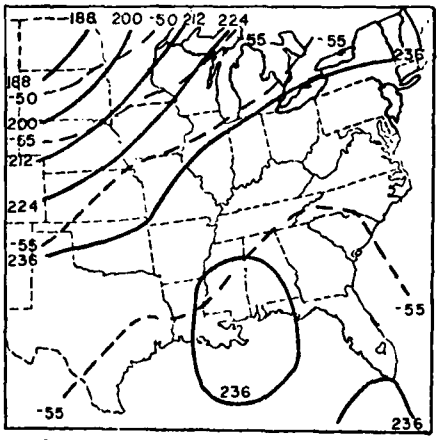

f. 200-mb contours and isotherms at 12 GMT on 25 August 1975.

Fig. 2. Synoptic conditions and locations of grid points, soundings, and the cross section over the central United States region.

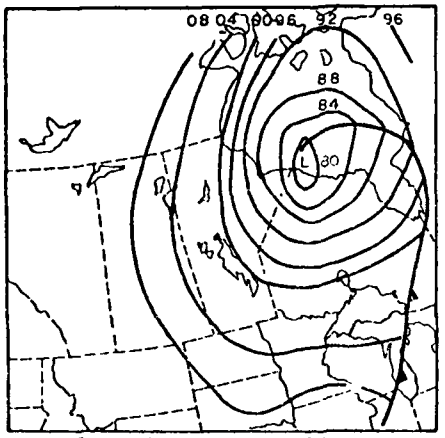

a. Surface isobars at 00 GMT on 26 August 1975.

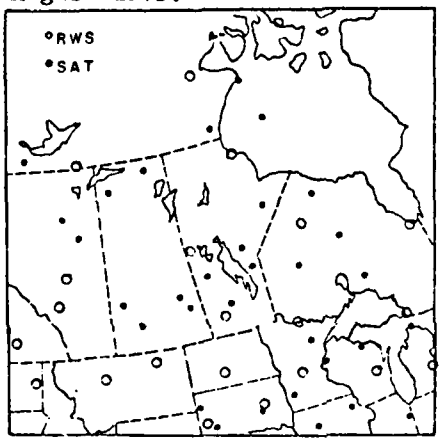

b. Rawinsonde (RWS) and satellite (SAT) sounding locations.

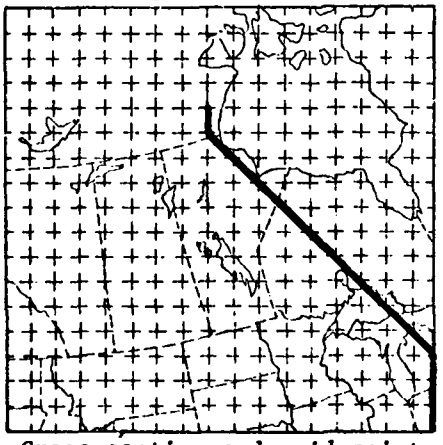

c. Cross section and grid point locations.

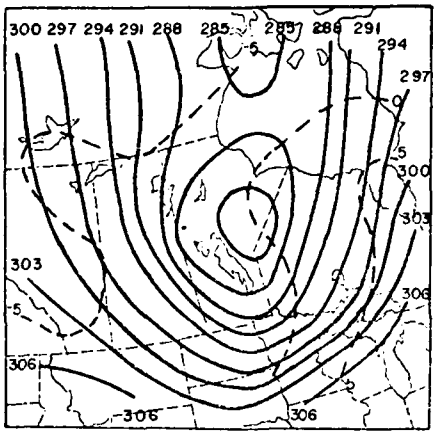

d. 700-mb contours and isotherms at 12 GMT on 25 August 1975.

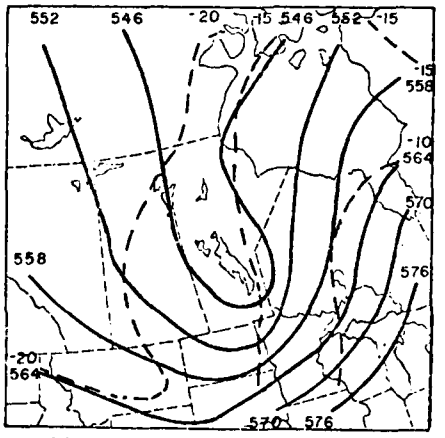

e. 500-mb contours and isotherms at 12 GMT on 25 August 1975.

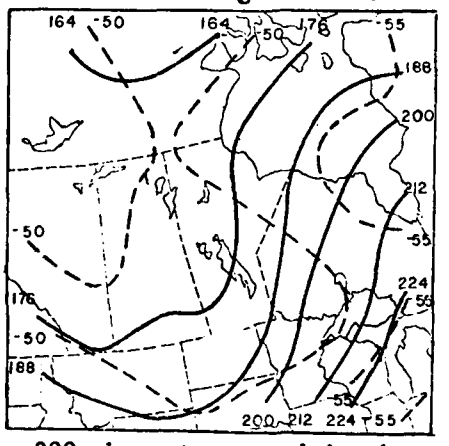

f. 200-mb contours and isotherms at 12 GMT on 25 August 1975.

Fig. 3. Synoptic conditions and locations of grid points, soundings, and the cross section over the Canada region.

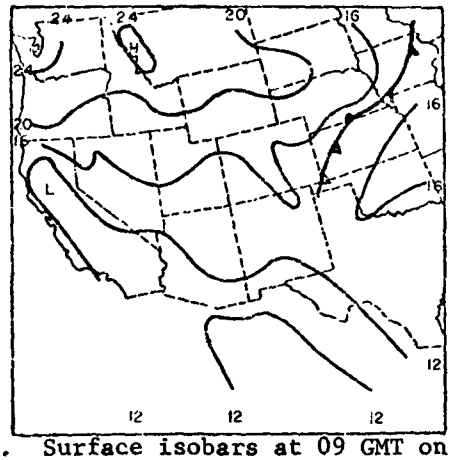

a. Surface isobars at 09 GMT on 3 September 1975.

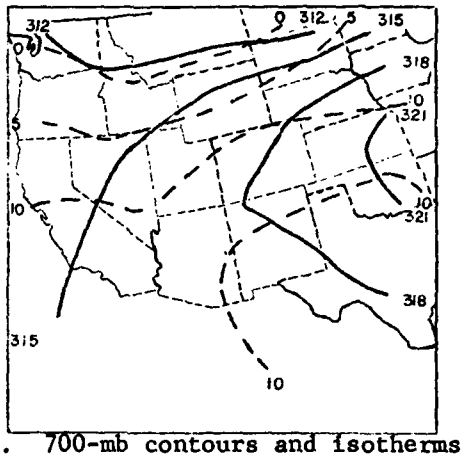

d. 700-mb contours and isotherms at 12 GMT on 3 September 1975.

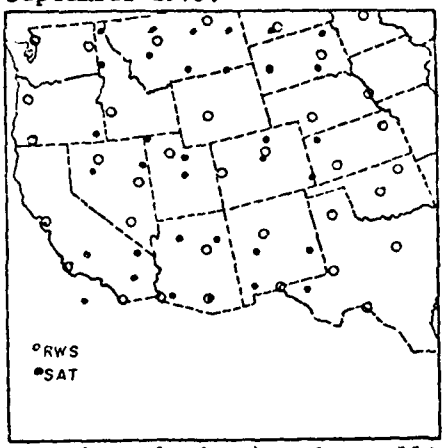

b. Rawinsonde (RWS) and satellite (SAT) sounding locations.

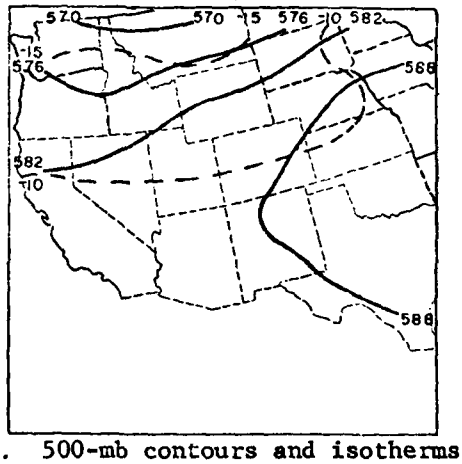

e. 500-mb contours and isotherms at 12 GMT on 3 September 1975.

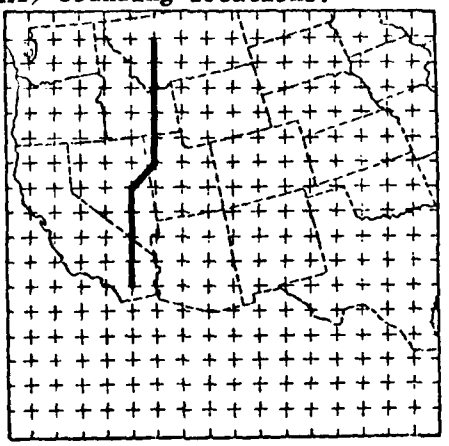

c. Cross section and grid point locations.

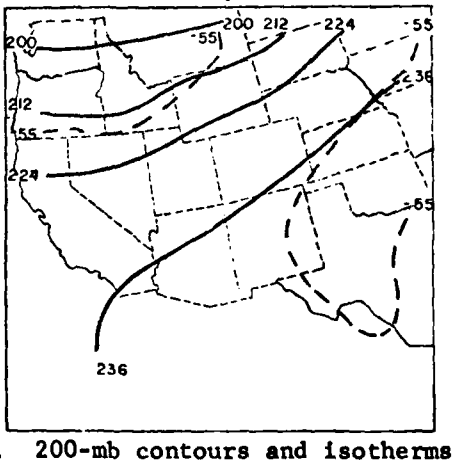

f. 200-mb contours and isotherms at 12 GMT on 3 September 1975.

Fig. 4. Synoptic conditions and locations of grid points, soundings, and the cross section over the western United States region.

later, there was again a frontal situation over the central United States, but the satellite swath being examined was over the western portions of the country. Here, as in the Caribbean region, there was little significant weather with only isolated thunderstorms in Arizona and New Mexico.

These four regions contain: 1) a frontal situation between polar and tropical air masses over the central United States where rawinsonde spacing is optimum; 2) a region just north of the United States in Canada containing a low-pressure center and an upper-level trough; 3) a region of weak anticyclonic flow and moist tropical and subtropical air in the Gulf of Mexico; and 4) a region of the western United States where elevation varies considerably and the atmosphere is fairly uniform. A combination of these four regions should yield a reasonable evaluation of the capabilities of satellite data for sensing synoptic features and structures of the atmosphere.

5. ANALYSIS PROCEDURE

a. Construction of gridded constant-pressure charts

There are two basic characteristics of the Nimbus-6 satellite soundings over the western hemisphere that must be considered when making comparisons between the satellite data and rawinsonde data. These characteristics are that the satellite soundings 1) are not taken at the same time as rawinsonde soundings, and 2) are not located at the same points on the surface as rawinsonde soundings.

One method of dealing with the first problem is to compare qualitatively the satellite data with each of the two adjacent rawinsonde sounding times, thereby taking into account the movement of systems, diurnal effects, and other changes that may have occurred between the times of the rawinsonde soundings. This approach was used by Horn, Peterson, and Whittaker (1976), among others. A second method is to make quantitative comparisons of the satellite data with both rawinsonde sounding times, and to present both sets of differences (Peterson and Horn, 1977). The method chosen in this study was to analyze each rawinsonde time individually, and to approximate the conditions at the intermediate satellite time through linear interpolation in time. These time-interpolated rawinsonde data were then used in the comparisons with satellite data, and gave better results than those obtained from comparisons of the satellite data with either rawinsonde time alone.

For the second problem, there are two approaches possible in the analysis of satellite and rawinsonde data when individual soundings of the two types are at noncoincident points. One approach is to pair the rawinsonde sounding stations with the nearest satellite sounding points, and to compare the pairs of soundings as if they had been at the same geographical location. The other approach is to use rawinsonde and satellite sounding data at their original locations, with a gridding procedure to place the two types of data onto a grid. The latter procedure was used in this study. The gridding process removes some of the spatial differences between satellite and rawinsonde soundings, and the use of appropriate grid spacing

and analysis parameters (see below) results in an analysis similar to that which would be achieved through hand analysis techniques.

For each of the four geographic regions considered in this study, a square grid of 18 x 18 points with a spacing of 158 km was established. The analysis technique presented by Barnes (1964) was used with four iterations and a scan radius determined by the approximate average station spacing. This technique utilizes a Fourier representation of the function to be gridded, and the scanning radius determines the maximum distance at which a grid-point value can be influenced by an actual data point. In order to smooth spurious high-frequency amplification, a Shuman smoothing procedure was applied to each gridded field (Shuman, 1957). Parameters of each grid are shown in Table 1 along with the time of the satellite pass for each region.

Table 1. Grid parameters for the four regions analyzed in this study.

Region	Left. Long.	Top Lat.	Scanning Radius, grid spaces RW	SAT	Number of Scans	Time of Sat. Pass
Caribbean	100°W	35°N	3 or 5*	3	4	1710 GMT
Central U.S.	105°W	50°N	3	3	4	1720 GMT
Western U.S.	125°W	50°N	3	3	4	0730 GMT
Canada	120°W	68°N	4	3	4	1730 GMT

*see text

The fairly even spacing of the satellite sounding points allowed the use of a uniform scan radius of three grid distances for satellite data in all regions. With rawinsonde data, however, availability and consistency varied considerably from region to region. Rawinsonde sounding points were most dense over the United States in the central and western regions. Canadian rawinsonde soundings were somewhat more sparsely spaced, and rawinsonde soundings in the southern portion of the Gulf of Mexico (Caribbean region) were very sparse.

Areas where stations are sparse or where there are stations with missing data at crucial locations can be gridded only through the use of an increased scan radius. Thus the United States regions had scan radii of three grid distances; the Caribbean region had a scan radius of three grid distances near the United States coast and five grid distances in the southernmost two-thirds of the region; and Canada had a scan radius of four grid distances. These differences between gridding procedures for the different regions, if taken into account, do not invalidate a comparison between regions, and reflect only the variation in spacing and consistency of rawinsonde soundings.

After the grid was established, all of the basic variables from the surface to 100 mb were placed on the grid for the particular region involved. Data sets were created with gridded surface fields of elevation, pressure, temperature, and dew-point temperature, and fields of temperature and dew-point temperature at each of the 21 pressure levels above the surface. This was done for both rawinsonde and satellite data. An auxiliary data set was created for rawinsonde-observed geopotential height, and observed u- and v-component wind data at the ten mandatory levels.

Since the rawinsonde data are available at 1200 and 0000 GMT only, the gridding procedure was applied to rawinsonde data at each time, and a linear time interpolation was applied to obtain the rawinsonde data at the intermediate time of the satellite pass. Use of this time-interpolation technique gives better results than those obtained from a comparison of the satellite data to either rawinsonde time by itself.

b. Variables considered and computational procedures

This study includes basic variables which are those supplied as part of the original data in rawinsonde or satellite soundings and derived variables which are those calculated from basic variables. Basic variables were listed in the previous section. Ten of the 21 pressure levels in the satellite data coincide with the ten mandatory levels from 1000 to 100 mb in rawinsonde data (1000, 850, 700, 500, 400, 300, 250, 200, 150, and 100 mb), while the remaining levels do

not necessarily coincide with rawinsonde significant-level data points. For purposes of comparison, therefore, rawinsonde temperature and dew-point temperature were obtained at the 11 non-coincident pressure levels by linear interpolation on a skew T/log P diagram. With the addition of the surface values for satellite soundings, comparable data sets for the two types of data were obtained.

Derived variables fall into three groups, the first being those that are related to temperature. The lapse rate of temperature was computed by using centered finite differences where the value at a given pressure level was determined by the values of temperature and geopotential height at the adjacent pressure levels above and below. Thus, the degree of smoothing is not constant with height, but satellite values can legitimately be compared with rawinsonde values since both are calculated over the same pressure layers. The rawinsonde calculations use rawinsonde-measured temperatures and calculated geopotential heights, while the satellite calculations use satellite-measured temperatures and computed geopotential heights based on the measured temperatures. In this way the rawinsonde and satellite computations are independent. The horizontal gradient of temperature is computed using a centered finite difference to approximate the x- and y-direction derivatives of temperature, and the end result is the magnitude of the horizontal temperature gradient and is independent of the orientation of any cross section. Potential temperature is computed using Poisson's equation.

The second group consists of those derived variables related to moisture. In this group are equivalent potential temperature, mixing ratio, and stability. Equivalent potential temperature was derived with the Rossby formula for pseudo-equivalent potential temperature, i.e.,

$$\Theta_e = \Theta_d \, e^{\left(\frac{Lw}{c_p T_{sc}}\right)}$$

where L is the latent heat of condensation, w is the mixing ratio, c_p is the specific heat at constant pressure, and T_{sc} is the temperature at saturation. The pseudo-potential temperature Θ_d, is given by

$$\theta_d = T\left(\frac{1000}{P - e}\right)^{\frac{R}{c_p}}$$

where T is the temperature, R is the gas constant for dry air, P is the pressure, and e is the water vapor pressure.

The third group of derived variables contains geopotential height and winds. The former was calculated at grid points by using virtual temperature, and integrated from the surface upward. The mean virtual temperature for a layer was defined as the arithmetic average of the values at the top and bottom of the layer. This method was found to yield values of geopotential height that were superior to those from other averaging methods in terms of root-mean-square differences between observed rawinsonde heights and computed satellite heights. Other methods of averaging that were investigated included several types of logarithmic averages. For the satellite computations, the surface temperature, dew point, and pressure were obtained from hourly synoptic data as described above.

Geopotential heights also were calculated from the 21 levels of interpolated rawinsonde temperature data. This was done to obtain an estimate of the error to be expected in height calculations resulting from the use of predetermined pressure levels rather than the set of significant levels which is used to compute the observed heights, and which changes from sounding to sounding.

c. Construction of cross sections

Computer programs were written to plot data on cross sections containing arbitrary numbers of soundings at arbitrary horizontal spacings, and at either the ten mandatory levels or the 21 pressure levels supplied in the satellite data. The computer-plotted data were then analyzed by hand. Two types of cross sections were constructed, viz., from sounding data at the locations of the sounding points and from gridded data.

There are several advantages to having both types of cross sections. Gridded sections take into account the variation perpendicular to the plane of the section, since the gridding procedure takes into

account variations in two dimensions on constant-pressure surfaces. The gridded sections also allow for the plotting of more soundings per cross section since grid points are generally closer together than sounding stations. Station-to-station sections allow examination of the data in cross-section form before smoothing or gridding takes place, and provide a check against the gridded data for consistency.

For placement of cross sections in each region, the locations of data points and synoptic features had to be taken into account. Cross sections perpendicular to fronts are desirable but not always possible due to the locations of the sounding points.

6. RESULTS

The results of this study are presented in three parts. The first involves quantitative differences--expressed as satellite values minus rawinsonde values--which were computed for several variables by using grid-point data on constant-pressure surfaces (850, 700, 500, 400, 300, 250, 200, 150, and 100 mb). The average and standard deviation of these differences were calculated at each pressure level and plotted as continuous profiles for each of the four regions. These profiles comprise the first section of the results.

The average difference at any pressure level represents a bias in the satellite data relative to rawinsonde data. If the profiles of these biases are consistent between regions, then their effect would be easily removed from future processing of satellite data by applying a correction which may be pressure-dependent.

The standard deviation of differences represents the variation of the magnitudes of a set of differences for a surface. In cases where the average is near zero, the standard deviation may be taken to represent an approximation to the RMS difference between the two types of data. Large variation of the magnitude of the differences represented by high values of standard deviation imply that comparison of satellite and rawinsonde values for that variable and pressure level yields poor results. While even large average differences may be removed by a fairly simple procedure, non-zero standard deviations are not easily removed and usually are interpreted as errors in the data.

The grid points over which the average and standard deviation were computed were chosen for the relevant portion of each region on the basis of the spacing of the original data points and the locations of missing data from either source. The relevant portion of a region includes that part which contains the unique features of the region, and which does not overlap any other region. The vertical difference profiles should, therefore, be representative of the region involved with its particular surface and atmospheric conditions.

Following the vertical difference profiles are analyses of constant-pressure charts and cross sections for the four regions. Most of these were taken from gridded data, and represent the horizontal and vertical variations of atmospheric parameters as depicted by satellite and rawinsonde data, as well as variations of quantitative differences between the two types of data.

Within each of these parts, results are presented for: 1) temperature-related variables; 2) moisture-related variables; and 3) geopotential height and wind. For each variable, results are presented for representative regions and discrepancies between regions are pointed out with some possible explanations.

a. Vertical difference profiles

1. Temperature-related variables

Temperature is probably the most basic of all meteorological parameters. Profiles of the average difference and the standard deviation of the differences between rawinsonde and satellite temperature values are shown in Fig. 5 for the four regions.

The magnitudes of the average and standard deviation of the differences are fairly small in the Caribbean region, but are larger with more vertical variation in the central and western United States regions. Average values in Canada are less than 0.75 C except near the tropopause (250 mb), and magnitudes of the standard deviation are intermediate between those of the Caribbean region and those of the United States regions. The explanation for the changes in profile shape and magnitude from region to region lies in the differing synoptic conditions present. The flat thermal field in the Caribbean, associated with the weak anticyclonic circulation and high tropopause, creates optimum conditions for accuracy in the satellite sounding data. This is because smoothing present in satellite soundings has little effect on the final values obtained due to the uniform vertical variation and small horizontal gradients in that region. The remaining regions, particularly the central United States and Canada, contain more temperature variation so that smoothing in satellite

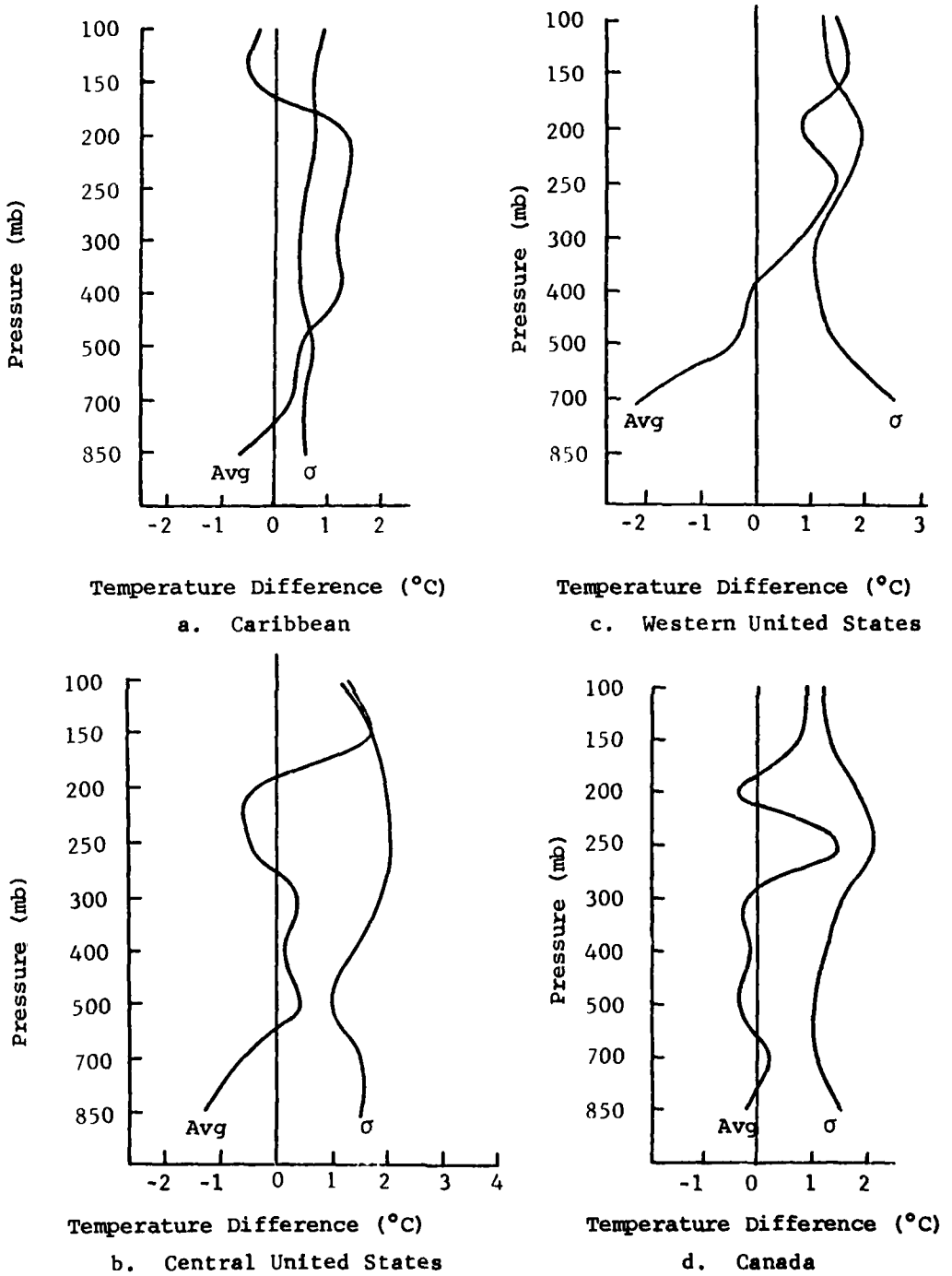

Fig. 5. Profiles of the average difference and standard deviation of the differences between satellite and rawinsonde temperatures (satellite values minus rawinsonde values) for four regions.

data results in higher difference magnitudes and less vertical consistency in the difference profiles.

Average differences in all regions tend to be largest near the tropopause which is near 100 mb in the Caribbean, near 150 to 200 mb in both of the United States regions, and near 250 mb in Canada. The small average differences (less than 0.4 C) below the tropopause which extend to the surface in Canada are probably characteristic of the satellite soundings in the polar air mass occupying most of that region.

Profiles of the average and standard deviation of the differences for lapse rate of temperature for the four regions are shown in Fig. 6. These show that through the lower levels of the troposphere, up to near 400 mb, the standard deviations of the differences are less than or equal to approximately 0.5°C km^{-1}. Average differences in those layers are also less than 0.5°C km^{-1}, and are smallest (near zero) in the Canada and Caribbean regions. Due to the vertical smoothing in the satellite soundings, the change of vertical lapse rate of temperature in satellite data associated with the tropopause occurs over a deeper layer than the corresponding change in rawinsonde data, so that the satellite data indicate a decrease which begins at a lower level than that in rawinsonde data. Therefore, differences tend to be negative (satellite values too low) below the tropopause in each region, while approaching zero and perhaps changing sign above the tropopause as the rawinsonde lapse rate decreases to approach the already-reduced satellite lapse rate. This effect is particularly evident in Canada, where the sign of the average difference changes at 250 mb, the approximate level of the tropopause in the polar air mass. The Caribbean profile shows the beginning of a similar pattern at 200 and 150 mb, but the high altitude of the tropopause puts the sign change (if present) above the 150-mb level where it cannot be seen in the figure.

The average difference curve for the central United States shows large negative values at the 200-mb level, which is below the tropopause in the tropical air south of the front in that region. The effect is not demonstrated well in the western United States due to

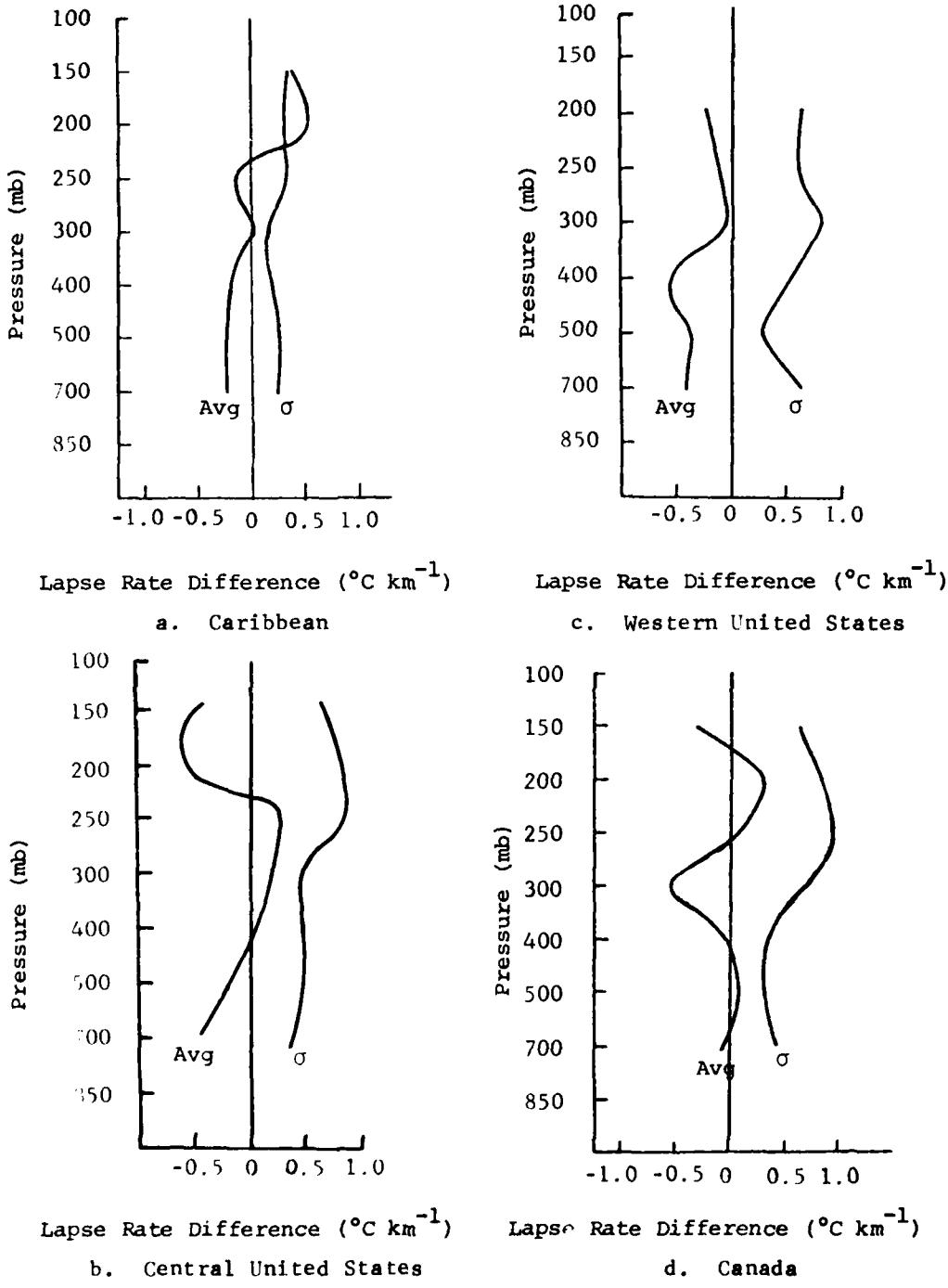

Fig. 6. Profiles of the average difference and standard deviation of the differences between satellite and rawinsonde vertical lapse rates of temperature (satellite values minus rawinsonde values) for four regions.

the presence of multiple tropopause layers in the air mass over that region.

The horizontal gradient of temperature as used here is the magnitude of the horizontal gradient vector, and is therefore not related to the direction or orientation of any cross section. Vertical difference profiles for the four regions for this variable are shown in Fig. 7.

Average differences are small, less than 2°C $(1000\ km)^{-1}$ in all regions, while standard deviations are near 1.7°C $(1000\ km)^{-1}$ in the Caribbean and are larger in the United States regions and the Canada region where values reach 5°C $(1000\ km)^{-1}$. This is in direct association with the magnitudes of the horizontal temperature gradients in these regions. The Caribbean region contains only small gradient values, thus allowing the differences there to be small; the polar front in Canada and the central United States causes gradients and differences to be somewhat larger. The similarity in shape and magnitude of the curves in the western United States to those for the central United States will be explained later in connection with the constant-pressure charts and cross sections for those regions. Average differences show that the satellite values are too small in Canada, too large in the Caribbean, and vary in the United States regions from too small near the surface to too large through the middle and upper troposphere.

Differences of profile shape and magnitude between regions have been related in this section to differences in atmospheric conditions. There are other differences from one region to another, however, that are not directly related to the atmosphere such as the magnitude and variation of the surface elevation. The Gulf of Mexico/Caribbean region is composed primarily of ocean surface so that the surface elevation is fairly uniform through most of the region. The central United States and Canada regions contain only a moderate amount of elevation variation.

Examination of the difference profiles for the temperature-related variables just discussed indicates that the standard deviations in the lower levels show the same change of magnitude from

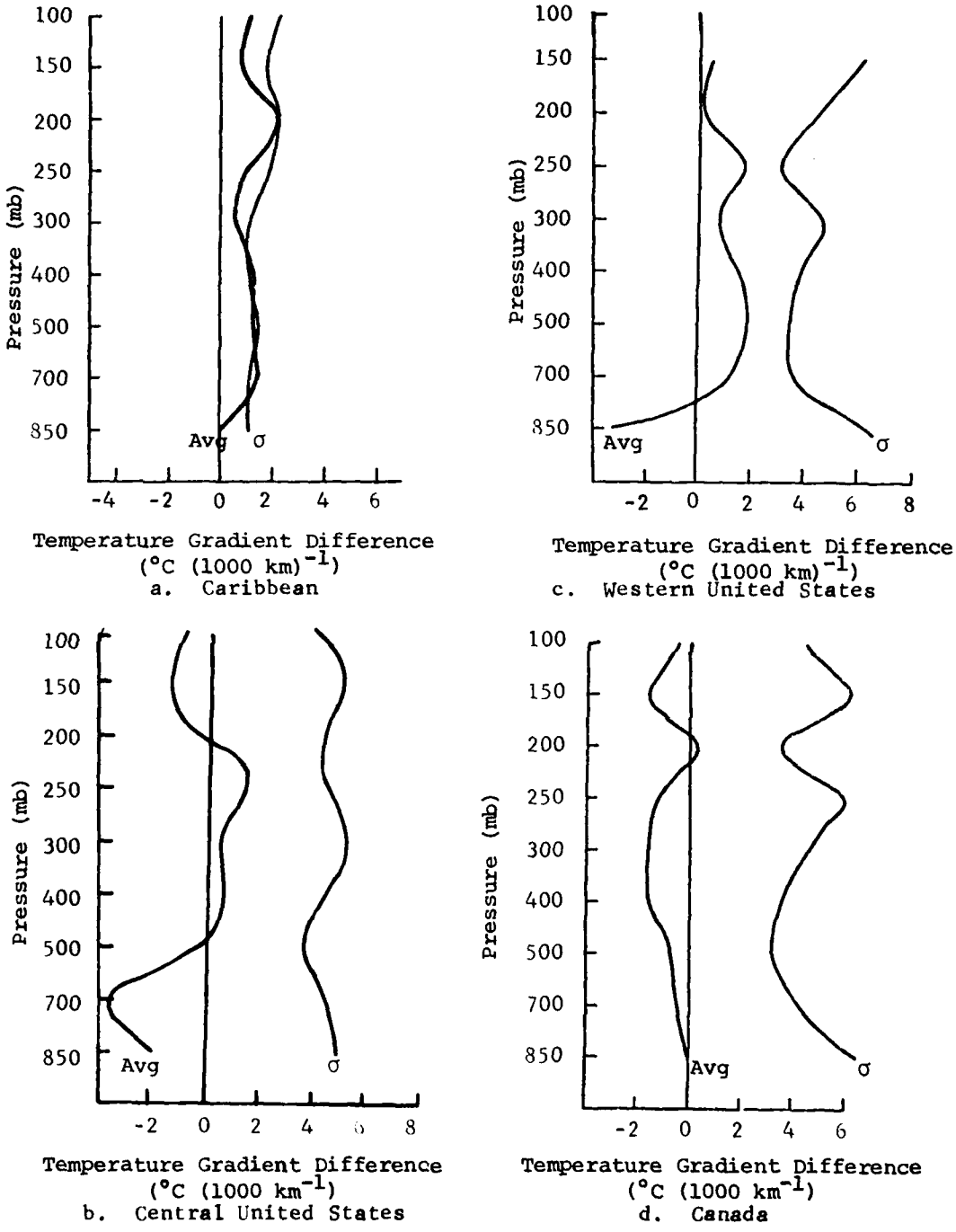

Fig. 7. Profiles of the average difference and standard deviation of the differences between satellite and rawinsonde horizontal temperature gradients (satellite values minus rawinsonde values) for four regions.

one region to another as the variation of the surface elevation. In other words, the lowest standard deviations (Caribbean) are associated with the lowest variation of the surface elevation, while the highest standard deviations (western United States) are associated with the largest variation of the surface elevation. This relationship can be observed in some of the variables discussed in the next section. The extent and cause of this seeming correspondence requires further study.

2. Moisture-related variables

Vertical difference profiles for dew-point temperature are shown in Fig. 8 for the four regions. The standard deviation of the differences in the central United States and Canada regions averages approximately 5°C in the lower troposphere where moisture is measured, while values of near 3.5°C and 7.5°C are typical for the Caribbean and western United States, respectively. Differences in the western United States are somewhat larger than those in the other three regions with values increasing above 400 mb to near 10°C. In all regions except Canada, the satellite indicates too much moisture relative to the rawinsonde with positive average differences at most levels. In Canada, however, where the fairly dry polar air is the main constituent, the satellite indicates too little moisture through most of the lower troposphere, which is probably another characteristic of the satellite soundings in that air mass. The large differences in the Caribbean at 500 mb will be discussed later.

Vertical difference profiles of mixing ratio are presented in Fig. 9. Noteworthy is the similarity of these curves to those of dew point, and the consistency of the curves of standard deviation for mixing ratio in all regions. Values of the standard deviation decrease from near 2 g kg^{-1} at 850 mb to very small magnitudes aloft where there is little moisture. The Caribbean profile shows that too little moisture is indicated by the satellite in the levels below 500 mb, and too much above 500 mb, which is a manifestation of the vertical smoothing present in the satellite data. Average differences for the central and western United States regions are quite similar

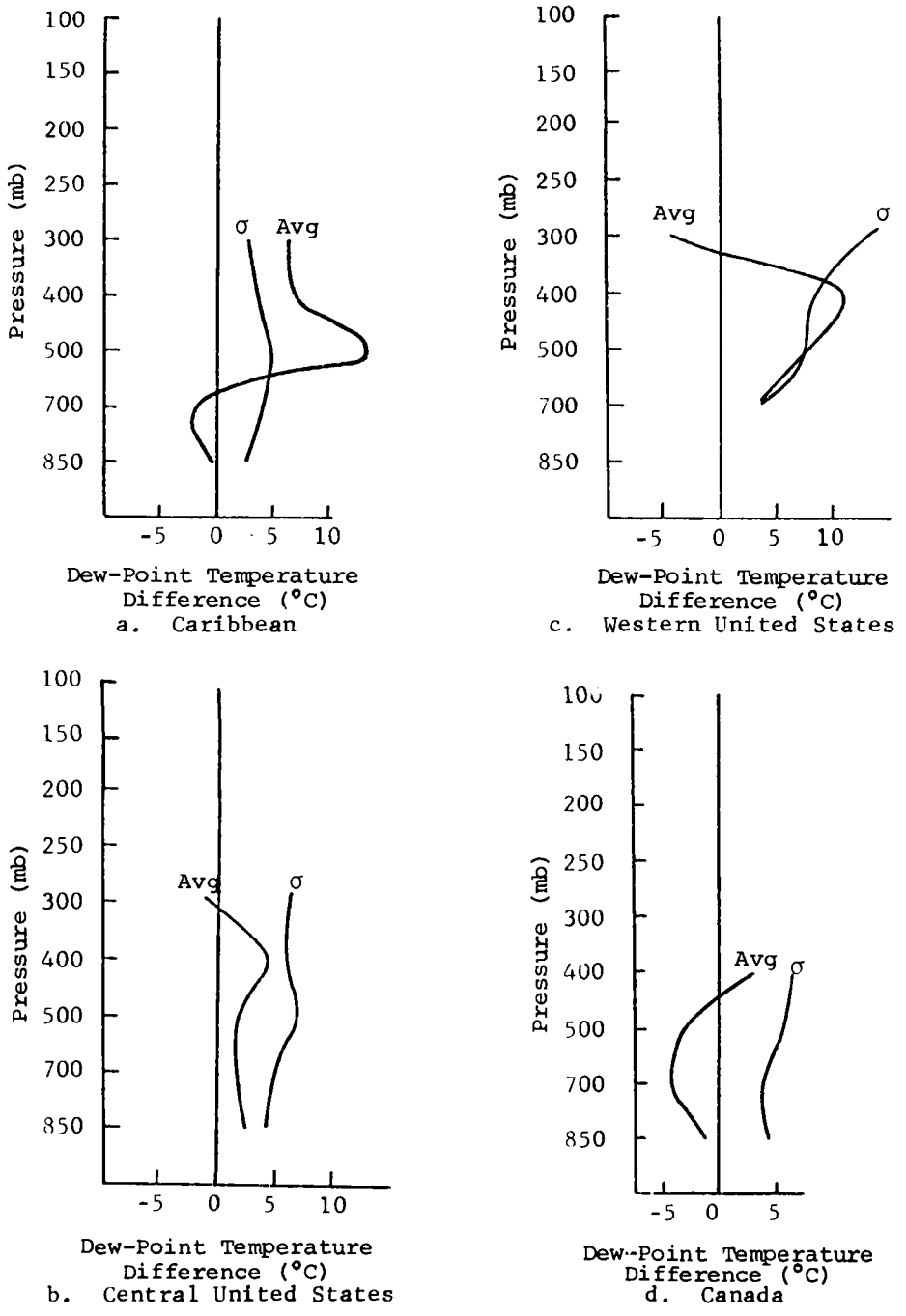

Fig. 8. Profiles of the average difference and standard deviation of the differences between satellite and rawinsonde dew-point temperatures (satellite values minus rawinsonde values) for four regions.

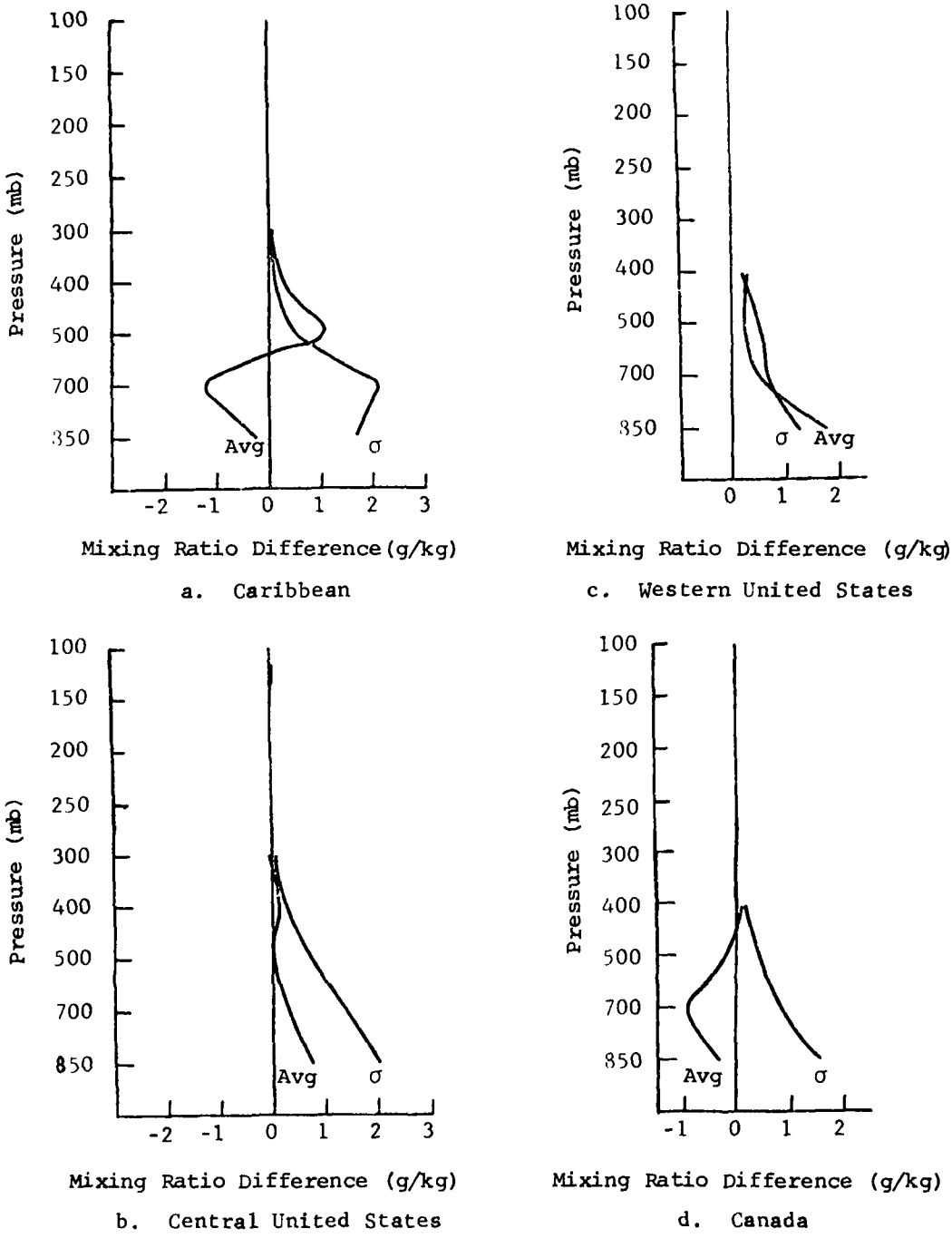

Fig. 9. Profiles of the average difference and standard deviation of the differences between satellite and rawinsonde mixing ratios (satellite values minus rawinsonde values) for four regions.

with values near 1 g kg^{-1} at 850 mb that decrease to near zero aloft; in Canada the satellite again is indicating too little moisture through most of the lower troposphere.

3. Geopotential height and wind

Vertical profiles of geopotential height for the four regions are shown in Fig. 10, where the solid lines represent average and standard deviations of differences between satellite and observed rawinsonde values. In this case, the observed rawinsonde geopotential height is that calculated by the National Weather Service from significant-level temperature and dew-point data obtained from rawinsonde soundings and supplied at mandatory levels in teletype data. Dashed lines in the vertical profiles represent the difference in terms of average and standard deviation between the same observed heights and those which were re-computed from interpolated rawinsonde temperatures at the 21 pressure levels given in the satellite data. These curves represent the discrepancy which can be expected in satellite data resulting from the use of a constant set of 21 pressure levels for height calculations rather than the significant levels. The real difference between the capabilities of satellite and rawinsonde to measure temperature as represented by geopotential height differences is, therefore, the difference between the solid and dashed curves. The difference between actual observations and the satellite is represented by the solid curves themselves.

Any difference between the satellite-computed geopotential height and the observed geopotential height can be attributed to: 1) temperature differences in the values of layer-mean virtual temperature; 2) surface elevation differences; and 3) surface pressure differences. The virtual temperature in a layer can be affected by errors in either the temperature or the dew-point temperature, so that large errors in dew point combined with small errors in temperature could yield appreciable height differences. The surface elevation was given with the satellite soundings, and represents a terrain height from a smoothed map for the satellite sounding point; the surface pressure was that obtained for the satellite sounding point from the

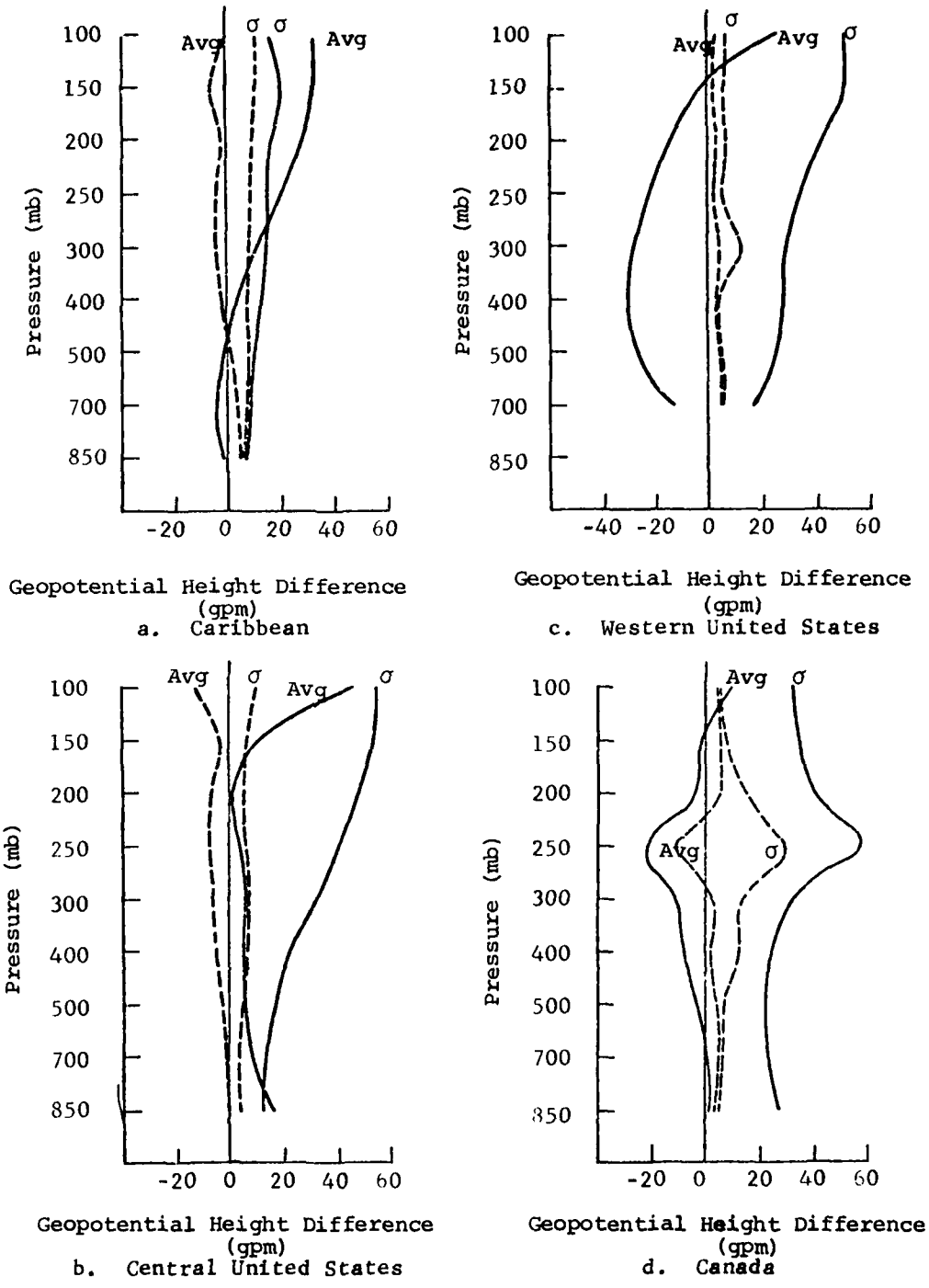

Fig. 10. Profiles of the average difference and standard deviation of the differences between satellite and rawinsonde geopotential heights (satellite values minus rawinsonde values) for four regions. See text for explanation of dashed lines.

surface hourly data. Either or both of these surface parameters could differ from those for rawinsonde stations where the surface elevation is nearly an exact value that is not taken from a smoothed terrain elevation map, and the surface pressure is that which was time-interpolated from 1200 and 0000 GMT data. Differences at the surface, however, account only for a constant difference throughout the troposphere, so that any changes in difference profiles occurring above 850 mb (the lowest level at which height differences were computed) are due to differences in temperature. The average difference between geopotential heights should, therefore, correspond with the vertical integral of the average temperature difference for the same region.

In general, the difference between satellite and rawinsonde geopotential heights is significantly greater than that between the observed and computed rawinsonde values. The latter tend to remain fairly constant throughout the troposphere while the former tend to increase toward the tropopause and decrease slightly above that level. Standard deviations tend to be smallest near the middle of the troposphere over all regions, and highest at the levels near the tropopause. This is reasonable, since these features are also characteristic of the temperature profiles.

The Caribbean region exhibits the smallest differences between satellite and rawinsonde values, with standard deviations increasing from near 8 m at 850 mb to 16 m at 100 mb. Standard deviation values in the other regions range from 12 to 56 m in the central United States, from 18 to 50 m in the western United States, and from 28 to 33 m in Canada where values of near 60 m are reached at 250 mb. Average differences are lower than standard deviations in all but the Caribbean region. A correction to remove the average difference (or bias) would improve the accuracy of the satellite geopotential heights in the Caribbean, but such a correction would not be helpful in any of the other regions, where standard deviations are significantly larger than average differences. The latter are, in fact, near zero through much of the troposphere in all but the western United States region.

In the Caribbean region, the differences between satellite and rawinsonde heights are not indicative of differences in temperature measurement up to approximately 300 mb, since the errors in rawinsonde computations based on temperatures at the satellite pressure levels are of nearly the same magnitude as the satellite differences. In the central United States, however, the standard deviation of the differences between satellite and rawinsonde data becomes significantly greater with altitude than the error in the rawinsonde data resulting from the use of the satellite pressure levels, so that much of the difference in the former can be attributed to differences in temperature measurement. In Canada, although the curves of satellite minus rawinsonde geopotential heights are 10 to 20 m greater in absolute magnitude than those for rawinsonde errors, no significant differences in temperature measurement are represented since the pairs of curves are parallel throughout the troposphere. Most of the difference is present at 850 mb and can be attributed to differences in surface variables.

There are four types of wind fields examined in this study. The first is the observed wind which is that wind derived from tracking the rawinsonde balloon as it ascends through the atmosphere. This will be referred to as the "real" wind. The other three types are geostrophic winds, which were calculated from 1) the observed geopotential height field given with rawinsonde data at mandatory levels--the "actual" geostrophic wind; 2) the re-computed rawinsonde geopotential heights based on the 21 levels of interpolated temperatures--the "rawinsonde" geostrophic wind; and 3) the 21 levels of satellite temperature values--the "satellite" geostrophic wind. The geostrophic approximation is only fair in estimating the real wind in areas where there is large curvature of the geopotential height field or where other types of significant accelerations are present. In these situations, a comparison of satellite-derived geostrophic wind with observed wind would not be a true indicator of the satellite sensing capabilities. Therefore, vertical difference profiles of geostrophic wind are presented based on differences between satellite geostrophic wind and actual geostrophic wind. Profiles are presented for four variables; namely, the u-component, v-component, scalar wind speed, and wind direction.

Vertical difference profiles for the u-component of the geostrophic wind are presented in Fig. 11. These show that the average difference in the u-component in all regions is fairly small, being 1-4 m s^{-1} throughout the troposphere. The standard deviation of the differences is somewhat larger, ranging from 4 m s^{-1} at 850 mb to near 15 m s^{-1} at 100 mb. There are slightly larger values in Canada at 250 mb.

Profiles of the v-component difference shown in Fig. 12 indicate that average differences are small, negative in the lower layers, and increase in absolute value to near -7 m s^{-1} at 100 mb. The exception to this is the western United States region, where differences are of the opposite sign but the same magnitude. Plots of scalar wind speed in the four regions, shown in Fig. 13, indicate that small average differences occur in the lower layers, with values near 5-7 m s^{-1} at the top of the troposphere. Standard deviations of differences tend to increase with altitude, with values between 5 and 15 m s^{-1}. Differences near the tropopause tend to be larger than those elsewhere in all four regions.

With the exception of the Caribbean region, the standard deviation of direction difference (Fig. 14) tends to average approximately 45°, and peak near the tropopause. The Caribbean region is quite different from the other regions due to the small wind speeds in that region that are associated with small magnitudes of height gradient.

Estimates of geostrophic wind from satellite temperatures via computed geopotential heights show similar magnitudes of differences in all four regions. This is significant especially in view of the fact that the magnitudes of the wind speed vary from fairly low values (10 m s^{-1}) in the Caribbean region to quite high values (50 m s^{-1}) in the upper-level flow over Canada. Differences in geopotential height change from region to region and are not related to those of geostrophic wind, which are fairly constant between regions. This implies that the accuracy of height gradients computed from satellite temperatures is independent of the accuracy of the height values themselves.

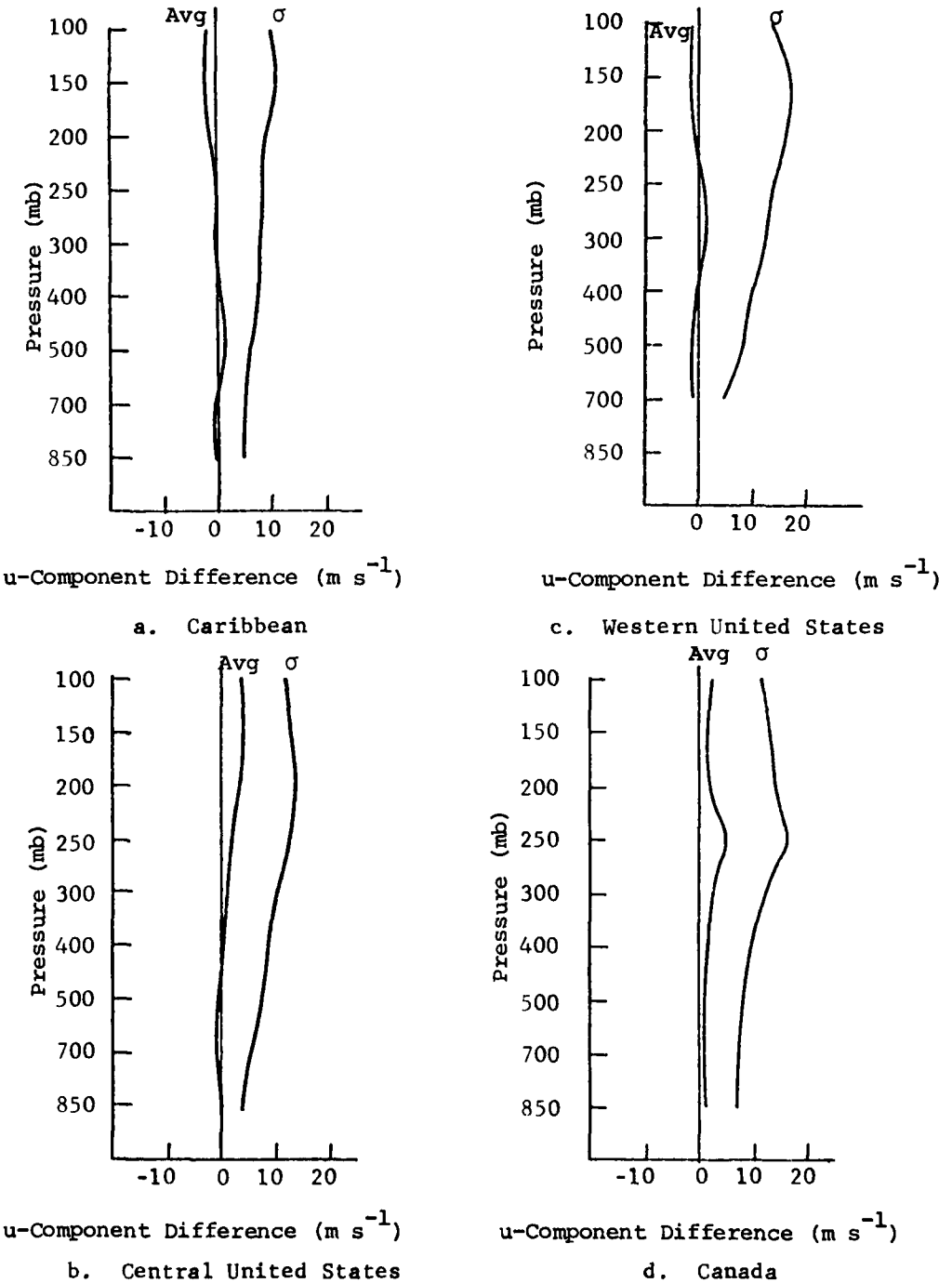

Fig. 11. Profiles of the average difference and standard deviation of the differences between satellite and rawinsonde geostrophic wind u-component (satellite values minus rawinsonde values) for four regions.

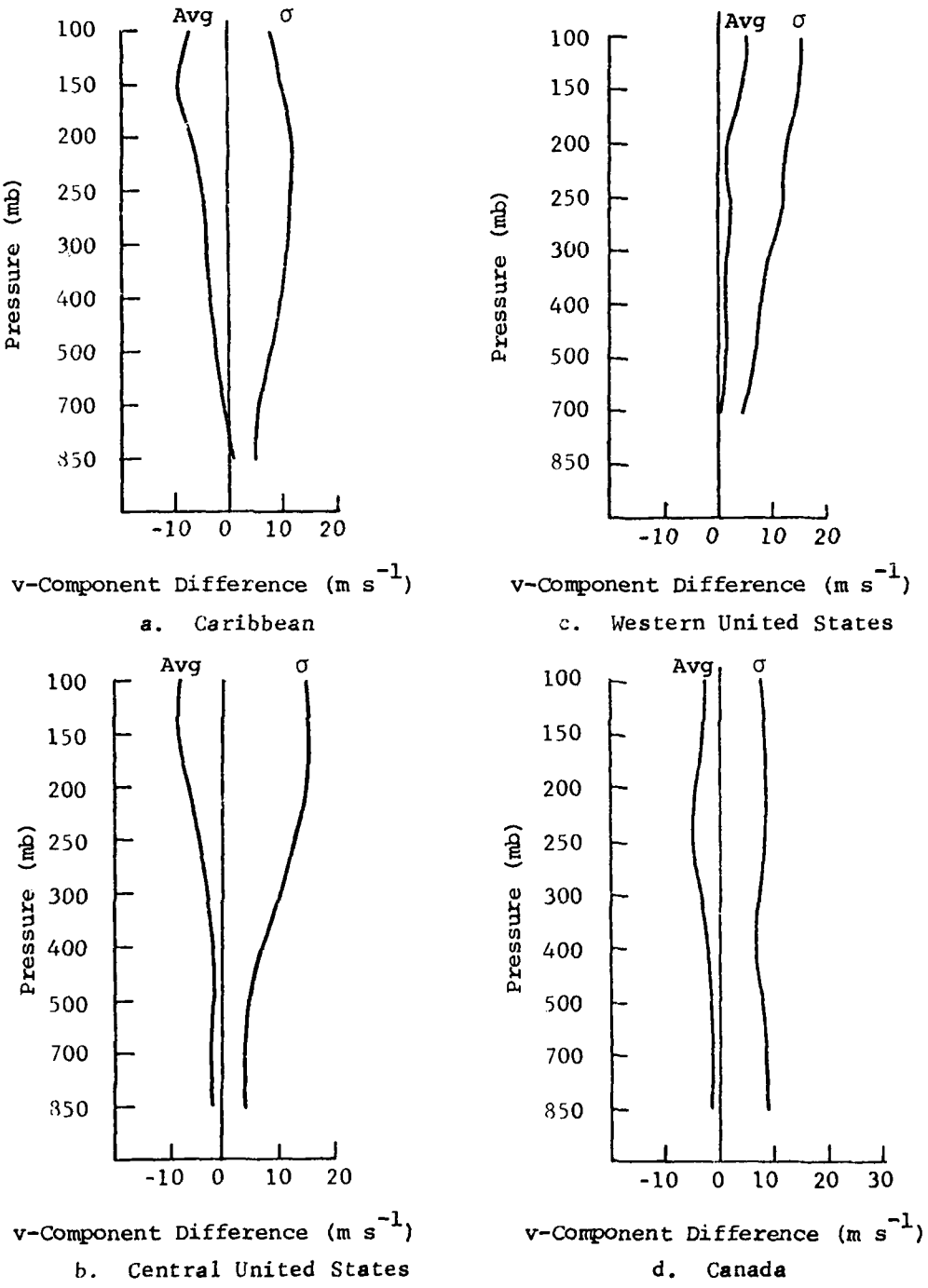

Fig. 12. Profiles of the average difference and standard deviation of the differences between satellite and rawinsonde geostrophic wind v-component (satellite values minus rawinsonde values) for four regions.

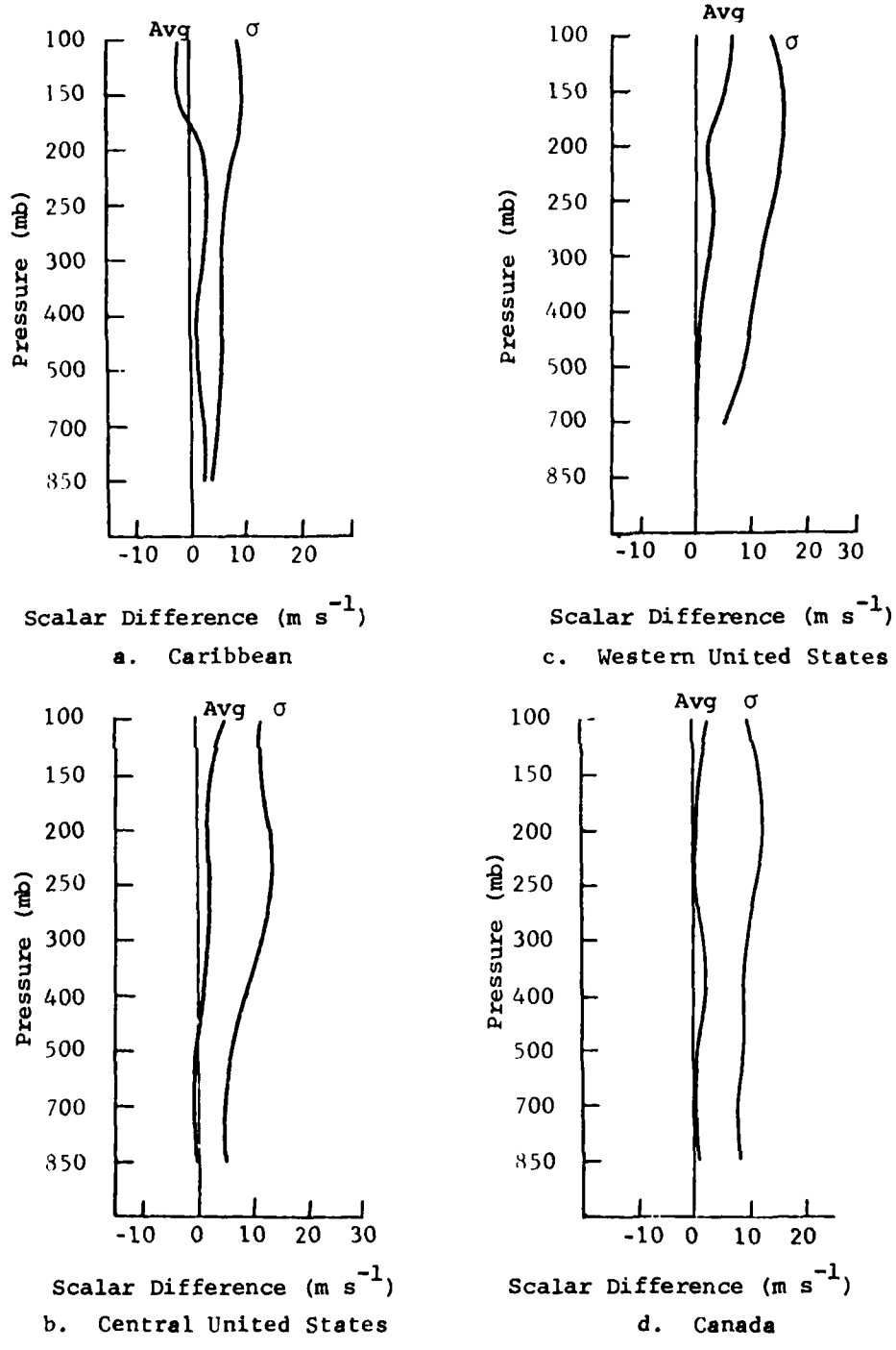

Fig. 13. Profiles of the average difference and standard deviation of the differences between satellite and rawinsonde geostrophic wind speeds (satellite values minus rawinsonde values) for four regions.

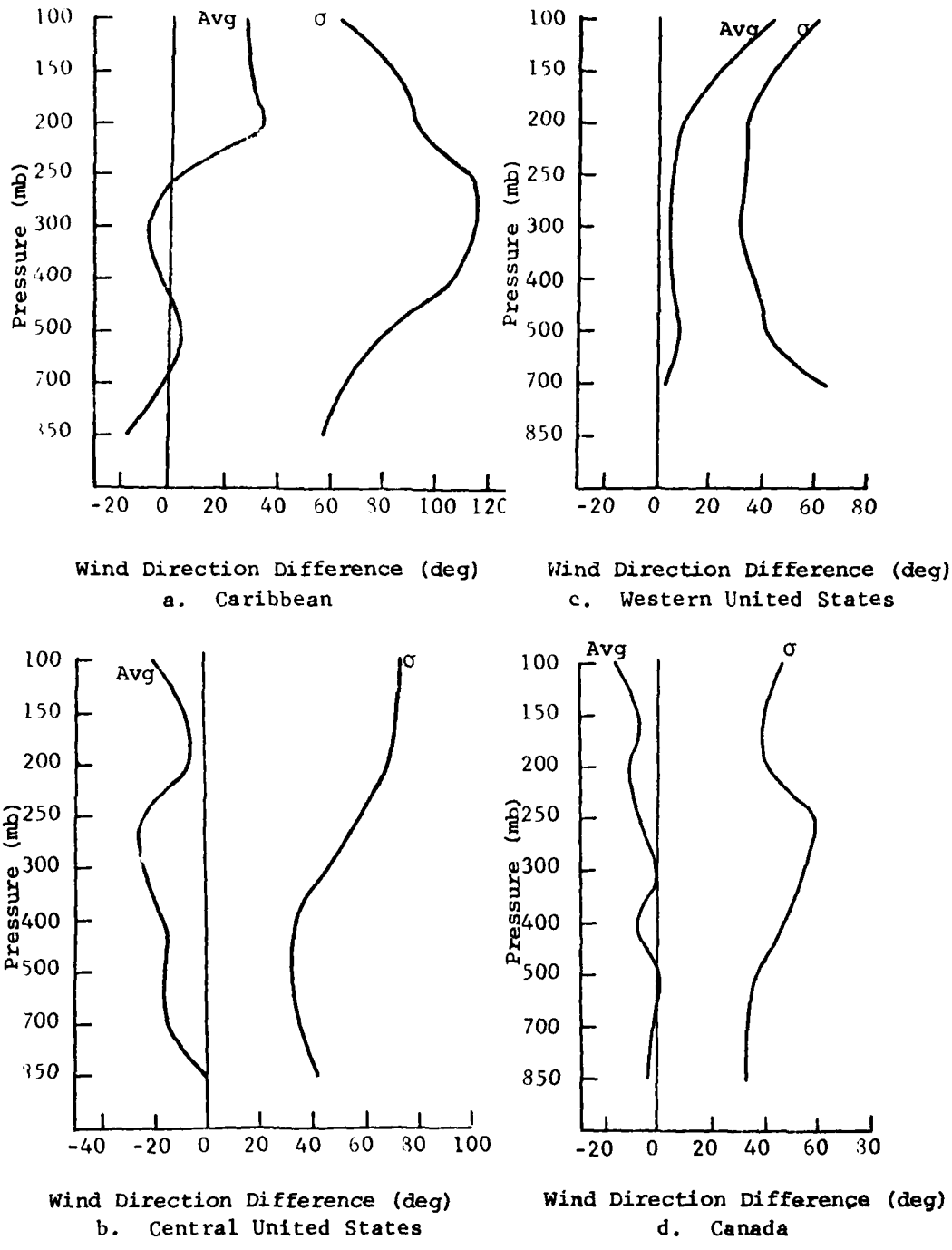

Fig. 14. Profiles of the average difference and standard deviation of the differences between satellite and rawinsonde geostrophic wind directions (satellite values minus rawinsonde values) for four regions.

4. Results from previous investigations

Other investigators have obtained similar profiles for differences between satellite and radiosonde data. Smith and Woolf (1974) used Nimbus-5 temperature soundings for comparison with radiosonde soundings along a line extending from approximately 60°S to 60°N near longitude 150°E. Since these data were put into cross-section form, other variables were computed and compared including horizontal gradient of temperature, geopotential height, and geostrophic wind. Waters et al. (1975) compared Nimbus-5 (Nimbus-E) Microwave Spectrometer soundings with radiosonde soundings at several locations, and obtained profiles of the RMS temperature deviation. The results of these studies are presented in Fig. 15, along with representative (central United States) profiles from the present study. A comparison of the previous results with results from this study indicates that the Nimbus-6 satellite data are slightly better than the Nimbus-5 data. This difference, however, depends on the synoptic conditions in the area of comparison.

b. Constant-pressure charts

1. Temperature-related variables

Fields of temperature at 850 and 500 mb for the Caribbean region are presented in Fig. 16. These show that the satellite temperature has very nearly the same magnitude as the rawinsonde temperature at both levels, with differences of approximately 1°C over most of the region. At 850 mb, the satellite values are slightly lower than the rawinsonde values, and there is only a vague agreement between the two patterns. At 500 mb, the satellite temperatures are slightly higher than rawinsonde temperatures, and both types of data show a weak thermal trough extending from the northwest in a southward direction toward the middle of the region. The temperature differences at the 850- and 500-mb levels should cause satellite lapse rates in the 850-500-mb layer to be too small, which corresponds to the value indicated at 700 mb in the difference profile of lapse rate (Fig. 6a). This value was computed from temperatures at 850 and 500 mb. There

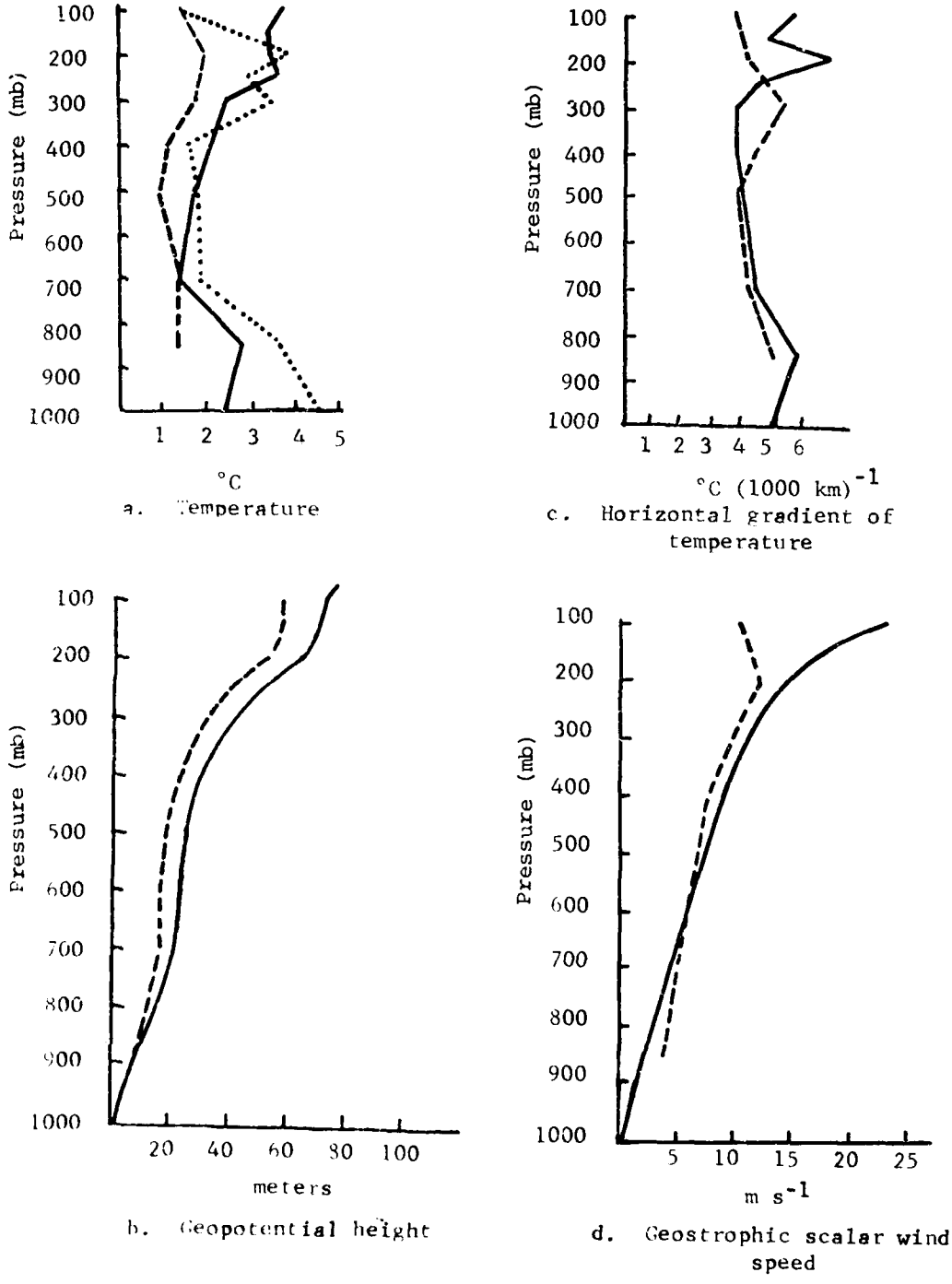

Fig. 15. Vertical profiles of standard deviations of differences between Nimbus satellite data and rawinsonde data. Solid lines are Nimbus-5 (Smith and Woolf, 1974); dashed lines are Nimbus-6 (this study). The dotted line on part (a) is from Waters et al. (1975).

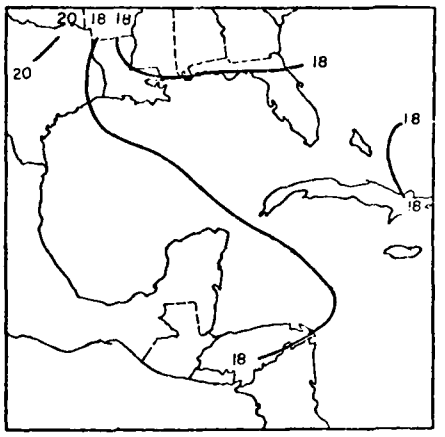

a. Rawinsonde (RW), 850 mb

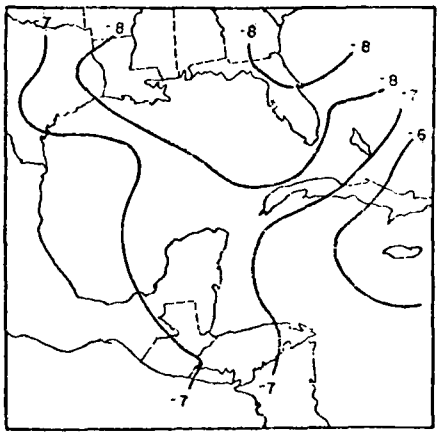

d. Rawinsonde (RW), 500 mb

b. Satellite (S), 850 mb

e. Satellite (S), 500 mb

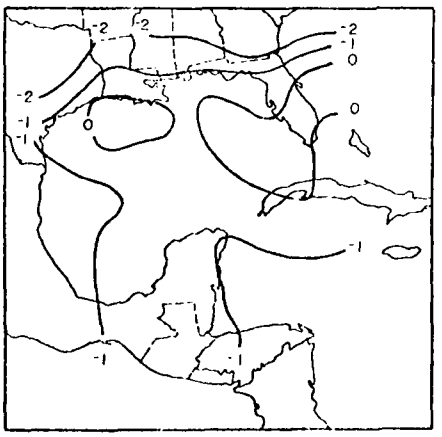

c. Differences (S-RW), 850 mb

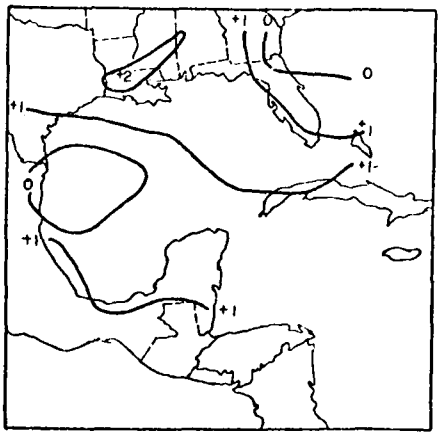

f. Differences (S-RW), 500 mb

Fig. 16. Charts of temperature and temperature difference (°C) at 850 and 500 mb over the Caribbean region.

is no obvious correspondence between the difference patterns and synoptic or cloud-related features.

Fields of temperature at the same two pressure levels for data in the central United States region are presented in Fig. 17. There is a surface front across the northwest portion of the region (see Fig. 2) that corresponds to the higher-than-average temperature gradient which is apparent in both types of data in that part of the region. Rawinsonde temperatures range from near 16°C just south of the front to near 8°C north of the front, while satellite temperatures range from near 16°C south of the front to near 6°C north of the front. This set of charts shows that, while temperature differences are largest just south of the front over Missouri at 850 mb (near 4°C), a reasonable correspondence exists between satellite and rawinsonde temperature data. The sign of the difference seems to be related to the location of the front, since positive differences are to the north and negative differences to the south of the front. This is in accordance with the horizontal smoothing in the satellite data, whereby each satellite datum represents an areal as well as a vertical average. In this region there seems to be a relation between negative temperature differences at 500 mb and clouds: the area centered over Iowa and the area of extreme northern Minnesota show negative differences, and there is medium-to-high cloudiness over those areas in the satellite picture. This correspondence is not evident in any of the other regions.

Temperature fields on constant-pressure surfaces for the western United States (Fig. 18) for the 850-mb level show a fairly strong temperature gradient from the middle of the region toward the northwest in the rawinsonde data, with warm pockets of 22°C and 24°C near the center of the region. The satellite data show a thermal trough oriented from northwest to southeast, with temperature gradients that are smaller in magnitude than those in the rawinsonde data. Differences are maximum (near 10°C) at the center of the satellite temperature trough, which is located to the south of the much straighter isotherms comprising the area of maximum gradient in the

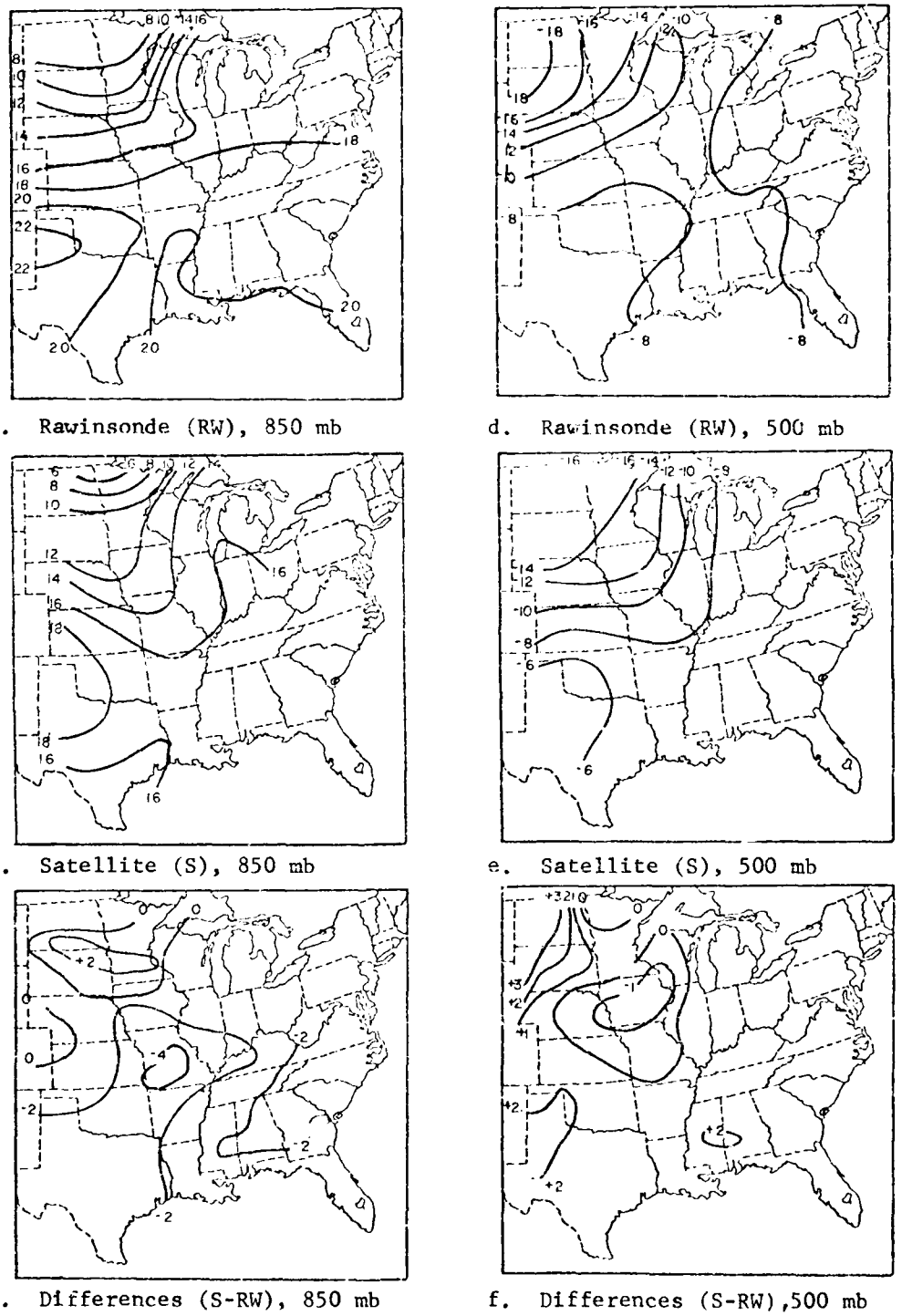

a. Rawinsonde (RW), 850 mb

d. Rawinsonde (RW), 500 mb

b. Satellite (S), 850 mb

e. Satellite (S), 500 mb

c. Differences (S-RW), 850 mb

f. Differences (S-RW),500 mb

Fig. 17. Charts of temperature and temperature difference (°C) at 850 and 500 mb over the central United States region.

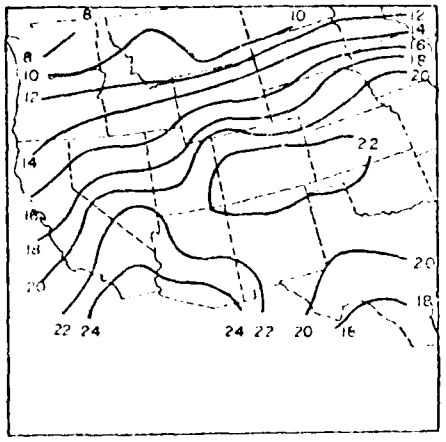

a. Rawinsonde (RW), 850 mb

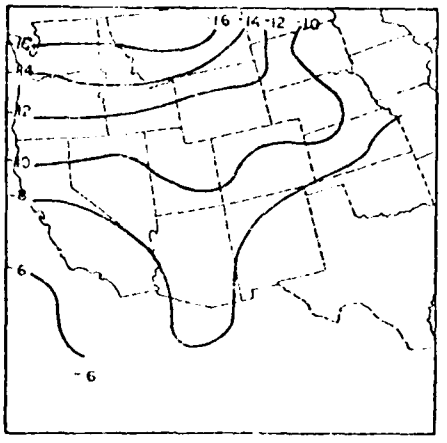

d. Rawinsonde (RW), 500 mb

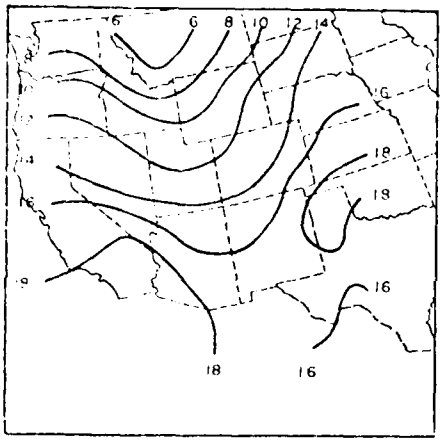

b. Satellite (S), 850 mb

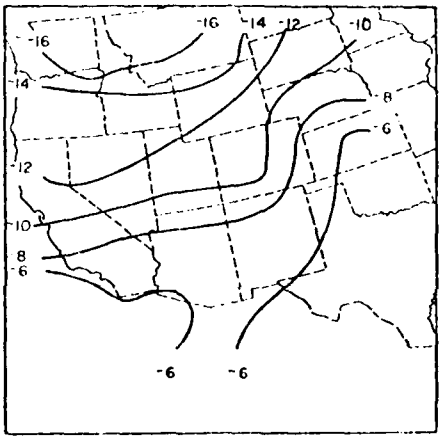

e. Satellite (S), 500 mb

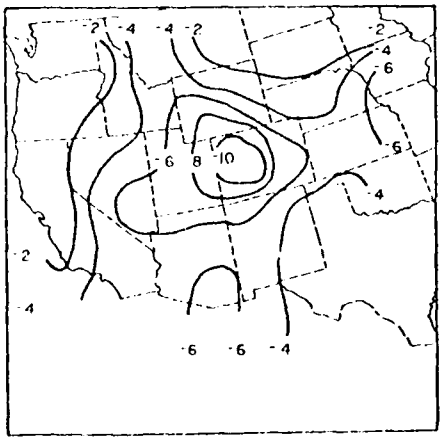

c. Differences (S-RW), 850 mb

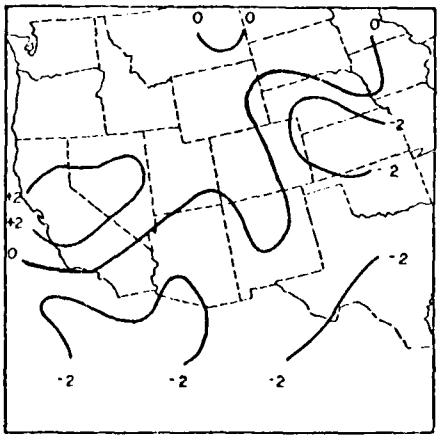

f. Differences (S-RW), 500 mb

Fig. 18. Charts of temperature and temperature difference (°C) at 850 and 500 mb over the western United States region.

rawinsonde data. Many of the mountains in this region reach above the 850-mb level, so that these large differences are probably associated with the gridding routine rather than with actual measurements.

The rawinsonde data also show a region of stronger thermal gradient at 500 mb in the northwest portion of the region, along with indications of a thermal trough through the middle of the region. Satellite data show this thermal trough to be fairly similar with gradients that are similar to those in rawinsonde data. Differences are small, with values of 2°C or less, and are positive in the southern part of the region.

Temperature charts at 850 and 500 mb for Canada are shown in Fig. 19. At 850 mb there is a region of strong packing of isotherms along the eastern boundary of the region associated with the surface front that is located just to the east (see Fig. 3). Gradient values west of the front are small except for a second area of isotherm packing toward the northwest. In the satellite data there is an indication of a cold trough behind the front that is also present in the rawinsonde data. Areas of largest difference in the chart of differences are near the northern edge of the region, where the satellite values are too low (negative differences).

At 500 mb there is a considerably weaker gradient behind the front than was present at 850 mb, particularly in rawinsonde data. Patterns indicated in satellite data are quite similar to those in rawinsonde data, and differences are fairly small throughout (less than 2°C).

In summary, the measurements of temperature obtained from satellite-observed radiances are accurate enough to depict fronts on constant-pressure charts, although the contrast in satellite temperatures across the front is less strong than that in rawinsonde temperatures. Satellite measurements tend to be somewhat smaller than rawinsonde measurements near the surface, and somewhat larger than rawinsonde measurements through the middle troposphere. These differences are not large enough to obliterate the temperature patterns on constant-pressure surfaces.

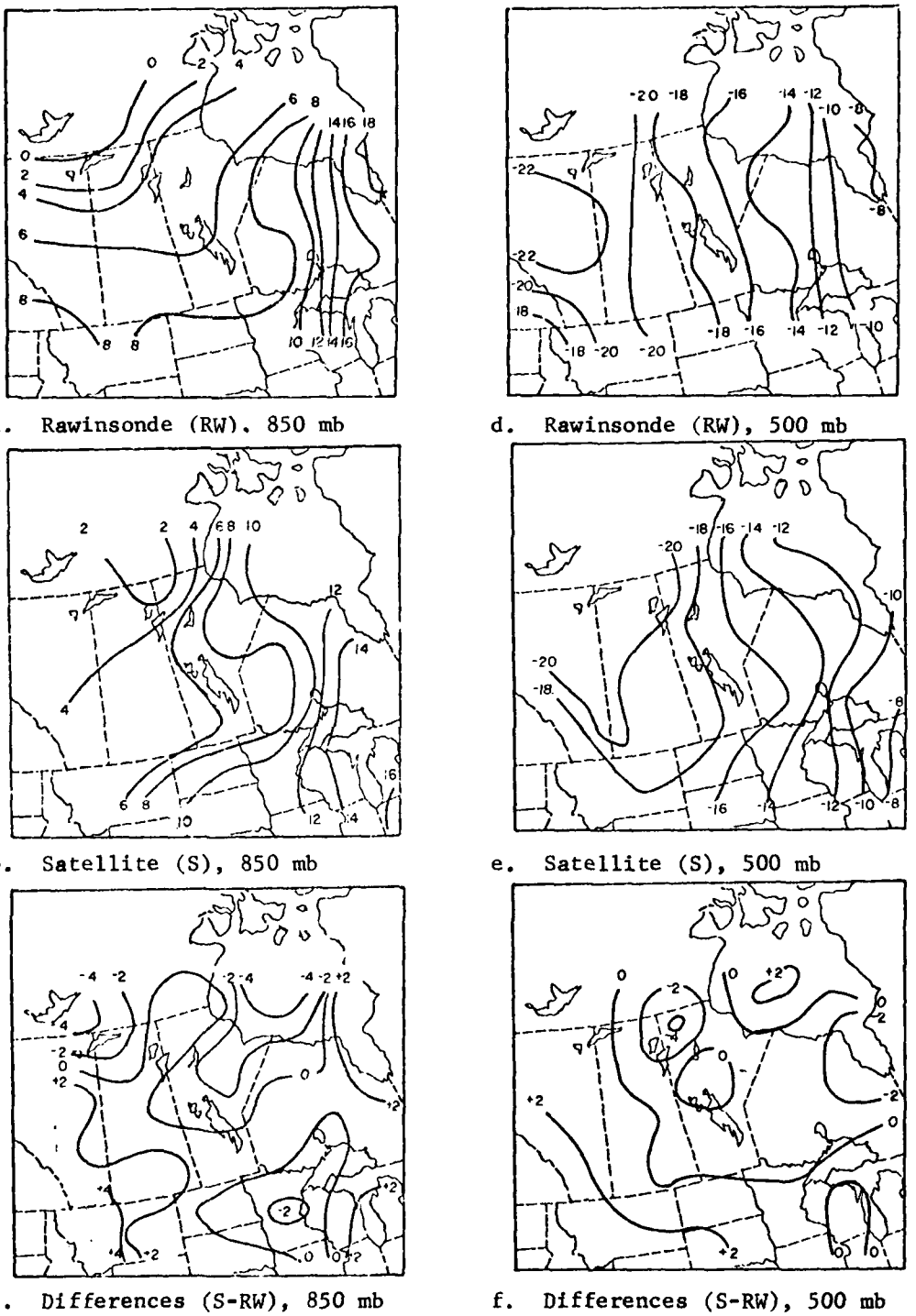

a. Rawinsonde (RW), 850 mb

d. Rawinsonde (RW), 500 mb

b. Satellite (S), 850 mb

e. Satellite (S), 500 mb

c. Differences (S-RW), 850 mb

f. Differences (S-RW), 500 mb

Fig. 19. Charts of temperature and temperature difference (°C) at 850 and 500 mb over the Canada region.

2. Moisture-related variables

The rawinsonde chart of dew-point temperature at 850 mb for the Caribbean region (Fig. 20) shows generally higher values toward the east, with dew points of near 15°C. These are associated with temperatures (see Fig. 16a) of near 18°C. The location of the area of highest dew point corresponds to that of a circular region of cloudiness in the 1630 GMT satellite picture. Both types of data indicate a general increase in dew point toward the east with smaller gradients in satellite data than in rawinsonde data. Satellite dew points are larger than rawinsonde dew points (positive differences) in a band extending from Texas to Central America, and smaller than rawinsonde dew points toward the northeast. Magnitudes of differences are generally less than 5°C.

Dew points for rawinsonde and for satellite data for the Caribbean region at 700 mb are also shown in Fig. 20. At this level, there is a dry area at the northern edge of the region over the United States with dew points of near -10°C. The air near the Mexican coast is shown to be fairly moist (values near 5°C), and a relative moisture minimum is indicated in the southeast corner of the region. The satellite data also show this relative minimum as well as the moisture increase to the west where values of 2.5°C and 5°C occur near the coasts of Mexico and Central America, respectively. The relative minimum over the United States and the relative maximum between Florida and the Yucatan peninsula are not indicated in the satellite data, thereby causing these to be areas of maximum difference at this level.

The chart of dew-point temperature at 500 mb for the Gulf of Mexico region is shown in Fig. 21. There is a region of dry air (-40°C dew point) located southwest of the Florida peninsula in the rawinsonde data, with highest values over the Texas coast and Mexico. In the satellite data, the region of moisture minimum is not present, although there is a general trend toward higher moisture content toward the western boundary of the region. Satellite dew points are quite

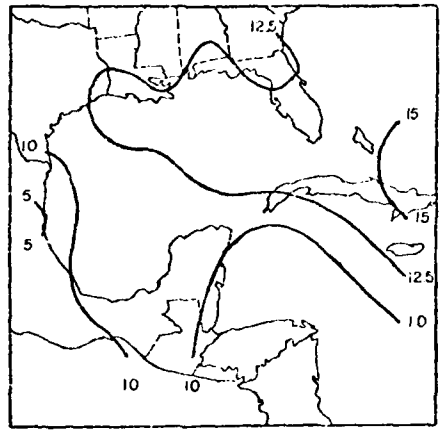

a. Rawinsonde (RW), 850 mb

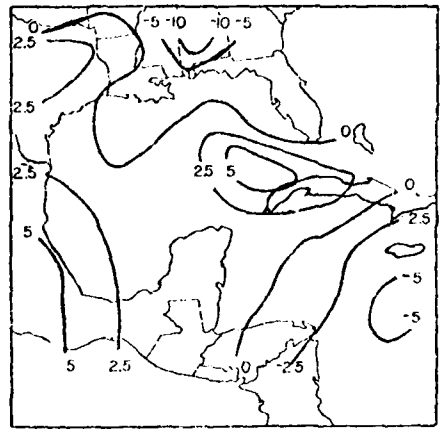

d. Rawinsonde (RW), 700 mb

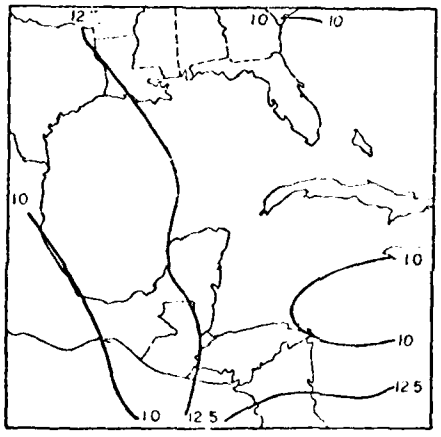

b. Satellite (S), 850 mb

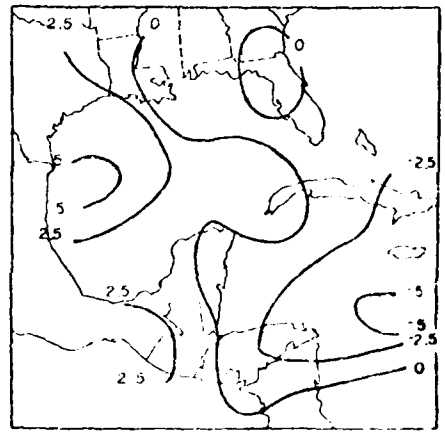

e. Satellite (S), 700 mb

c. Differences (S-RW), 850 mb

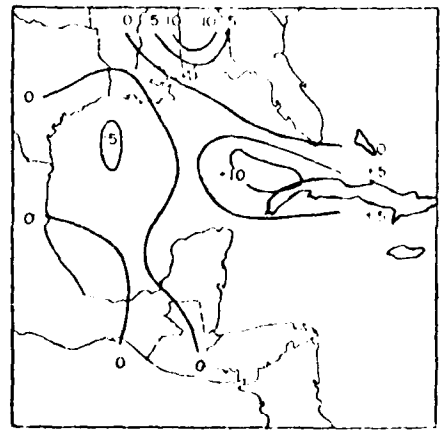

f. Differences (S-RW), 700 mb

Fig. 20. Charts of dew-point temperature and dew point difference (°C) at 850 and 700 mb over the Caribbean region.

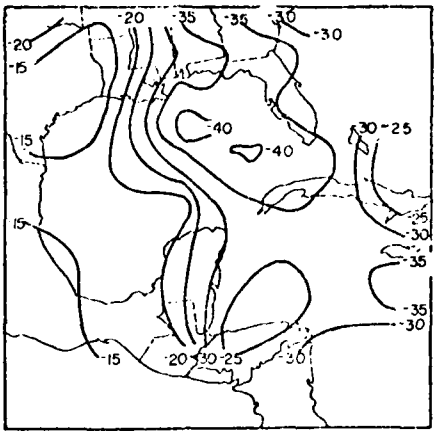

a. Rawinsonde (RW), 500 mb

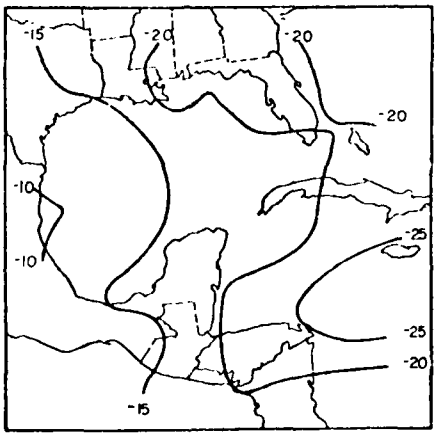

b. Satellite (S), 500 mb

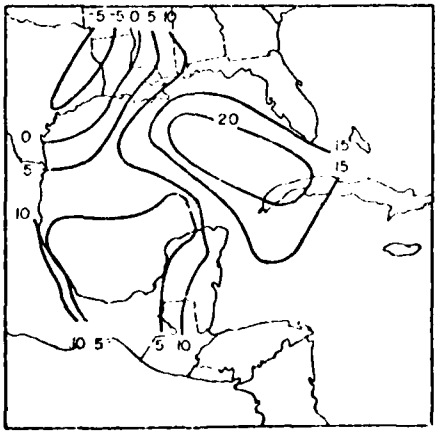

c. Differences (S-RW), 500 mb

Fig. 21. Charts of dew-point temperature and dew point difference (°C) at 500 mb over the Caribbean region.

smoothed and generally too high relative to rawinsonde values at this level. Large differences are indicated southwest of Florida with smaller differences (less than 10°C) elsewhere. The area southwest of Florida, where the rawinsonde indicates very dry conditions and the satellite does not, causes the vertical profile of average differences for dew point in this region (Fig. 8a) to show maximum values at this level.

A chart showing the dew-point temperature over the central United States at 850 mb is shown in Fig. 22. This shows the contrast in moisture across the front in this region with typical values of 10°C to 15°C south of the front, and values of 0°C or less north of the front. The satellite data are consistent with the rawinsonde data in terms of the general pattern, with indications of moist air south of the front and dry air north of the front (values of 10-12°C and 4-6°C, respectively). The gradients in dew point in the satellite data at this level are not sufficient to provide a precise indication of the frontal position. On the other hand, the front can be located fairly easily in the rawinsonde data since the gradient is quite strong in a band from Michigan to Colorado. Differences (Fig. 22c) are generally between 0°C and 5°C, although values of 10°C occur just behind the front. As with temperature, the front marks a line separating positive differences to the north from negative differences to the south.

The dew-point temperature map for rawinsonde data at 500 mb in the central United States region, also presented in Fig. 22, shows many areas of strong gradient of moisture content which are not present in the satellite data. Maximum differences are located parallel to and just south of the front with values reaching 10°C. These differences do not correspond with cloudiness.

For the western United States region, dew-point temperature charts for the 850- and 700-mb levels are shown in Fig. 23. There is a region of strong gradient at 850 mb along a line from Nebraska to Arizona, with more moisture indicated to the south and less moisture indicated to the north. Satellite dew-point temperatures are somewhat higher than those in rawinsonde data, but a similar though

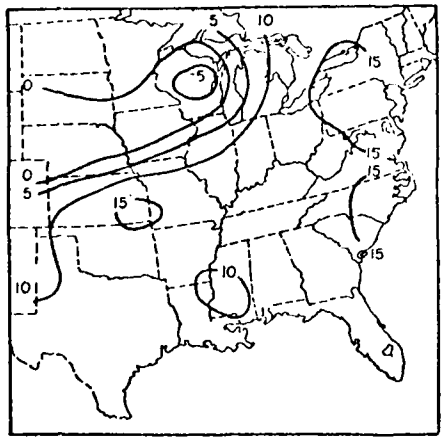

a. Rawinsonde (RW), 850 mb

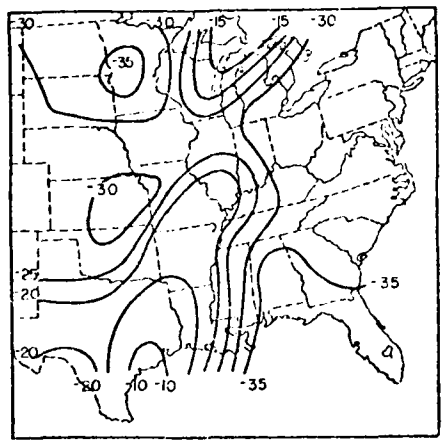

d. Rawinsonde (RW), 500 mb

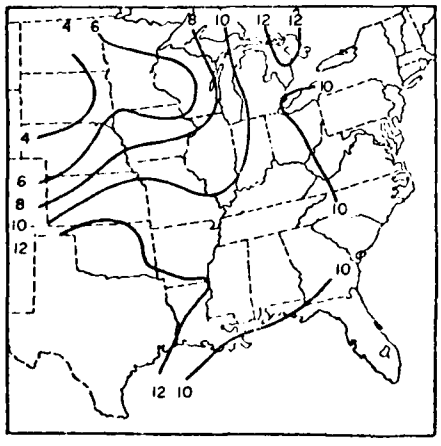

b. Satellite (S), 850 mb

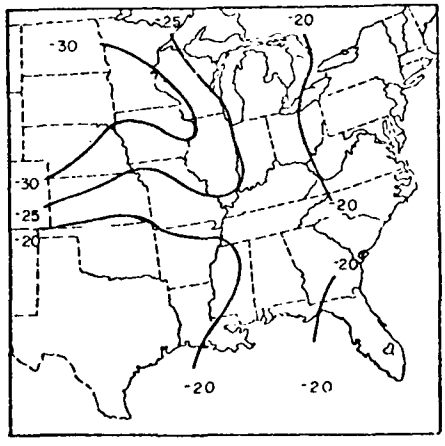

e. Satellite (S), 500 mb

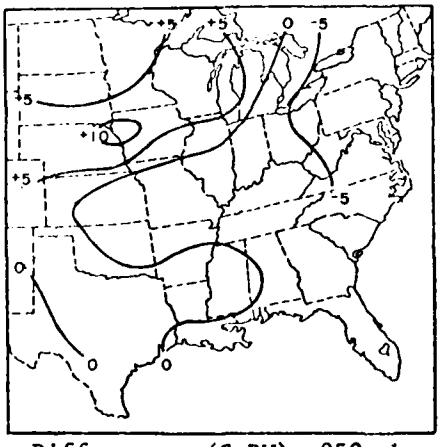

c. Differences (S-RW), 850 mb

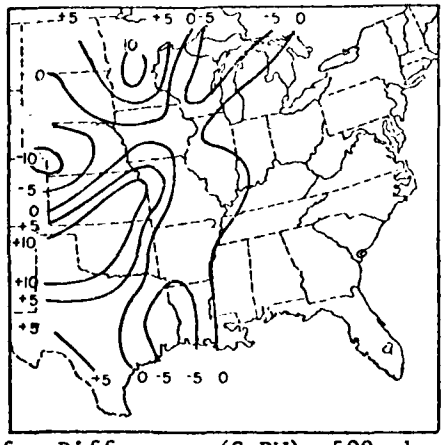

f. Difference (S-RW), 500 mb

Fig. 22. Charts of dew-point temperature and dew point difference (°C) at 850 and 500 mb over the central United States region.

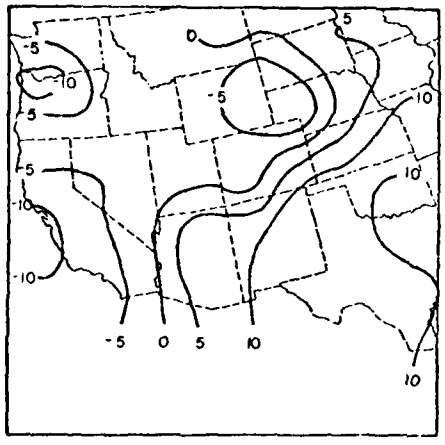

a. Rawinsonde (RW), 850 mb

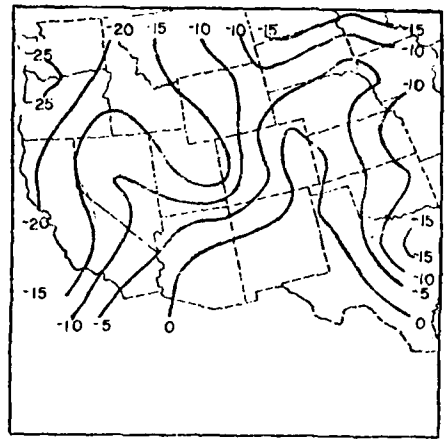

d. Rawinsonde (RW), 700 mb

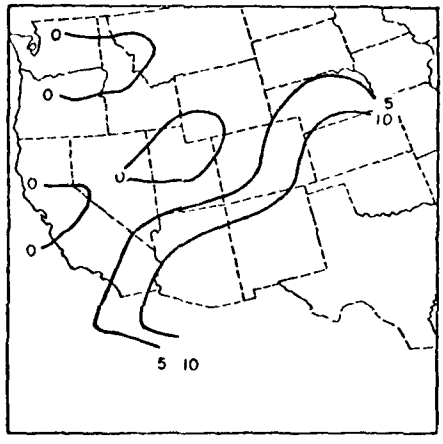

b. Satellite (S), 850 mb

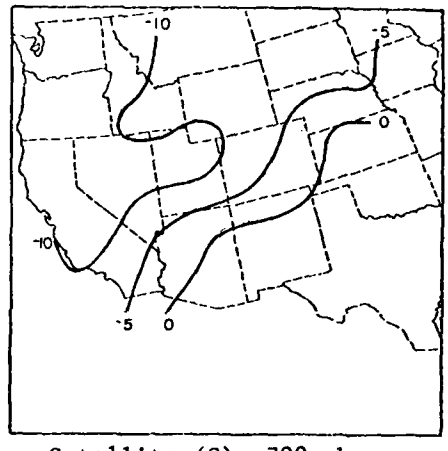

e. Satellite (S), 700 mb

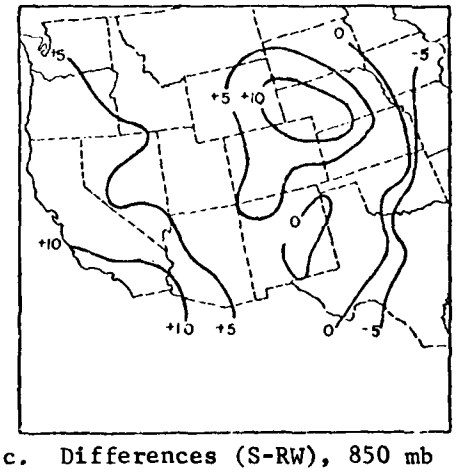

c. Differences (S-RW), 850 mb

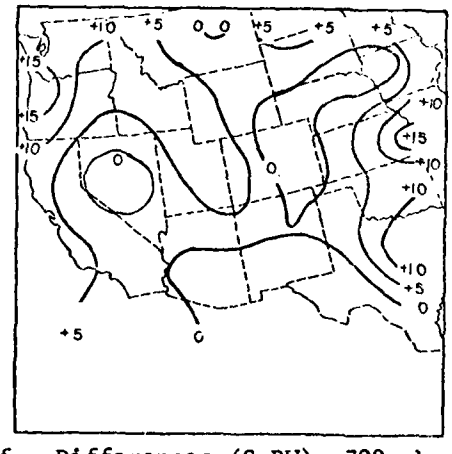

f. Differences (S-RW), 700 mb

Fig. 23. Charts of dew-point temperature and dew point difference (°C) at 850 and 700 mb over the western United States region.

somewhat smoothed line of higher gradient is present. This line is characteristic of a front, and while no front is depicted on the National Weather Service charts for this region, there seem to be indications of the presence of one. The altitude of the mountains affects the gridding of the data at this level.

There are similar lines of strong gradient at 700 mb in both the rawinsonde and satellite data, but the satellite pattern is considerably smoothed compared to the rawinsonde pattern. Differences (Fig. 23f) are generally positive and exhibit almost a random pattern.

The dew-point chart for 500 mb (Fig. 24) shows a band of moisture maxima through the middle of the region. Values to the northwest are lower (less moisture) than those to the southeast. In the satellite data, although the gradient is smaller, the "frontal band" is also well indicated. Differences are positive over the major portion of the region and show only a vague alignment with the "front."

The presence of front-like bands of concentrated gradient in the rawinsonde and satellite data for this region offers an explanation for the similarity experienced in most variables between the vertical difference profiles for the western and central United States regions. If both contain contrasts between similar air masses, then the difference patterns and magnitudes for the two regions would be expected to be similar.

The dew-point temperature charts for Canada are shown in Fig. 25 for the 850- and 700-mb levels. The dew-point patterns in the rawinsonde data at these levels do not seem to correspond well with the front that is located along the eastern edge of the region (see Fig. 3). This is due in part to the close proximity of the front to the edge of the region. Differences at 700 mb (Fig. 25f) are negative through most of the region, and at 850 mb (Fig. 25c) are positive in the center of the region and large and negative in the southwest corner. The signs of the average differences at these levels (see Fig. 8) are opposite to those in the United States regions due to the different moisture content that is characteristic of the polar air mass.

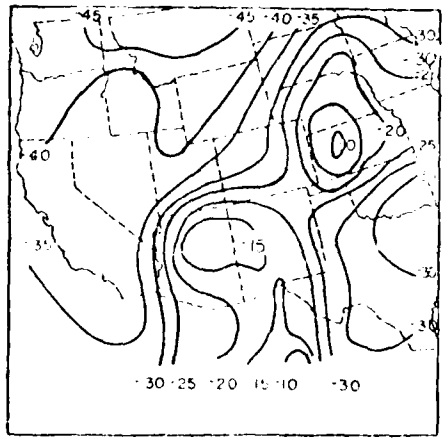

a. Rawinsonde (RW), 500 mb

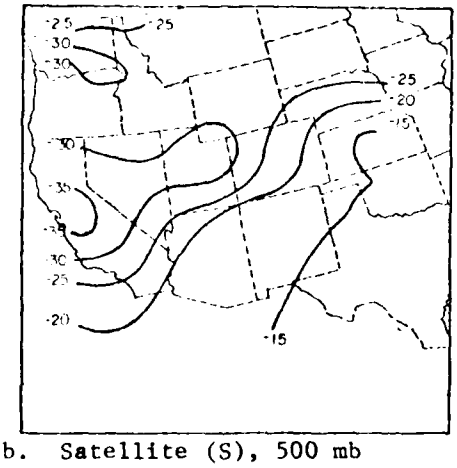

b. Satellite (S), 500 mb

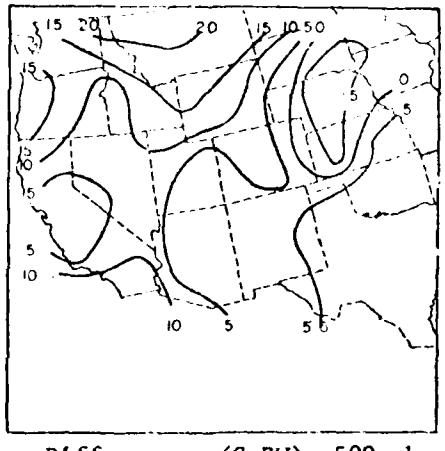

c. Differences (S-RW), 500 mb

Fig. 24. Charts of dew-point temperature and dew point difference (°C) at 500 mb over the western United States region.

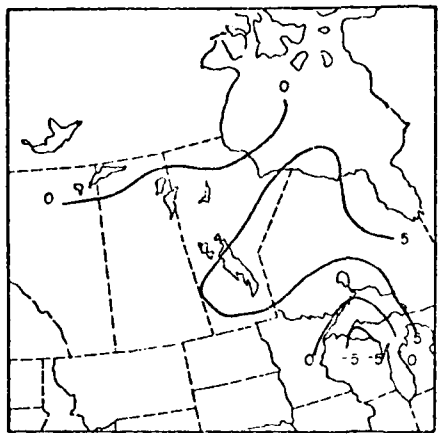

a. Rawinsonde (RW), 850 mb

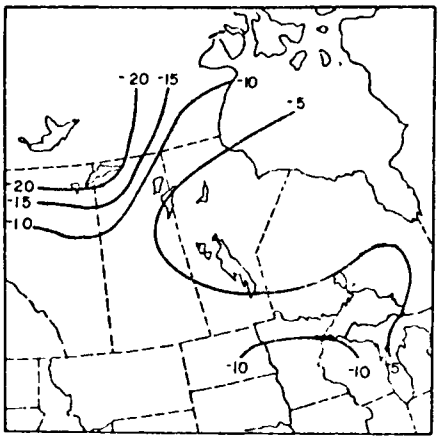

d. Rawinsonde (RW), 700

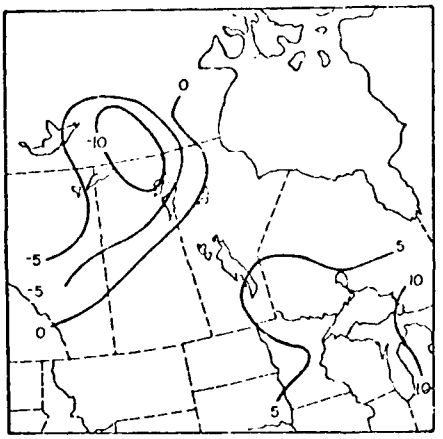

b. Satellite (S), 850 mb

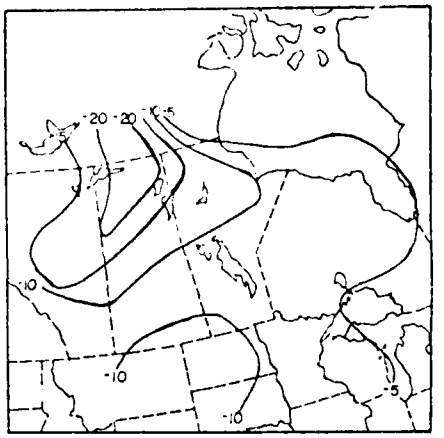

e. Satellite (S), 700 mb

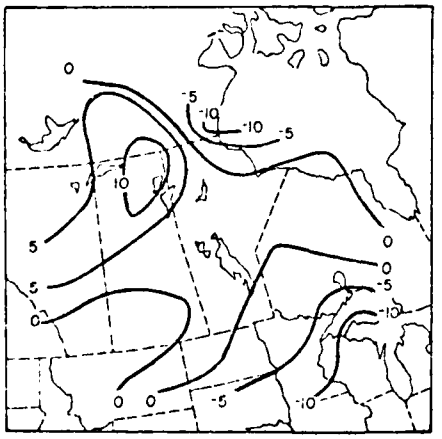

c. Differences (S-RW), 850 mb

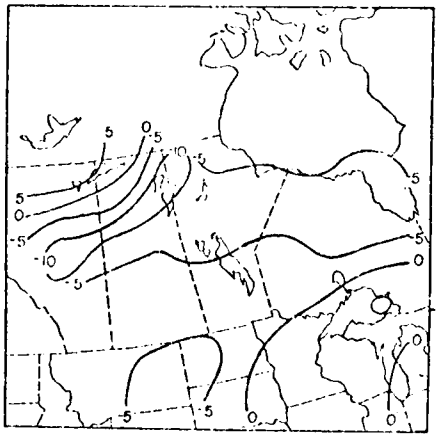

f. Differences (S-RW), 700 mb

Fig. 25. Charts of dew-point temperature and dew point difference (°C) at 850 and 700 mb over the Canada region.

3. Geopotential height and wind

In this study, fields of geostrophic wind were derived from both the rawinsonde and the satellite geopotential heights. These winds are shown in the form of wind barbs plotted on charts with geopotential height contours for each region. Also shown are wind barbs for the observed wind, plotted at the same points as the geostrophic wind. This provides a comparison of the differences between the observed and geostrophic wind fields in each region.

The geopotential height and wind fields at 500 mb for the Caribbean region are shown in Fig. 26. The main feature is the small magnitude of the height gradient associated with the fairly weak anticyclonic flow over the whole region. The 500-mb satellite-derived height field shows the same low gradient values and nearly the same values of geopotential height, with a pattern that is similar to that in rawinsonde data. Differences are small with the maximum difference being no larger than 20 m. The geostrophic wind fields do not agree well with the observed wind field in either rawinsonde or satellite data. The scalar wind speeds are close to those for the observed wind, but the directions are quite different at many points. For small values of wind speed, small changes in height gradient will cause large changes in the direction of the geostrophic wind, so that large differences in the wind direction may be expected in a situation of weak flow such as this. This effect was also seen in the vertical difference profiles for wind direction discussed in the previous section. The observed wind depicts the anticyclonic flow around the high-pressure center in the western Atlantic.

The 500-mb geopotential height and associated wind fields for the central United States region are shown in Fig. 27. Rawinsonde data in this region show the southern portions of the cyclonic system from which the front extends, while the satellite data show a pattern that is similar but somewhat less organized. Difference magnitudes are somewhat larger than those in the Caribbean. The

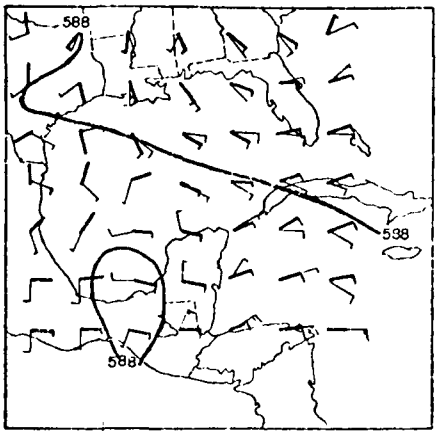

a. Rawinsonde (RW)

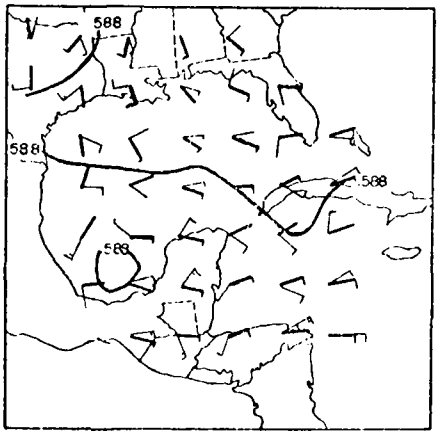

b. Satellite (S)

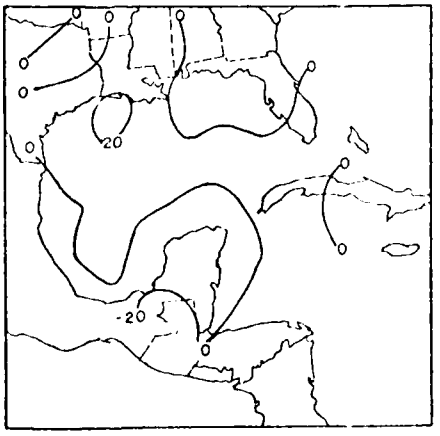

c. Difference (S-RW)

Fig. 26. Charts of geopotential height (m/10) with wind barbs for geostrophic (thin line) and observed (thick line) wind (m s^{-1}) at 500 mb over the Caribbean region.

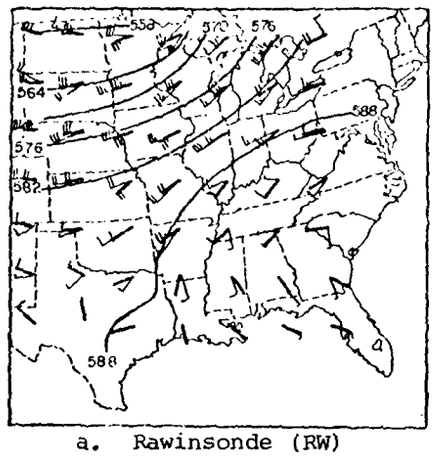

a. Rawinsonde (RW)

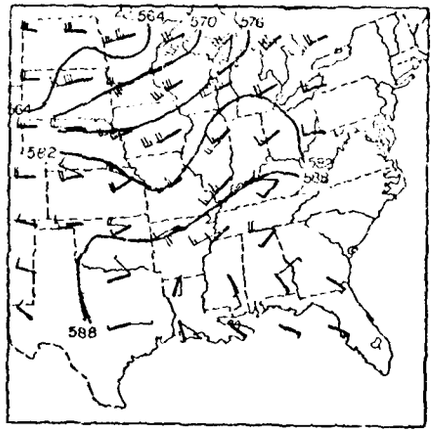

b. Satellite (S)

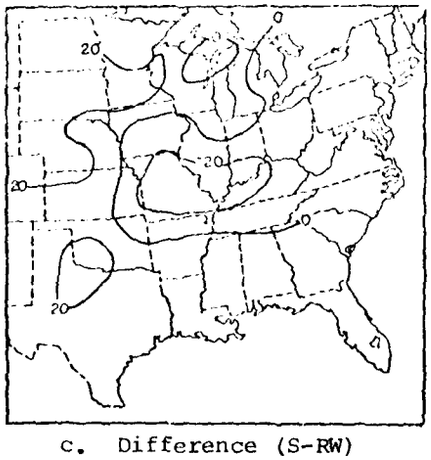

c. Difference (S-RW)

Fig. 27. Charts of geopotential height (m/10) with wind barbs for geostrophic (thin line) and observed (thick line) wind (m s^{-1}) at 500 mb over the central United States region.

front generally divides negative height differences to the south from positive height differences to the north, corresponding to the relationship of the temperature differences to the front (Fig. 17). The observed wind field shows the cyclonic flow through most of the region, along with the anticyclonic flow in the southeast corner that is associated with the high-pressure cell in the Atlantic that is influencing the atmosphere over the Gulf of Mexico and the southeast United States. The rawinsonde and satellite geostrophic wind fields show reasonable similarity in both speed and direction.

The geopotential height and wind fields for the western United States are shown in Fig. 28. There is an area of slightly stronger-than-average height gradient in both types of data along the northern edge of the region, with smaller gradient values elsewhere. The satellite and rawinsonde patterns are similar, but differences become fairly large (80 m) at the western edge of the region. Elsewhere, differences are generally less than 20 m and the average difference is approximately 26 m. In this region also, the geostrophic wind represents a good approximation to the observed wind.

In Canada, the fields of geopotential height and wind at 500 mb (Fig. 29) show that the satellite and rawinsonde geopotential height fields are somewhat different. The low-pressure trough in the rawinsonde data is located over the north-central portion of the region, while in the satellite data the same trough is located more to the southeast. Differences exceed 40 m in places, and one of the areas of largest difference is associated with the displacement of the low-pressure trough in the satellite data. The geostrophic wind fields from satellite and rawinsonde heights are fairly similar, except in the area to the west of the satellite pressure trough.

On these synoptic-scale constant-pressure charts, the geostrophic wind fields from the rawinsonde and satellite data agree fairly closely, and each deviates from the observed wind to approximately the same extent.

4. Results from previous investigations

In a recent study (Peterson and Horn, 1977), the 500-mb geopotential height and geostrophic wind fields from rawinsonde and Nimbus-6

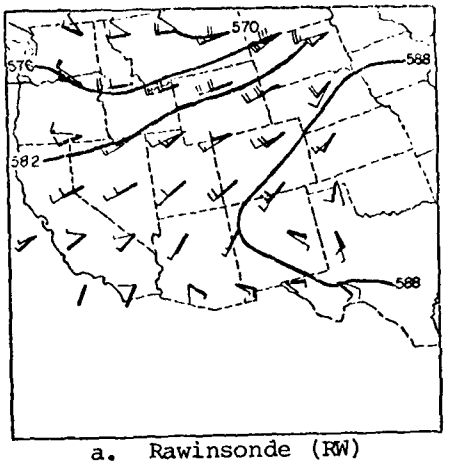

a. Rawinsonde (RW)

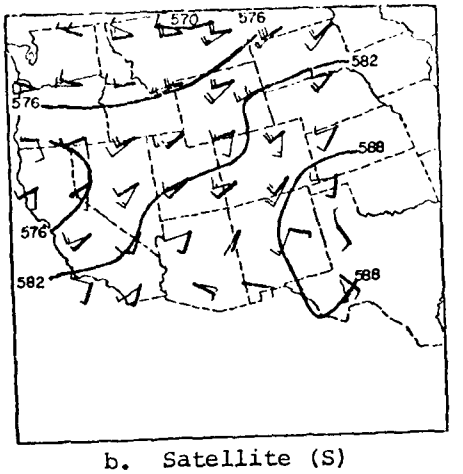

b. Satellite (S)

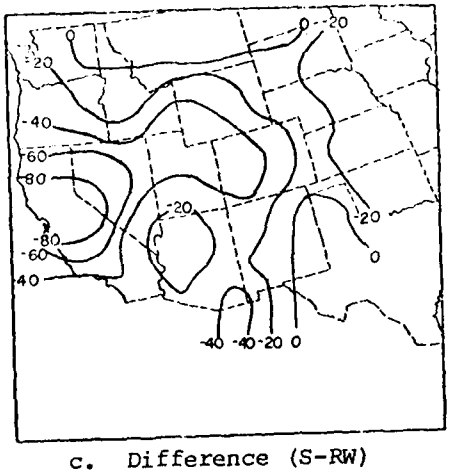

c. Difference (S-RW)

Fig. 28. Charts of geopotential height (m/10) with wind barbs for geostrophic (thin line) and observed (thick line) wind (m s^{-1}) at 500 mb over the western United States region.

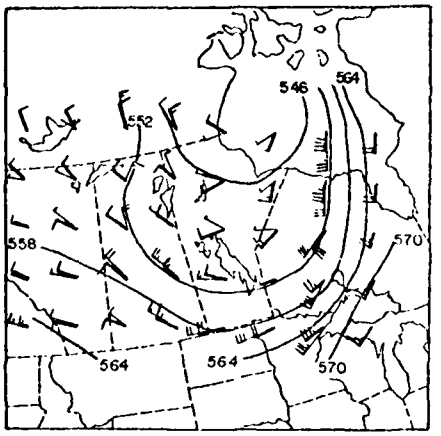

a. Rawinsonde (RW)

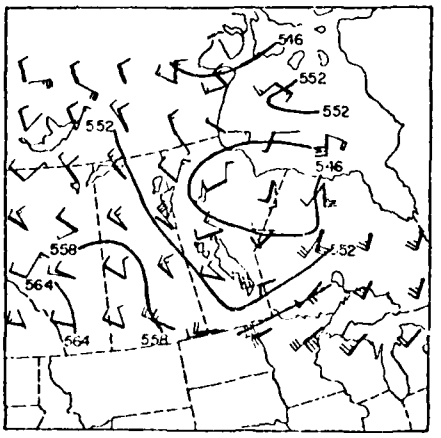

b. Satellite (S)

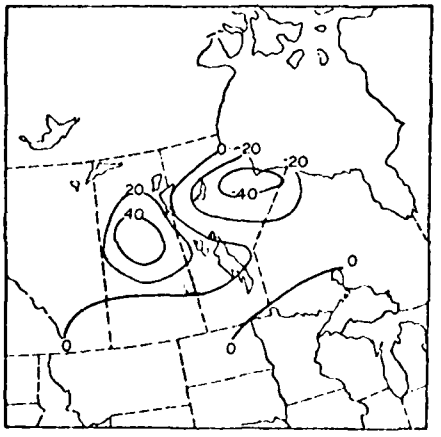

c. Difference (S-RW)

Fig. 29. Charts of geopotential height (m/10) with wind barbs for geostrophic (thin line) and observed (thick line) wind (m s^{-1}) at 500 mb over the Canada region.

satellite data were computed and compared. The data were taken over the eastern and central parts of the United States, and a procedure similar to the one used in this study was used, in that the data were gridded and comparisons were based on grid-point values. The time is approximately 1 week earlier than that selected for the present study, so that results should be fairly similar. Table 2 shows results for the Peterson and Horn study in the upper three rows, and

Table 2. Comparison of results for 500-mb geopotential height between Peterson and Horn (1977) and the present study.

		Nimbus-6 minus RAOB (12 GMT)		Nimbus-6 minus RAOB (00 GMT)		Nimbus-6 minus RAOB (avg)	
		avg	std. dev.	avg	std. dev.	avg	std. dev.
Peterson and Horn (1977)	8/18/75	-2.8*	24.5	-11.9	22.4	-	-
	8/19/75	-2.1	26.3	-14.0	28.0	-	-
	8/20/75	8.8	24.8	-15.2	30.1	-	-
This study	Caribbean	-	-	-	-	-1	10
	Central U.S.	-	-	-	-	-2	18
	Western U.S.	-	-	-	-	-28	26
	Canada	-	-	-	-	-4	24

*Units are m.

for the present study in the lower four rows. Since comparisons were made with each rawinsonde time individually in the former and with time-averaged rawinsonde data in the latter, the results can be compared only on a qualitative basis. There is little difference between values of standard deviation of differences, with both studies showing values of near 25 m. Table 3 shows a similar comparison for geostrophic scalar wind speed, where the values from Peterson and Horn are somewhat lower than those for this study. This may be due to slight differences in the analysis procedures. Both studies seem to indicate that the satellite is capable of producing wind

fields that are fairly reasonable in terms of comparisons with rawinsonde fields.

Table 3. Comparison of results for 500-mb geostrophic scalar wind speed between Peterson and Horn (1977) and the present study.

	Nimbus-6 minus RW (12 GMT)		Nimbus-6 minus RW (00 GMT)		Nimbus-6 minus RW (avg)	
	avg	std. dev.	avg	std. dev.	avg	std. dev.
8/18/75	-1.0*	3.5	-0.7	3.8	-	-
8/19/75	-0.4	3.5	-2.2	5.0	-	-
8/20/75	-0.4	3.7	-0.1	3.9	-	-
Caribbean	-	-	-	-	3	5.5
Central U.S.	-	-	-	-	-0.5	7
Western U.S.	-	-	-	-	0	9
Canada	-	-	-	-	0.5	8

*Units are m s^{-1}.

c. Cross sections

The locations of the cross sections for the four regions used in this study are illustrated in Figs. 1 through 4. Each figure of cross sections presented contains three parts: 1) a cross section derived from rawinsonde data; 2) a cross section derived from satellite data; and 3) a cross section of differences expressed as satellite values minus rawinsonde values. As in the case of the vertical difference profiles and the constant-pressure charts, positive differences indicate that satellite values are higher than rawinsonde values. In some cases, the patterns evident in the cross sections of differences have an obvious relation to the synoptic conditions or some other feature of the region involved. In many other cases, however, there is no obvious relation between the difference patterns and any characteristic of the atmosphere or surface of the particular region.

1. Temperature-related variables

The flatness of the temperature field in the Caribbean region is perhaps better illustrated in the cross section of temperature for the region (Fig. 30) than in the constant-pressure charts for temperature shown previously.

Noteworthy in this cross section is the difference in indicated height of the tropopause, with the satellite data indicating a somewhat lower altitude than the rawinsonde data in the northern part of the section. This is probably an effect of vertical smoothing in the satellite data. Quantitative differences are quite small through most of the section, with negative values predominating in the lowest layers and positive values aloft. The presence of relatively large differences near the tropopause is no longer unexpected. There are no other obvious patterns in the difference section.

The cross section of temperature for the central United States region (Fig. 31) shows the front in the northern part of the section to be relatively weak in terms of temperature contrast in the rawinsonde data, and weaker in the satellite data. This makes the front difficult to locate in the satellite cross section, but neither type of data locates the front except as being somewhere in a broad zone of baroclinity. In this region only, the front was located by use of individual rawinsonde soundings, and the frontal position so obtained was also used with the satellite data. In the other regions, structural features were diagnosed from rawinsonde and satellite data independently. One feature of the difference cross section is the presence of negative differences through most of the troposphere in the air south of the front. A layer of positive differences (satellite too high) is present just under the tropopause in both air masses, as a result of the vertical smoothing.

The temperature cross section for Canada (Fig. 32) traverses a segment of the same polar front as in the central United States but is located farther north and is, therefore, closer to the low-pressure center. The region of baroclinity near the center of the section indicates the frontal position with equal definition in both

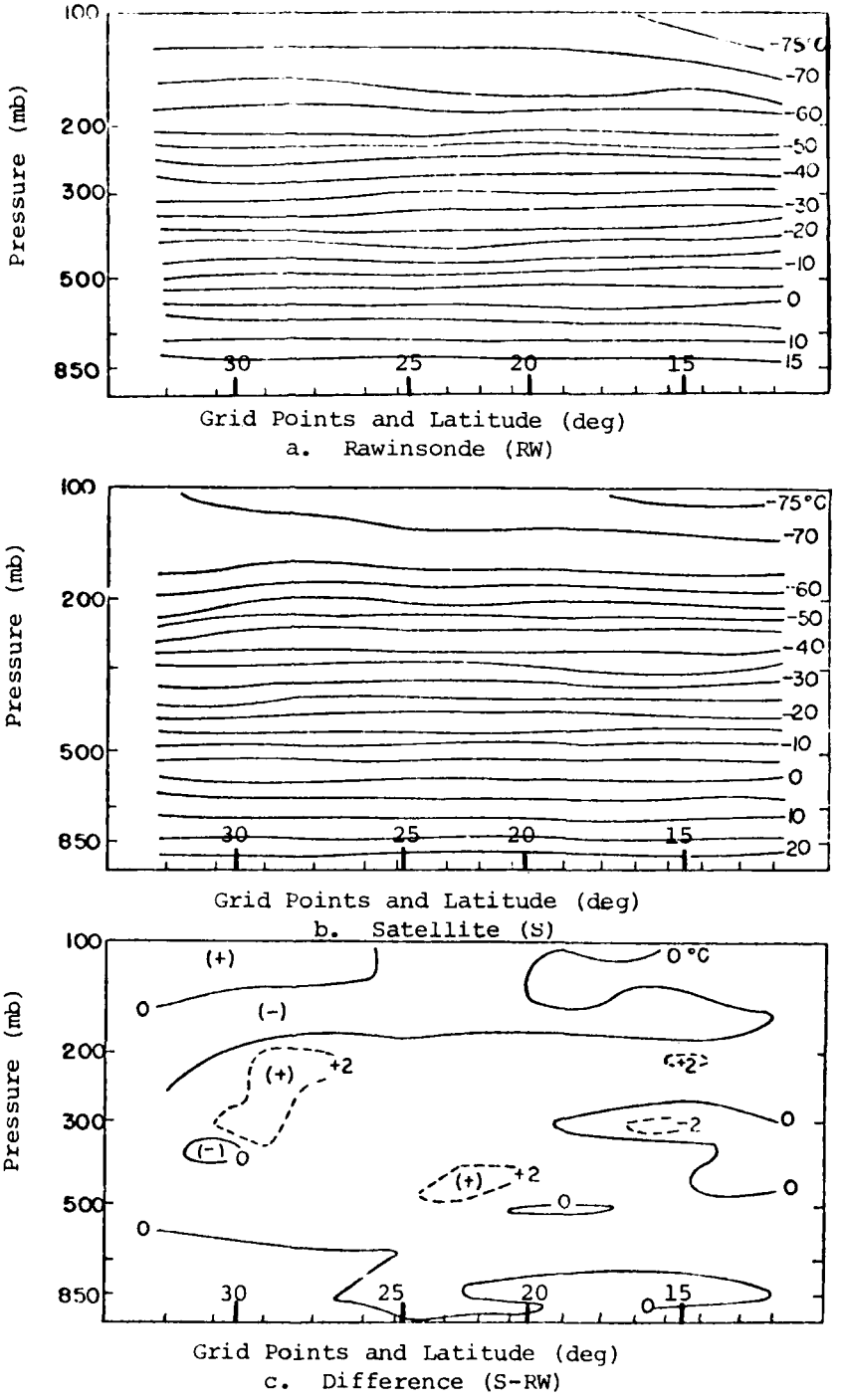

Fig. 30. Cross sections of temperature and temperature difference (°C) for the Caribbean region on 25 August 1975 at 1700 GMT. (See Fig. 1 for path of cross sections.)

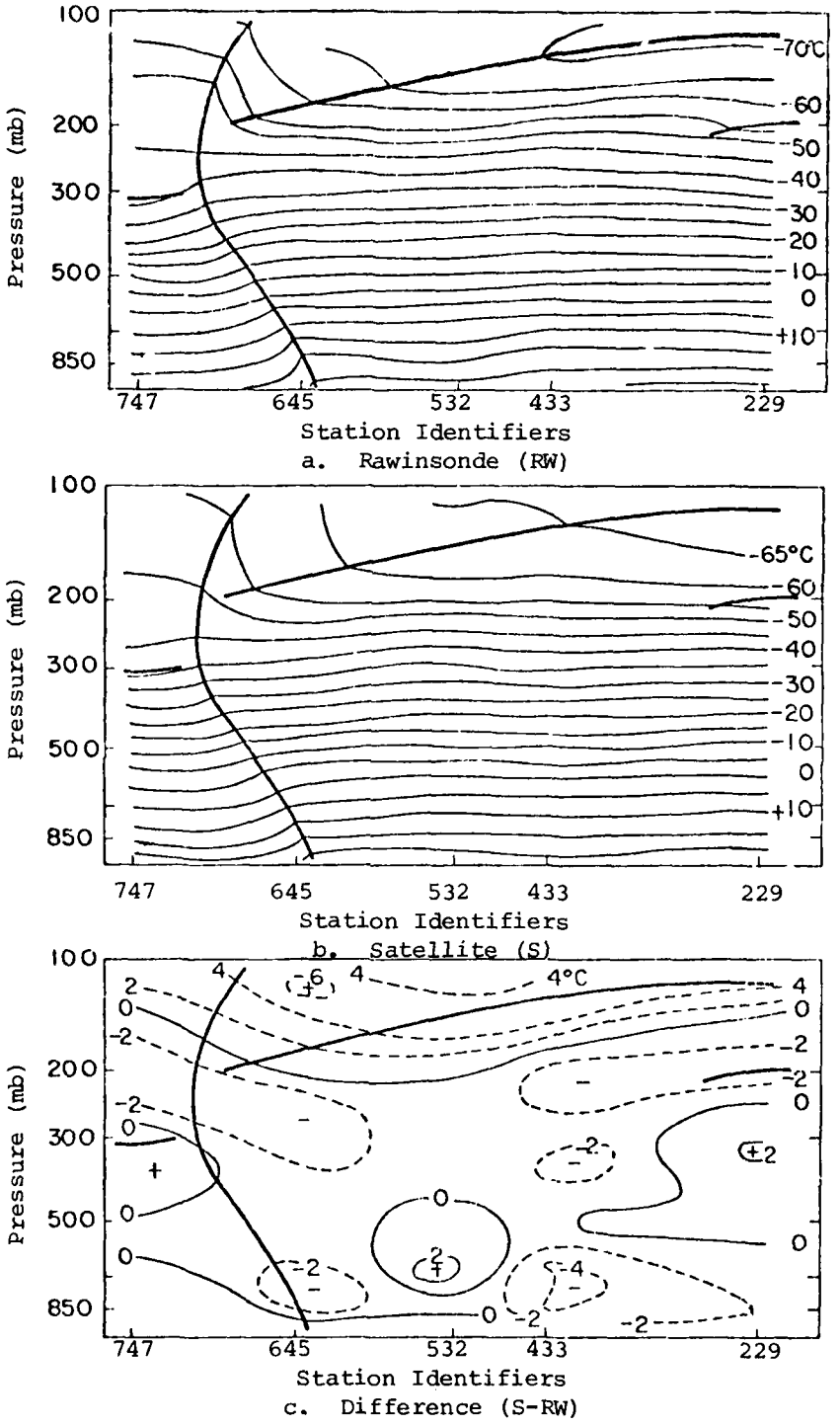

Fig. 31. Cross sections of temperature and temperature difference (°C) for the central United States region on 25 August 1975 at 1700 GMT. (See Fig. 2 for path of cross sections.)

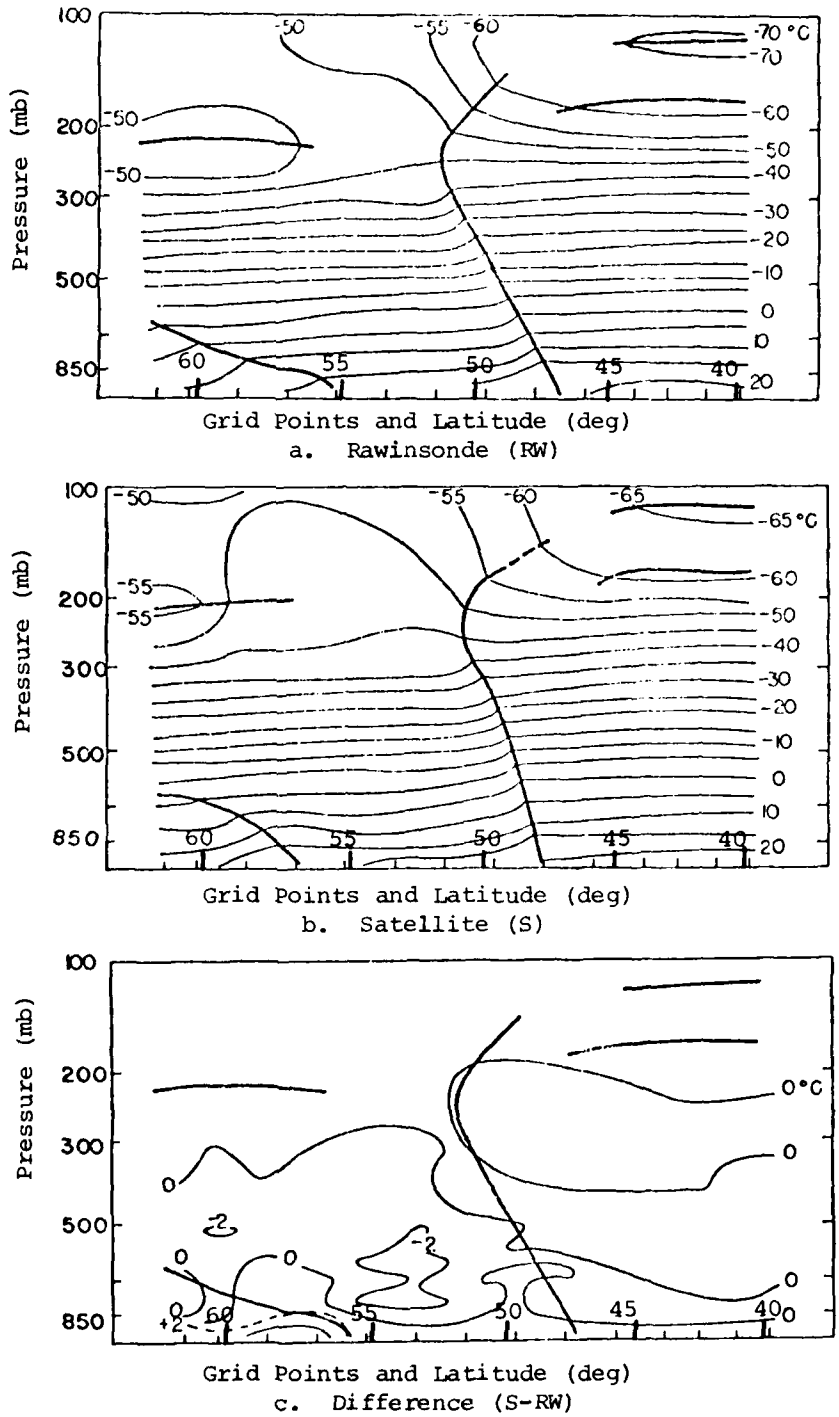

Fig. 32. Cross sections of temperature and temperature difference (°C) for the Canada region on 25 August 1975 at 1700 GMT. (See Fig. 3 for paths of cross sections.)

rawinsonde and satellite data. The tropopause is well-defined in both types of data for both air masses. In this region, smoothing in the satellite data does not significantly worsen the depiction of synoptic features, i.e., the front and tropopauses, as compared to rawinsonde data. This may be partly a result of the increased smoothing necessary in gridding the sparsely-spaced rawinsonde soundings. In the difference cross section, negative differences predominate in the mid-troposphere (700 to 350 mb) in the polar air while positive differences predominate in those layers in the air south of the front. Weinreb (1977) found that differences in temperature between satellite and rawinsonde measurements are associated with differences in mixing ratio as measured by the two systems. When the air is measured to be too dry, the temperature is found to be too low, and vice versa. This difference cross section, combined with that for mixing ratio (discussed later), exhibits this correspondence across the front.

The temperature cross section for the western United States region, shown in Fig. 33, depicts an area of baroclinity in the northern one-third of the section in both types of data, but particularly in the satellite data. There is also a change in indicated tropopause height in both types of data near 45°N. Hence, there is some evidence for a weak front located north of the center of the section. This explanation is supported by the cloud pattern present in the satellite picture at 2015 GMT; however, a front has not been included in the analysis due to its uncertainty of position. In the difference cross section for this region, as in Canada, there are negative values in the mid-troposphere in the northern half of the section, with a slight tendency toward positive values from 300 to 570 mb near the southern end, although the pattern is not as clear as in the difference cross section for Canada. Negative differences are quite large at 850 mb and in a shallow layer above that level, and negative differences are dominant below about 400 mb. Many of the mountains of this region extend above 850 mb, however, so that temperature or difference values near that level may not be representative of the atmosphere.

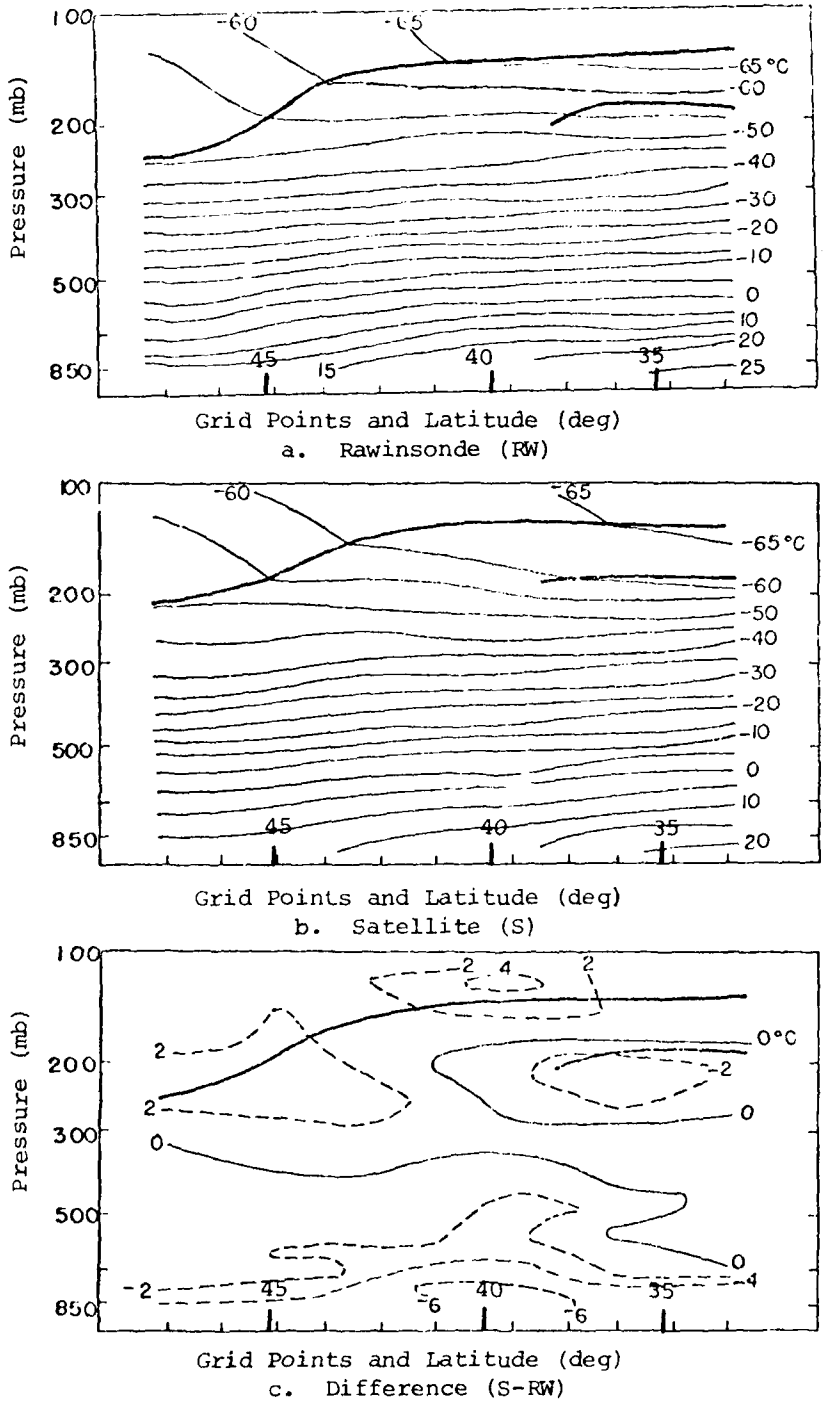

Fig. 33. Cross sections of temperature and temperature difference (°C) for the western United States region on 3 September 1975 at 0730 GMT. (See Fig. 4 for path of cross sections.)

Cross sections with weak baroclinic zones in temperature show the same zones to be slightly more baroclinic in potential temperature for both rawinsonde and for satellite data. As an example of this, the potential temperature cross section for Canada is shown in Fig. 34. The regions of baroclinity just north of the front are slightly more emphasized than they are in temperature (Fig. 32), as is the change in vertical gradient at the tropopause. This is due to the nature of the definition of potential temperature. As with temperature, there are negative differences in the difference cross section north of the front, and positive differences in the mid-troposphere south of the front.

Vertical smoothing in the satellite data causes temperature lapse rates to begin decreasing at a lower level than in rawinsonde data, so that temperature differences should be positive (satellite values too high) just below the rawinsonde-indicated tropopause. Temperature lapse rate differences should be negative in those layers. This effect is illustrated in the cross sections of temperature lapse rate for the central United States region shown in Fig. 35. Here, in the air mass south of the front, the satellite decrease begins lower than the rawinsonde decrease, so that differences below the tropopause are negative. The tropopause in the tropical air mass, which is south of the front and occupies most of the region, is above 200 mb, so that differences should approach maximum negative values near that level. This was also shown in Fig. 5b, the vertical difference profile for temperature in the central United States region.

The cross section of differences shows that differences are fairly small throughout the section, and tend to be aligned in horizontal layers. This is reasonable, since the variation of lapse rate within any given air mass is fairly small, so that differences will be horizontally consistent.

In the western United States region, the cross section of differences in lapse rate (Fig. 36) again shows negative values below the rawinsonde-indicated tropopause in the northern end of the section, but shows positive differences at that level near the southern end due to the indications of a double tropopause in that area in the rawinsonde data which are not present in the satellite data. The same

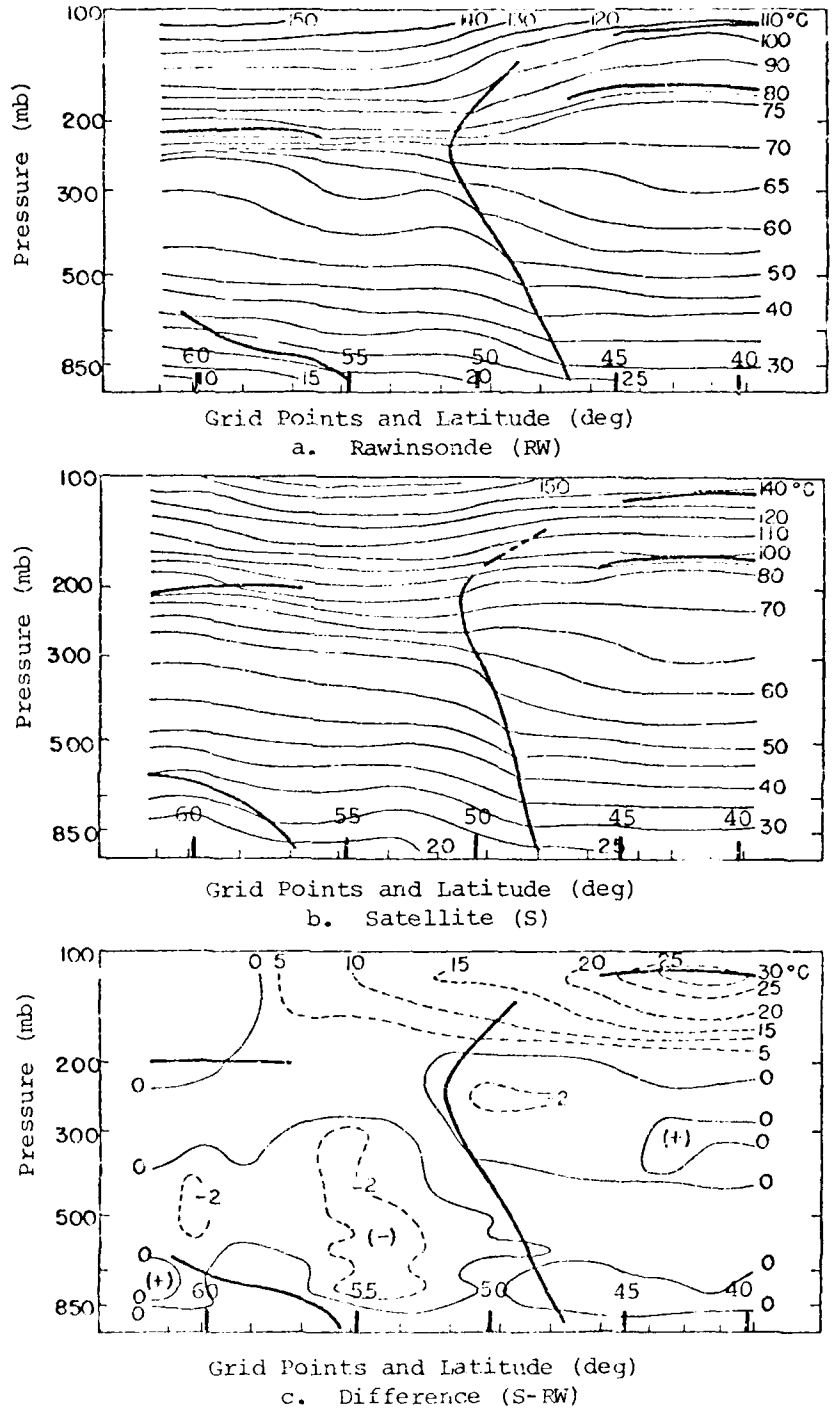

Fig. 34. Cross sections of potential temperature and potential temperature difference (°C) for the Canada region on 25 August 1975 at 1700 GMT. (See Fig. 3 for path of cross sections.)

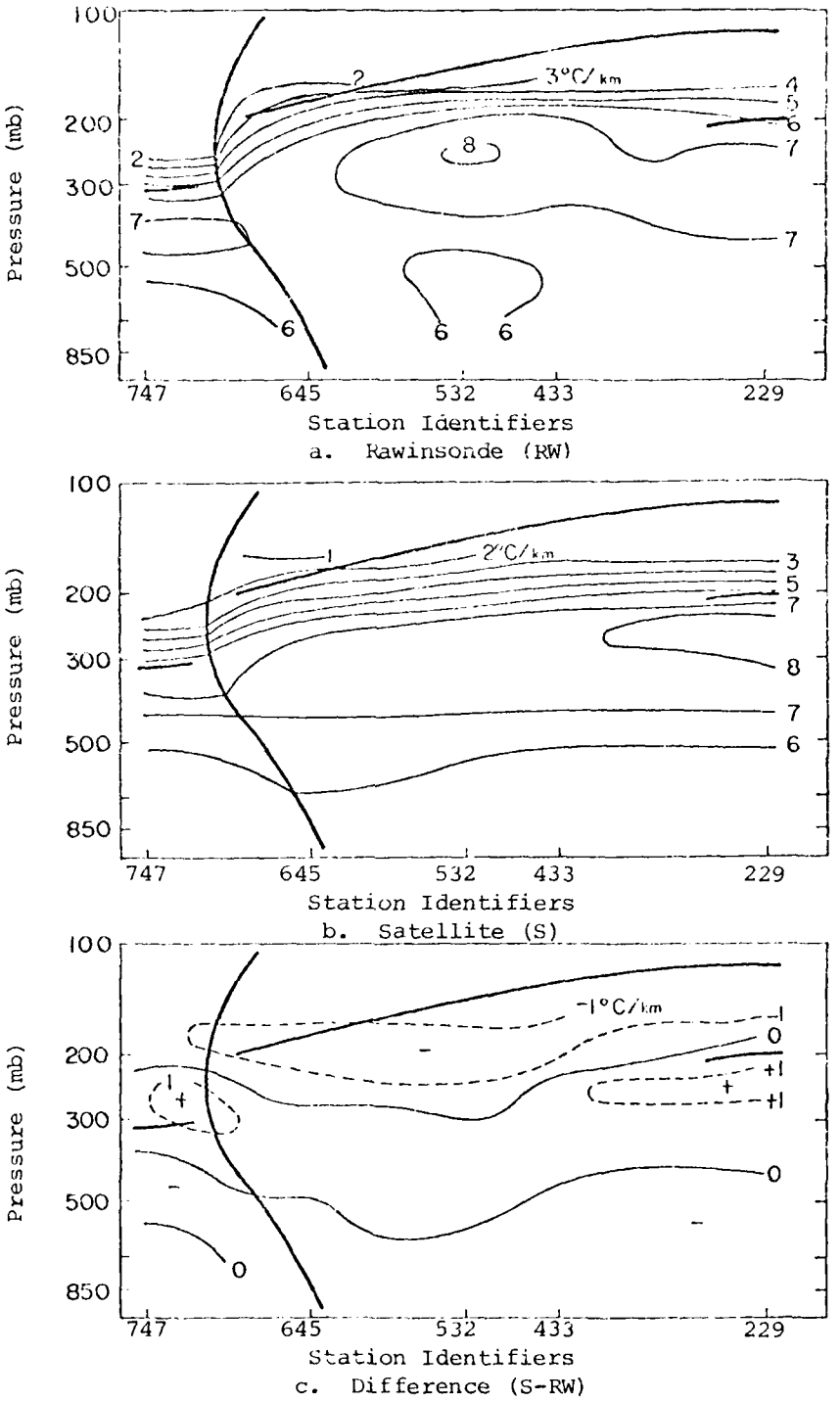

Fig. 35. Cross sections of vertical lapse rate of temperature and lapse rate difference (°C/km) for the central United States region on 25 August 1975 at 1700 GMT. (See Fig. 2 for path of cross sections.)

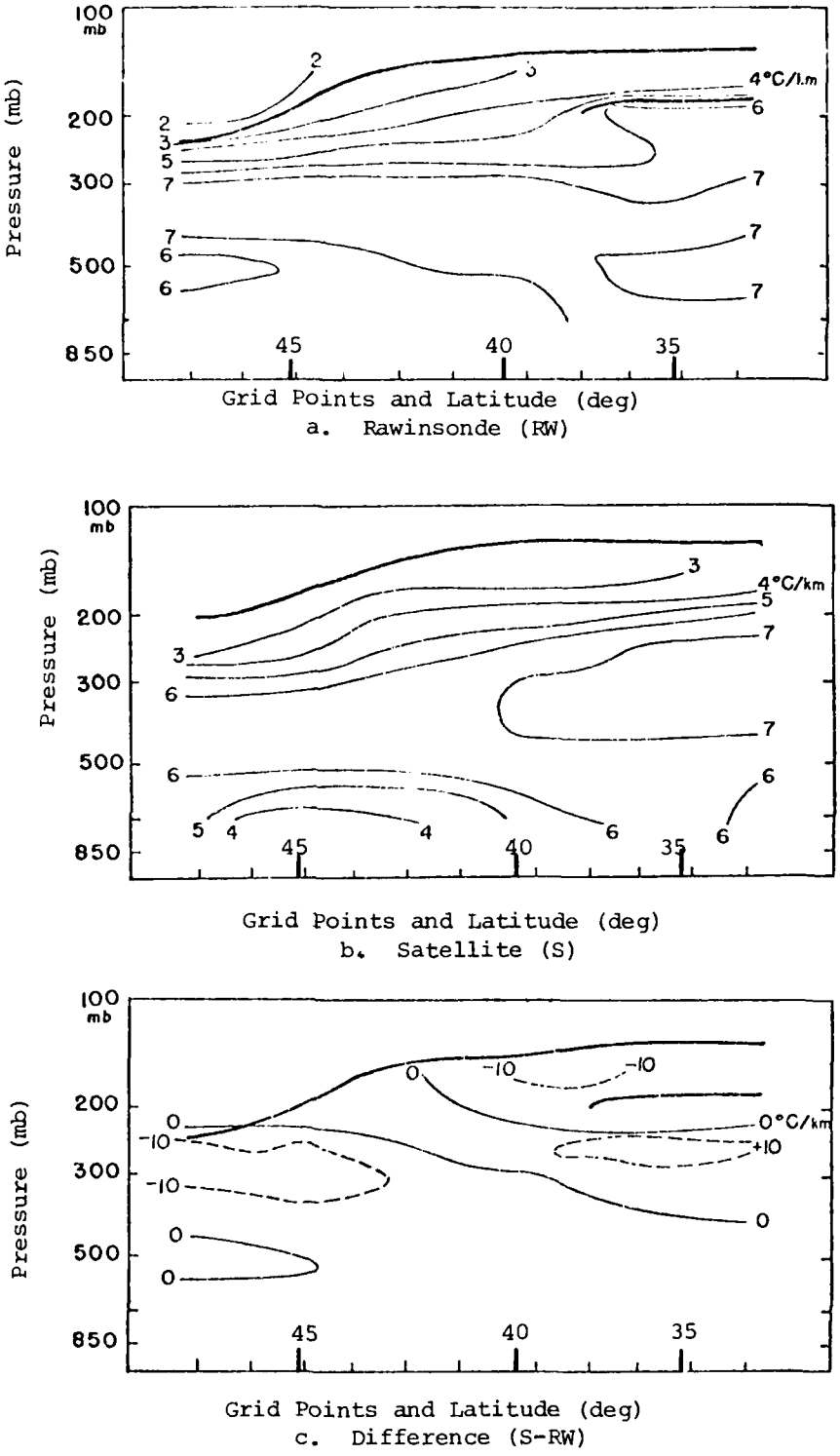

Fig. 36. Cross sections of vertical lapse rate of temperature and lapse rate difference (°C/km) for the western United States region on 3 September 1975 at 0730 GMT.

vertical smoothing is present as in the other regions. The indication of a change in the level of the tropopause in the northern third of the section in the satellite data is better defined than the same feature in the rawinsonde data.

Fig. 37, which shows the cross section of temperature lapse rate for Canada, indicates the change in tropopause level and air mass structure across the front. Vertical smoothing in the satellite data is not detrimental to the definition of either the front or the tropopause in this region, a fact that may be due in part to the greater contrast across the polar front at this point than was present farther south in the central United States region where the contrast was weak and the front difficult to locate in both types of data. The difference cross section shows that in this region there is a contrast not only in lapse rate values but also in the differences across the front. In the 500-300-mb layer, differences are positive south of the front and negative north of the front, an effect of the lower tropopause in the polar air. Also, the 500- and 700-mb lapse rate differences are negative in the air south of the front and positive in the air north of the front.

Cross sections of horizontal temperature gradient are shown in Figs. 38 and 39 for the western United States and Canada regions, respectively. The former shows maximum values near 700 mb and above 200 mb in the northern third of the section, corresponding to the location of the weak front which may be present. These features are similarly defined in the satellite data as was the case with temperature and lapse rate of temperature. In Canada, the cross section of horizontal gradient of temperature shows a column of maximum values in the center of the section corresponding to the location of the front, and generally small values elsewhere. There is a minimum in gradient values at 250 mb, the location of the jet maximum which will be mentioned later. This cross section in satellite data corresponds well with the rawinsonde section and with the synoptic situation. Differences are largest just behind the front in the mid-troposphere where satellite gradients underestimate rawinsonde gradients by near 10°C $(1000\ km)^{-1}$ at 300 mb. This is expected

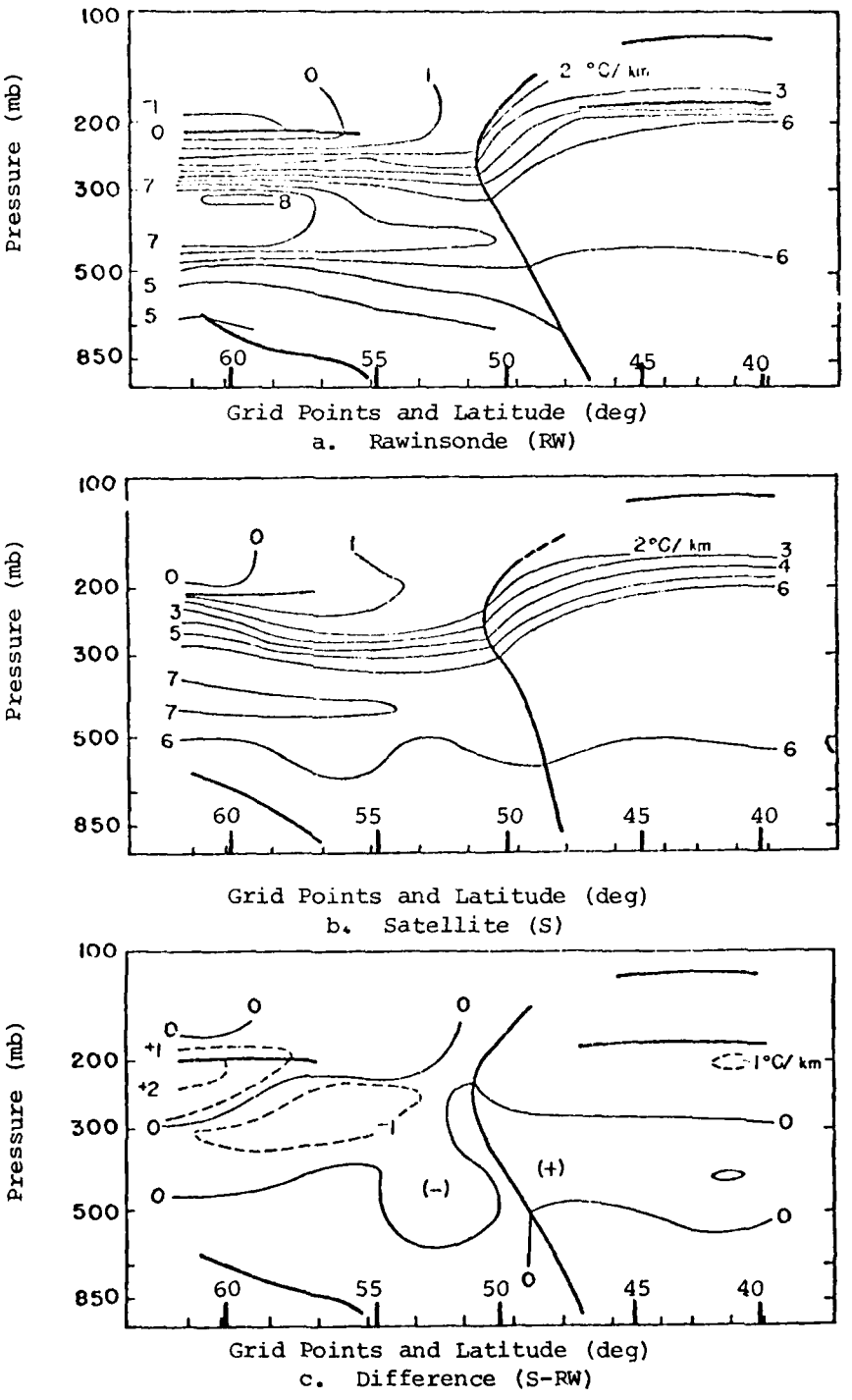

Fig. 37. Cross sections of vertical lapse rate of temperature and lapse rate difference (°C/km) for the Canada region on 25 August 1975 at 1700 GMT. (See Fig. 3 for path of cross sections.)

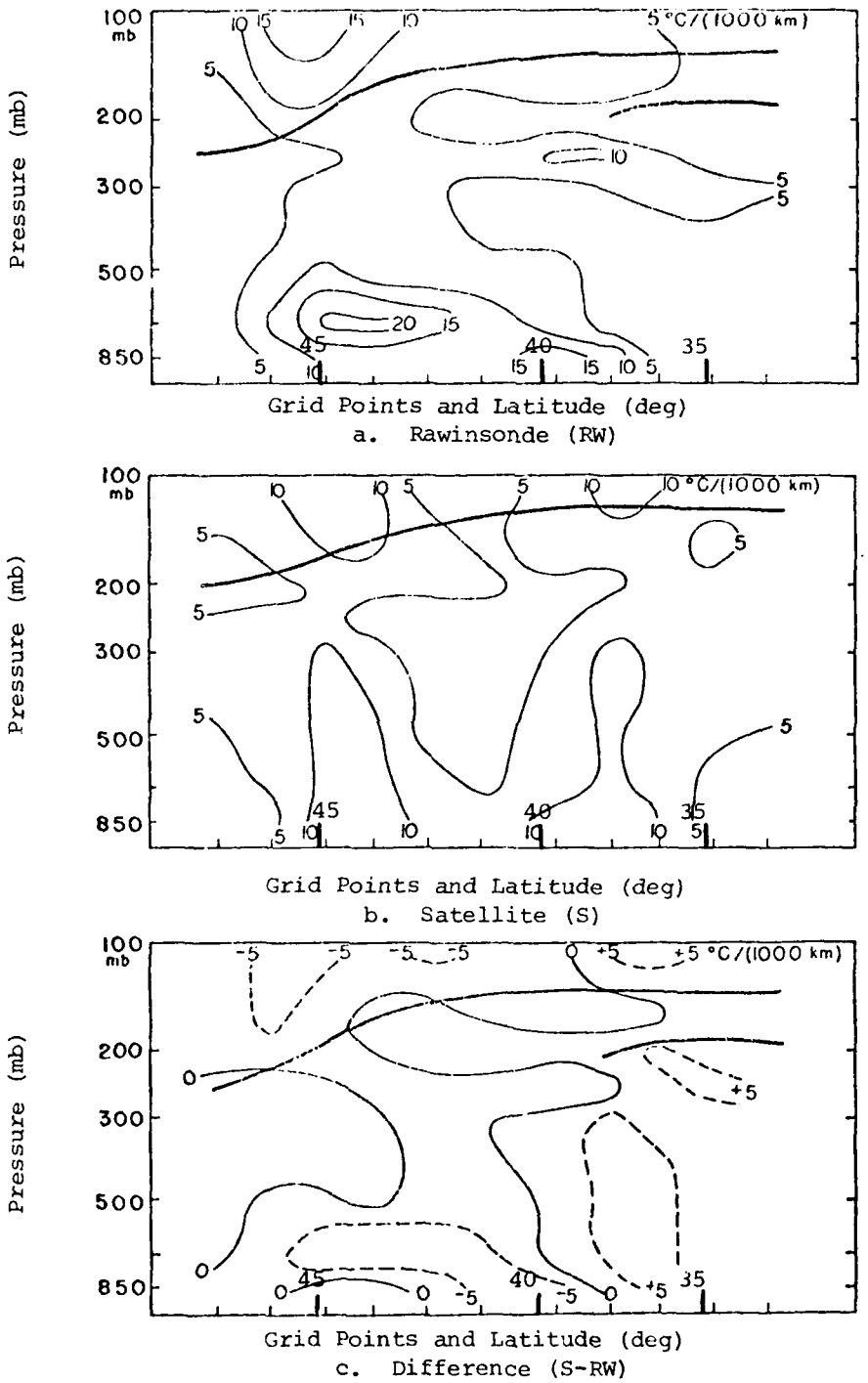

Fig. 38. Cross sections of horizontal temperature gradient and gradient difference (°C/1000 km) for the western United States region on 3 September 1975 at 0730 GMT. (See Fig. 4 for path of cross sections.)

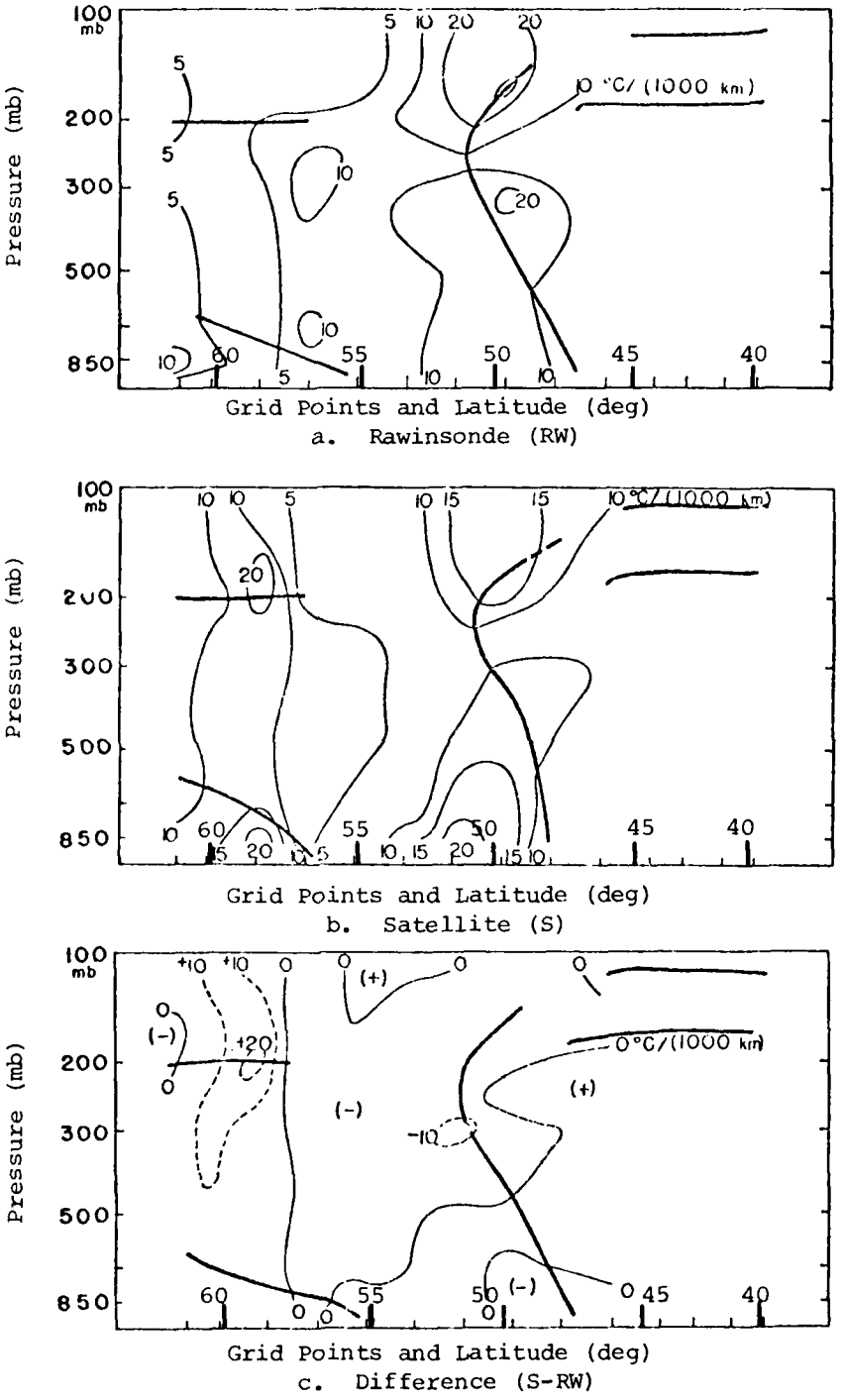

Fig. 39. Cross sections of horizontal temperature gradient and gradient difference (°C/1000 km) for the Canada region on 25 August 1975 at 1700 GMT. (See Fig. 3 for path of cross sections.)

because of the horizontal smoothing in the satellite soundings which represent an area approximately 300 km on a side.

2. Moisture-related variables

Cross sections of dew-point temperature for the Caribbean, central United States, and Canada are shown in Figs. 40, 41, and 42, respectively. At the time of the satellite pass, there is a circular region of cloudiness over eastern Cuba in the Caribbean, and some clouds located just south of the western end of that island. Examination of the rawinsonde sounding locations versus those of the satellite for the area near Cuba (Fig. 1) shows that rawinsonde measurements for grid points in that area come from soundings in southern Florida. The cross section for this region passes over western Cuba. The rawinsonde data show a moisture maximum near and just below 350 mb and a second maximum at 700 mb, both located near the center of the section. The 500-mb level shows little horizontal change through that part of the section. In the satellite data, however, the moisture maxima in the lower and middle troposphere are joined together and include the 500-mb level. Hence, there are relatively large differences between satellite and rawinsonde data at 500 mb in this region. Some of this difference probably is due to the sparseness of the rawinsonde soundings in the region.

The cross section of rawinsonde dew point for the central United States region shows a moisture increase across the front from north to south associated with pre-frontal shower activity, and fairly strong contrast across the front. The satellite section indicates much less contrast across the front with greatly smoothed patterns. Differences are largest where the rawinsonde gradients are largest. The frontal position is difficult to locate on the basis of the satellite dew-point cross section alone, but with prior knowledge of the approximate location, it is possible to place a front on the satellite dew-point cross section. Without such knowledge, however, it would be difficult to locate this front on either the satellite cross section of temperature or the satellite cross section of dew-point temperature.

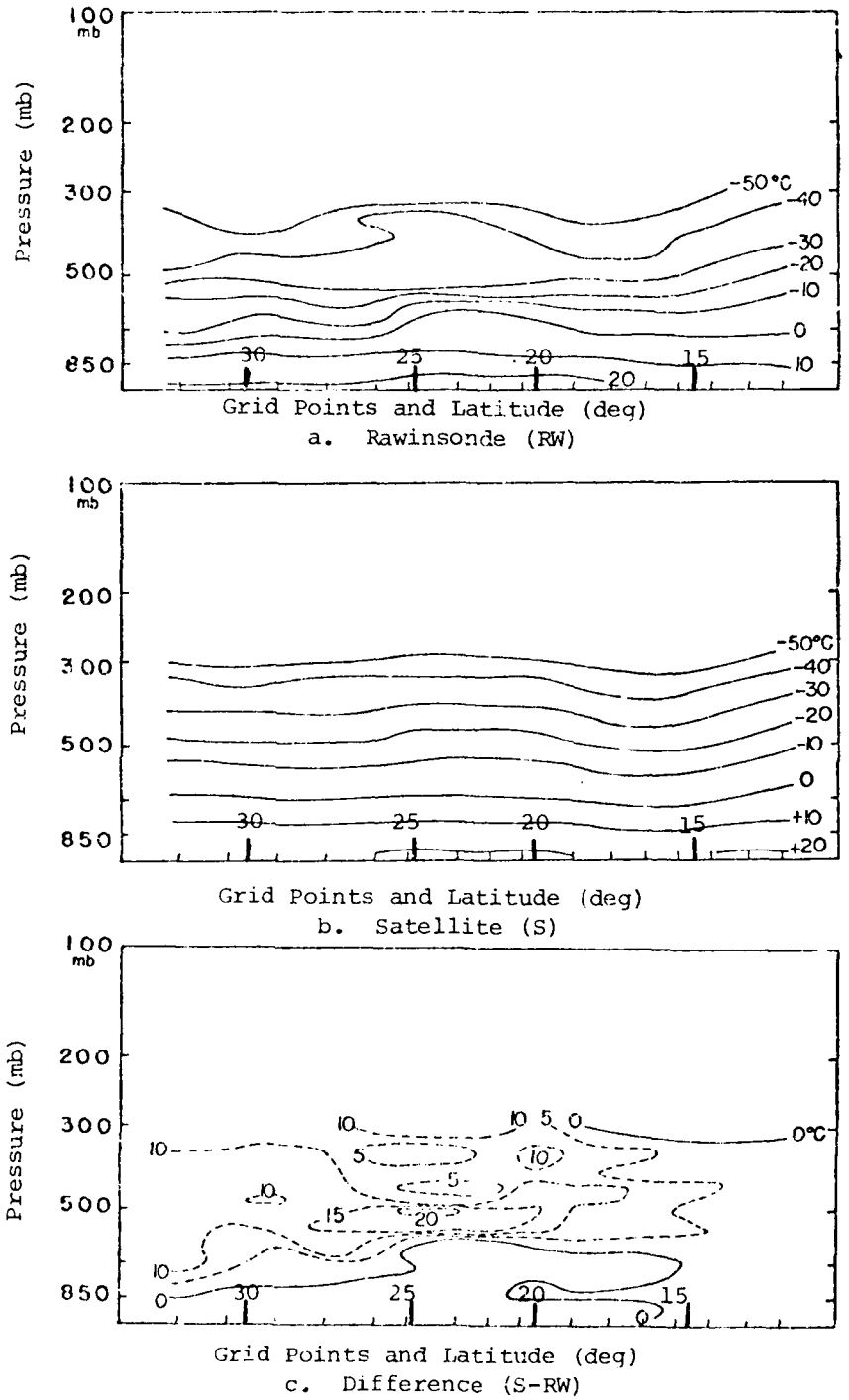

Fig. 40. Cross sections of dew-point temperature and dew point difference (°C) for the Caribbean region on 25 August 1975 at 1700 GMT. (See Fig. 1 for path of cross sections).

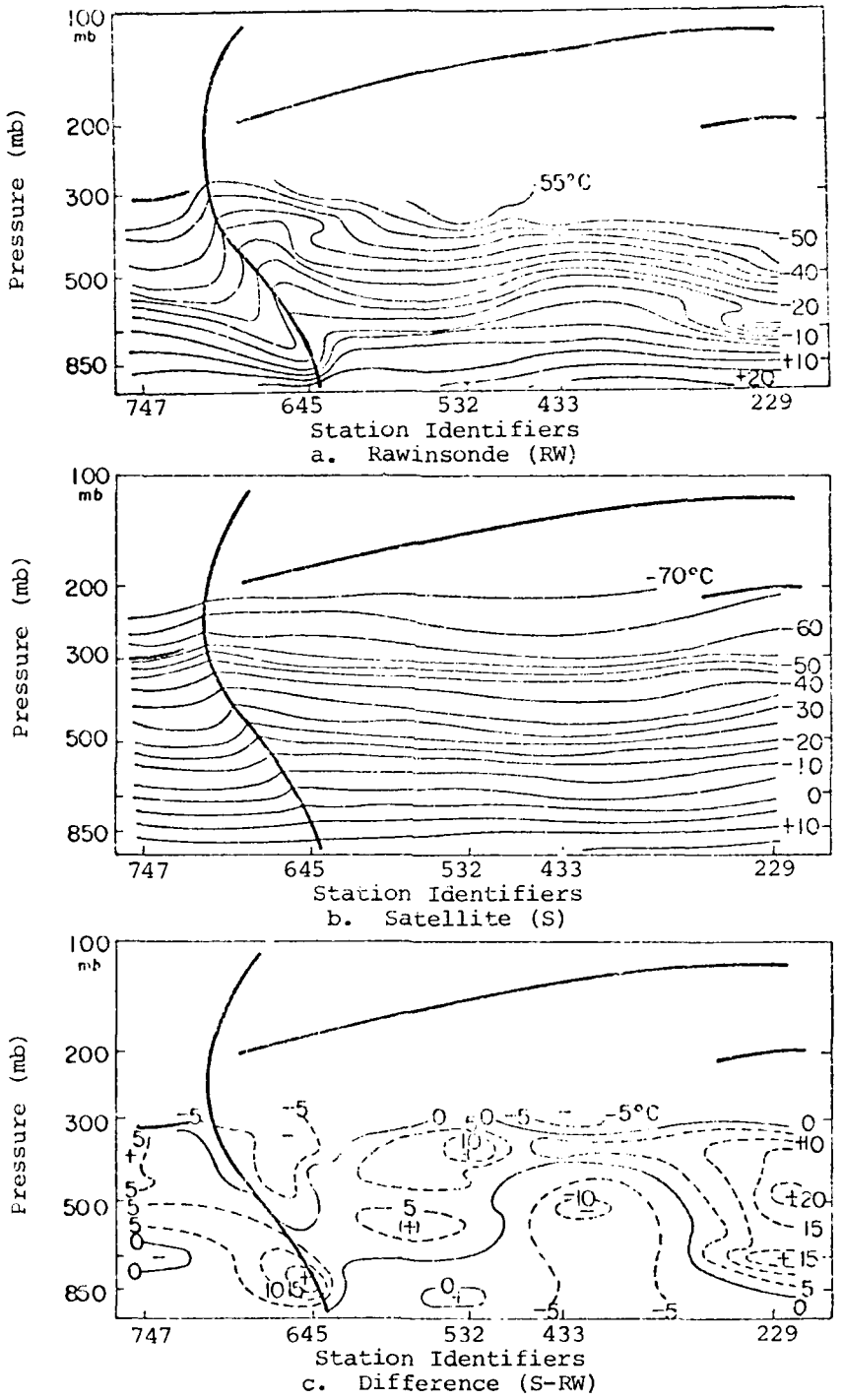

Fig. 41. Cross sections of dew-point temperature and dew point difference (°C) for the central United States region on 25 August 1975 at 1700 GMT. (See Fig. 2 for path of cross sections.)

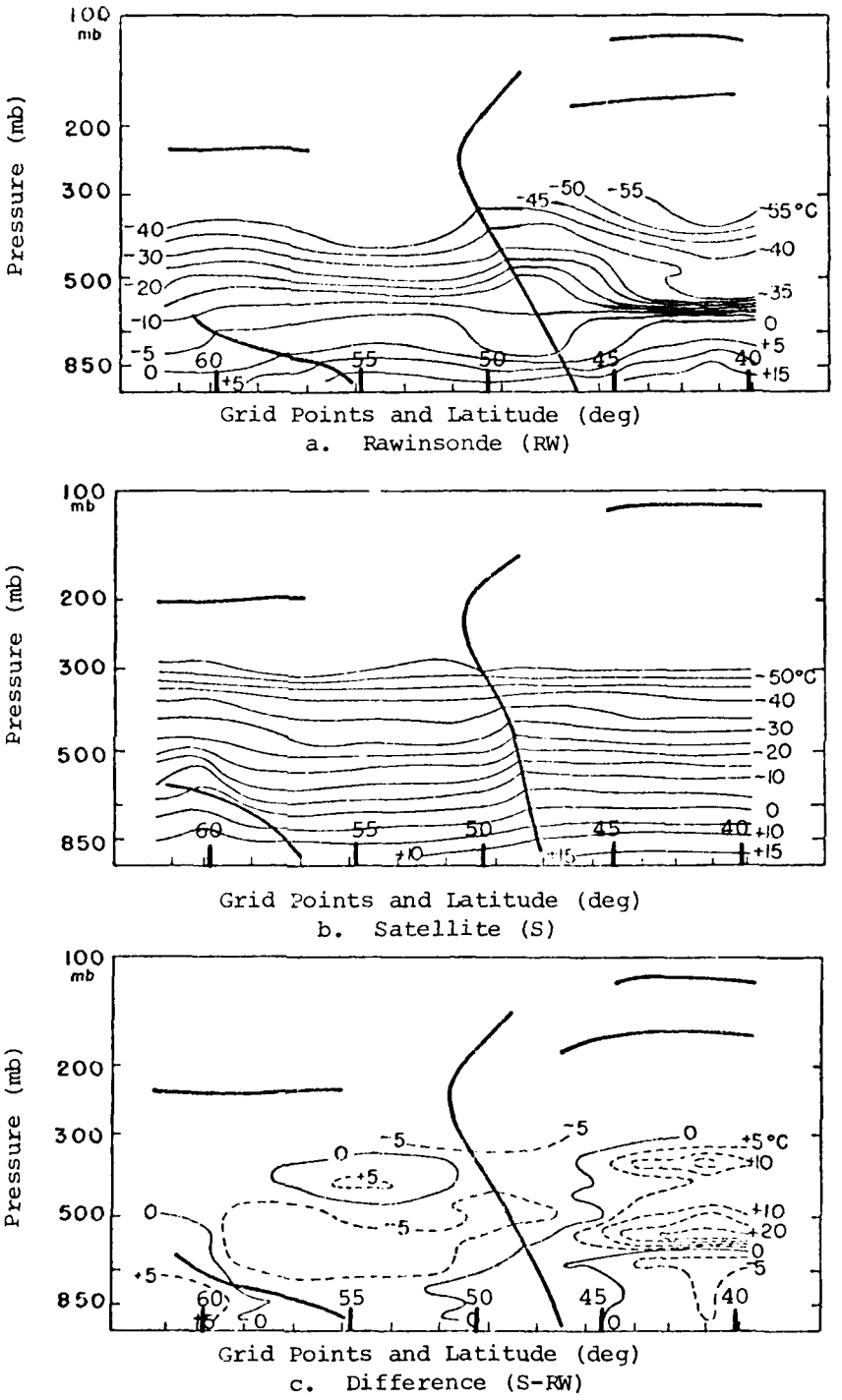

Fig. 42. Cross sections of dew-point temperature and dew point difference (°C) for the Canada region on 25 August 1975 at 1700 GMT. (See Fig. 3 for path of cross sections.)

In Canada the cross section of dew-point temperature shows a strong contrast across the front with little contrast near the surface and just below 500 mb. The satellite section shows smoothed patterns, although it is possible to place a front on the section. At 850 and 700 mb, as in the constant-pressure charts for this variable, there is little contrast across the front. There are negative values in the difference cross section in the polar air, which is consistent with the negative temperature differences (Fig. 32) and the relationship between temperature and moisture measured by satellite that was found by Weinreb (1977).

Fig. 43 shows cross sections of mixing ratio for Canada with good indications of both the polar and arctic fronts near the surface in both types of data. Near the polar front on the surface the satellite indicates too little moisture in the tropical air mass and too much in the polar air mass. Near the arctic front, the difference changes sign and becomes negative at approximately the mid-point between the two fronts. The sign changes once again at the arctic front, so that there are indications of too little moisture southward and too much moisture northward of the front relative to rawinsonde data. This is an effect of smoothing in the satellite data, and is not seriously detrimental to the usefulness of the satellite data in this region.

Cross sections of equivalent potential temperature for the central United States and Canada are shown in Figs. 44 and 45, respectively. There is a great degree of similarity between the rawinsonde patterns for the two regions and between the satellite patterns for the two regions. The difference in air mass structure and stability is shown in both types of data for these regions which depict different segments of the same polar front. Both types of data show good contrast across the front. This appears to be a reliable variable to examine from satellite data for depiction of frontal contrasts between air masses. Differences in equivalent potential temperature measurements are largest near the surface, where the largest differences in moisture measurement occur.

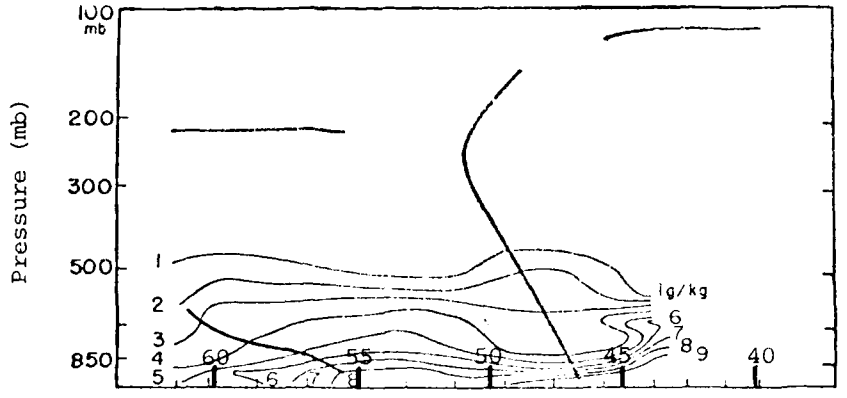

Grid Points and Latitude (deg)
a. Rawinsonde (RW)

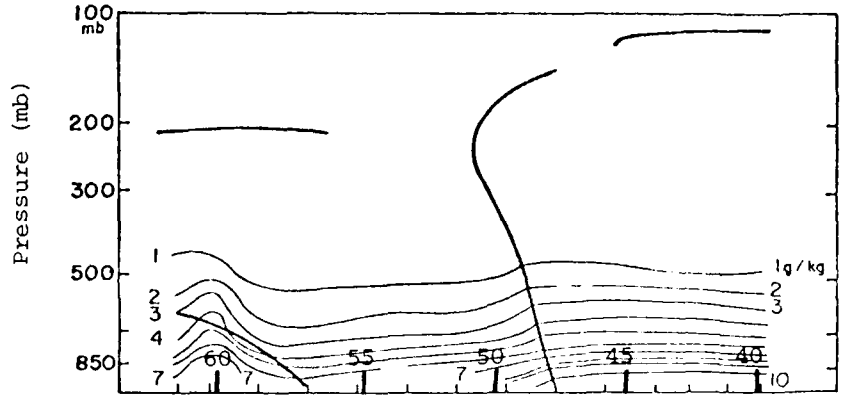

Grid Points and Latitude (deg)
b. Satellite (S)

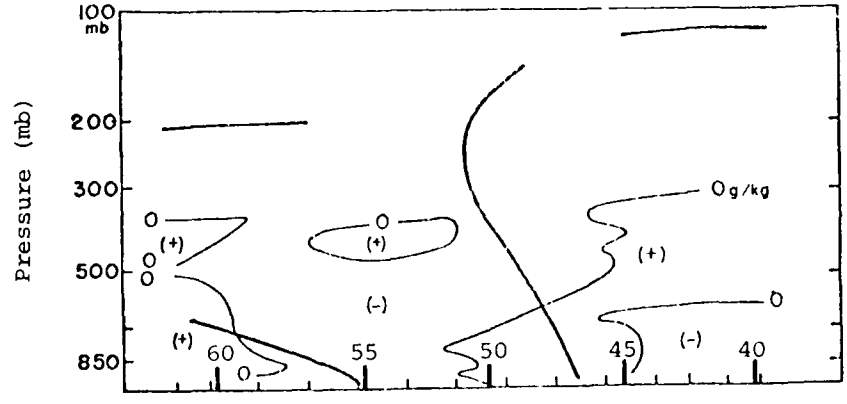

Grid Points and Latitude (deg)
c. Difference (S-RW)

Fig. 43. Cross sections of mixing ratio and mixing ratio difference (g/kg) for the Canada region on 25 August 1975 at 1700 GMT. (See Fig. 3 for path of cross sections.)

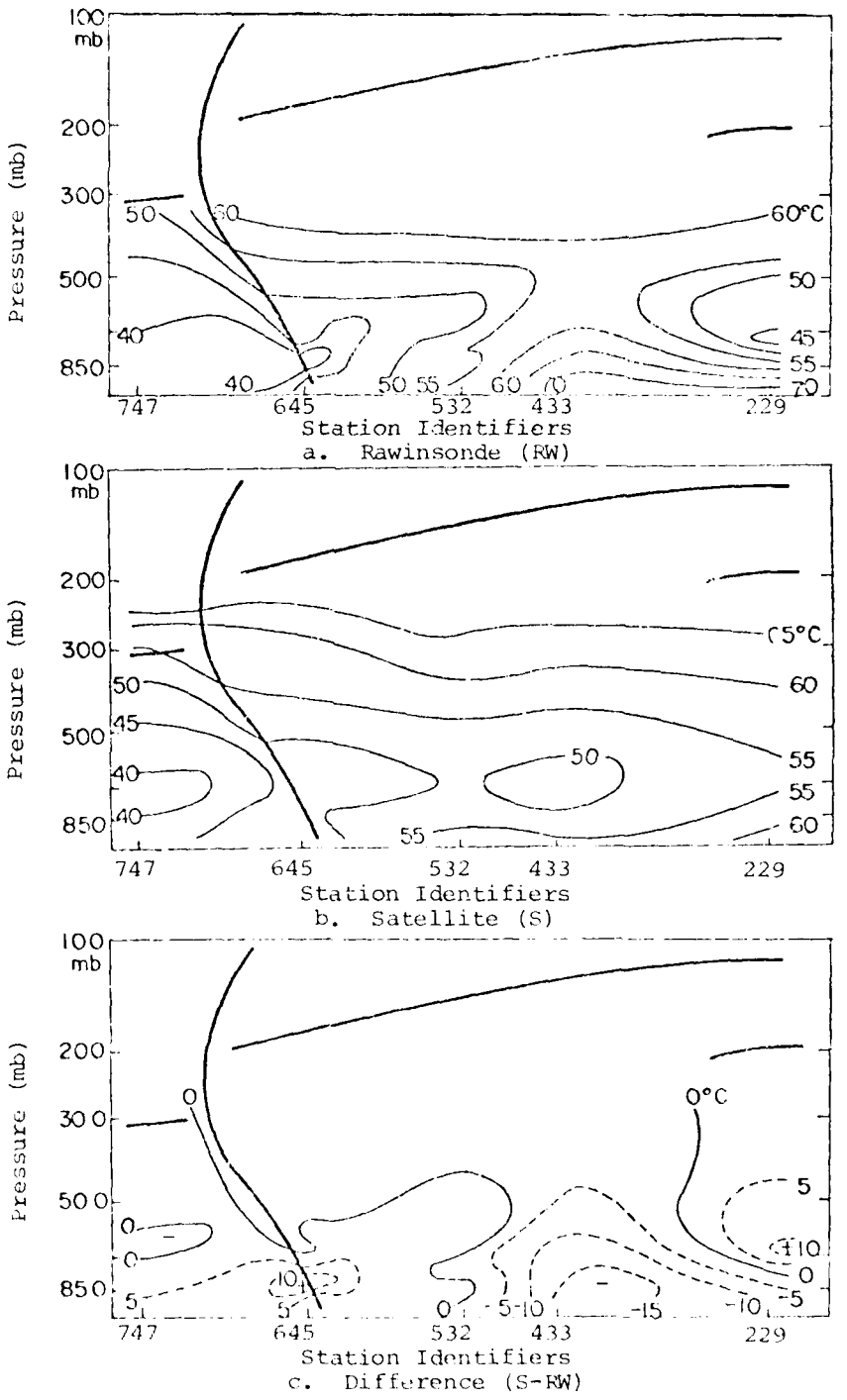

Fig. 44. Cross sections of equivalent potential temperature and equivalent potential temperature difference (°C) for the central United States region on 25 August 1975 at 1700 GMT. (See Fig. 2 for path of cross sections.)

AD-A094 480 TEXAS A AND M UNIV COLLEGE STATION DEPT OF METEOROLOGY F/G 4/1
ATMOSPHERIC STRUCTURE DETERMINED FROM SATELLITE DATA.(U)
JAN 81 K S KNIGHT, J R SCOGGINS DAAG29-76-G-0078
UNCLASSIFIED NASA-RP-1071 NL

2 of 2
AD A094480

END
DATE FILMED
2-81
DTIC

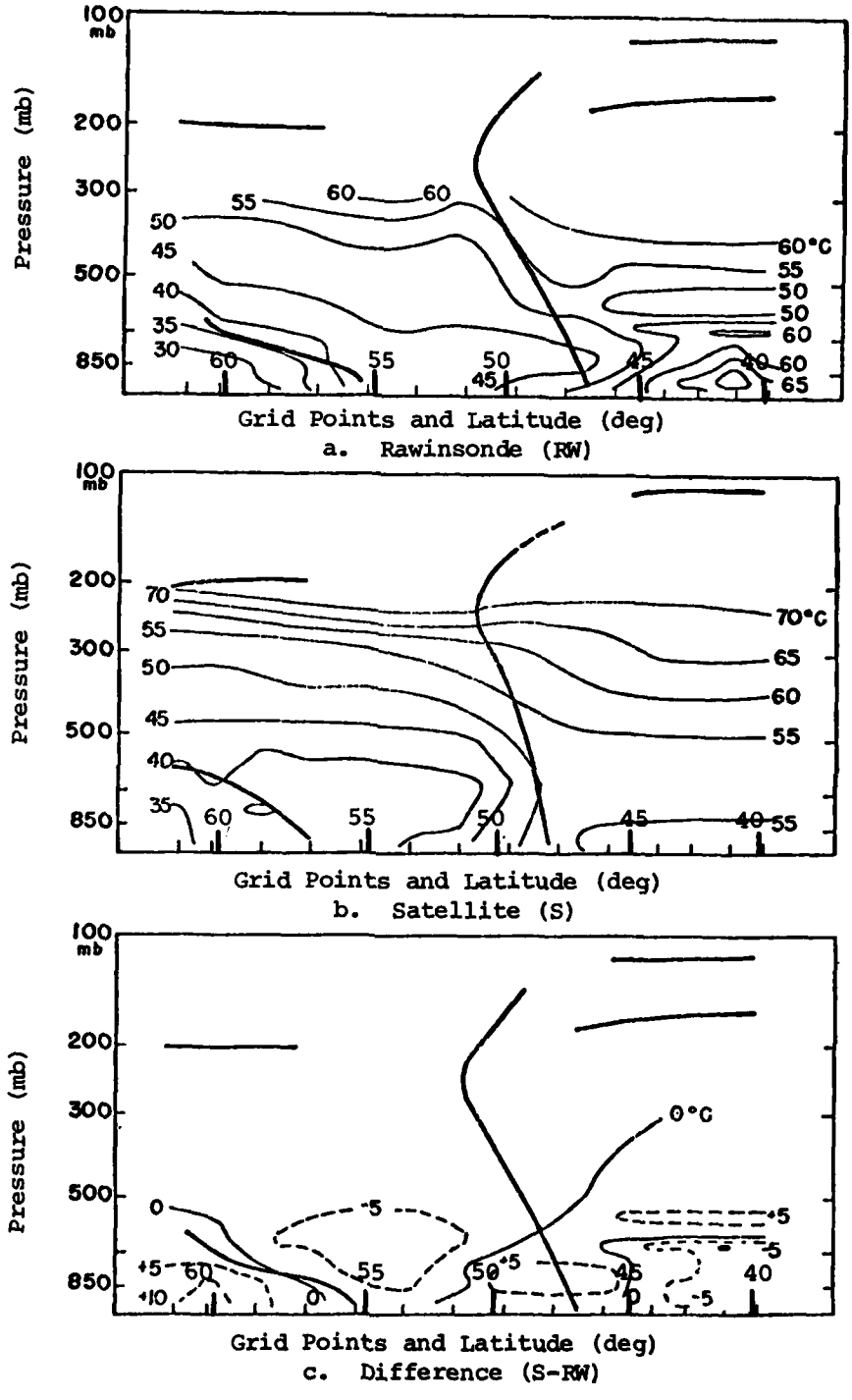

Fig. 45. Cross sections of equivalent potential temperature and equivalent potential temperature difference (°C) for the Canada region on 25 August 1975 at 1700 GMT. (See Fig. 3 for path of cross sections.)

3. Wind

Cross sections of wind used in this study are taken from appropriate sets of grid points on constant-pressure charts at mandatory levels. This is the same procedure that was used in constructing cross sections of gridded data for other variables. These cross sections represent the spatial distribution of the variable and are not dependent on the orientation of the cross section. Wind values, therefore, are not to be taken as an estimate of the wind normal to the cross section, but as indications of the spatial distribution of wind in the x- or y-direction which may be at some non-perpendicular angle to the cross section.

A cross section of the observed wind (v-component) for Canada is shown in Fig. 46 along with the cross sections of the v-component of the actual geostrophic wind and the satellite geostrophic wind. These show quite good agreement as to location of the jet core, with the geostrophic values being higher than the observed values, as is expected in a cyclonic circulation system such as the one in this region. The frontal position is defined equally well in both types of data.

A similar set of cross sections for the u-component wind in the western United States region is presented in Fig. 47. The observed wind shows an extension of higher velocities southward from the north end of the section associated with the baroclinity which was indicated beneath those levels in the cross sections of horizontal temperature gradient and temperature. The geostrophic wind shows a maximum core at the southern extreme of the observed tongue of higher velocities, and another maximum associated with the tropopause south of the center of the section. This second core is more pronounced in the satellite data, and is an area of large differences between rawinsonde and satellite winds in this region.

d. Summary of results

For temperature and variables which depend only on temperature, there is a strong correspondence between rawinsonde and satellite

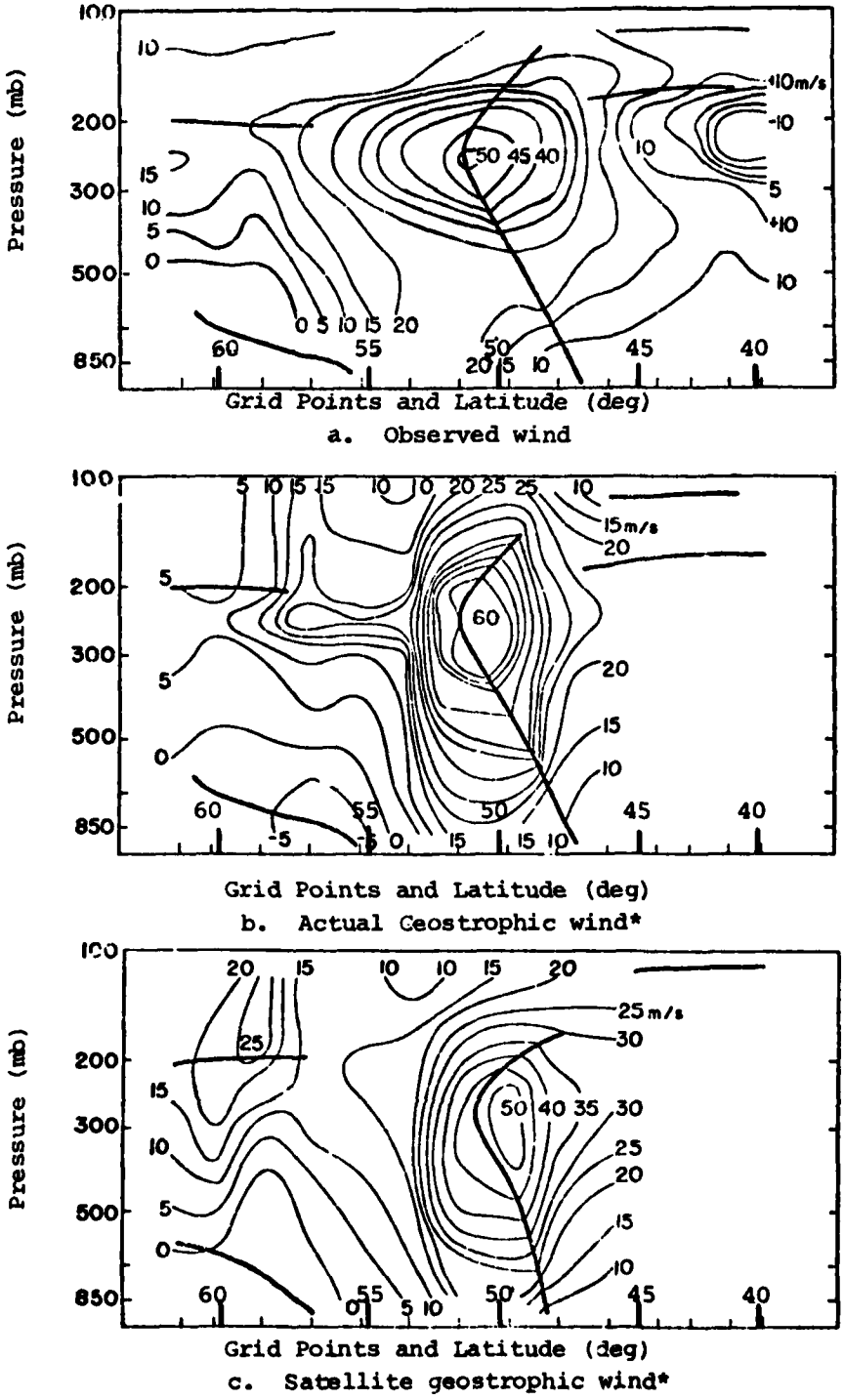

Fig. 46. Cross sections of observed and geostrophic v-component wind (m s^{-1}) for the Canada region on 25 August 1975 at 1700 GMT. (See Fig. 3 for path of cross sections.)
*see text

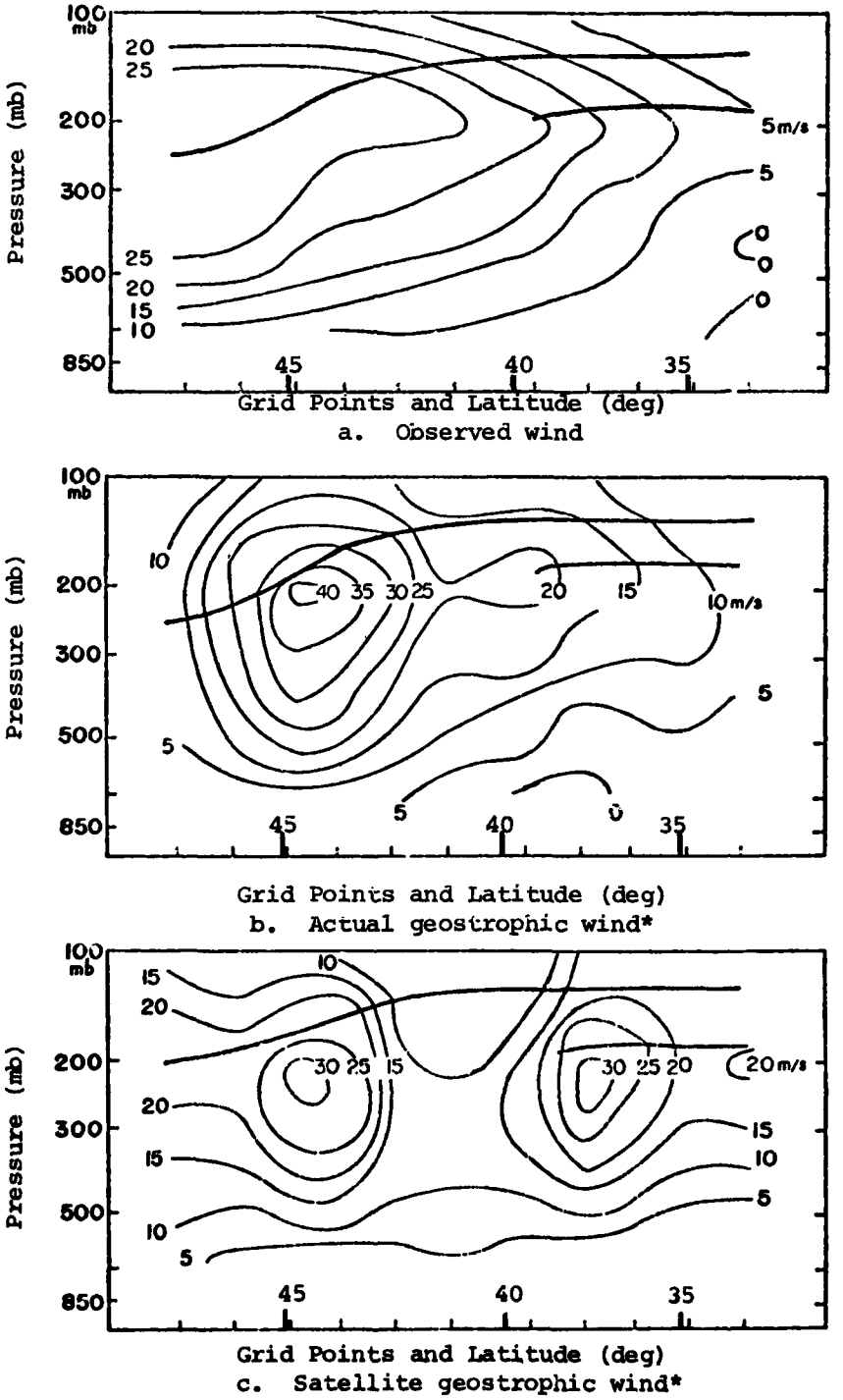

Fig. 47. Cross sections of observed and geostrophic u-component wind ($m\ s^{-1}$) for the western United States region on 3 September 1975 at 0730 GMT. (See Fig. 4 for path of cross sections.)

*see text

data. Temperature differences are significant only in regions of strong vertical or horizontal gradients. In cross sections and constant-pressure charts, the satellite data yield similar patterns to rawinsonde data, except that frontal contrasts are somewhat smoothed so that gradients behind fronts are not quite as strong in the satellite data. The temperature pattern from satellite data will show enough detail, however, that a reasonable location for a front can be found. This location may be inadequate for mesoscale purposes but is probably adequate for the synoptic scale. Satellite and rawinsonde values show differences of smallest magnitude in low-gradient situations such as in the Caribbean region in this study. Vertical lapse rate of temperature shows good correspondence with the synoptic situation and small differences from rawinsonde data in all regions. Horizontal temperature gradient near a front corresponds best in terms of patterns in situations of strong gradient, and best in terms of magnitudes in situations of weaker gradient. In the Canada and Caribbean regions, where satellite soundings are substantially more densely spaced than rawinsonde stations, the satellite data perform well enough to indicate large-scale features.

For dew-point temperature and other measurements of moisture, the satellite soundings present a smoothed version of rawinsonde soundings. In the case of frontal contrasts, the smoothing is severe enough to cause difficulty in locating fronts in satellite data. Mixing ratio patterns seem most able to locate fronts near the surface, and equivalent potential temperature, which combines temperature and moisture measurements, is shown to be a good variable for distinguishing between air masses in the regions of the central United States and Canada. Examination of dew point itself seems to yield poor results in terms of the depiction of frontal contrasts and in terms of quantitative differences between satellite and rawinsonde values.

Geopotential height computed from satellite temperature measurements shows fairly small differences near the surface and in the lower layers of the atmosphere, with differences between satellite and rawinsonde measurements increasing to significant

magnitudes in the upper levels. In the lower and middle troposphere, some of the differences between observed and satellite-derived geopotential height are due to the use of a constant set of 21 pressure levels, rather than significant levels which change from sounding to sounding and depend on the characteristics of the sounding. There is, however, a significant portion of the difference in geopotential height measurements that is due to temperature differences between the two types of data. While profiles of differences in geopotential height changed shape and magnitude from one region to another, differences in geostrophic wind remained approximately the same between regions. Large differences in wind occurred in places where the satellite data indicated a second wind maximum core that was not present in the rawinsonde data. This is a recurring problem with satellite geopotential height measurements, i.e., secondary maxima of geostrophic wind are also found by other investigators in places where such maxima are not indicated in rawinsonde data (Arnold et al., 1976).

Vertical difference profiles of most variables in the western United States and central United States regions are similar in shape and magnitude. The central United States region contains a front that was strong enough to be analyzed on National Weather Service charts, while the western United States has no analyzed front, although cross sections and constant-pressure charts show indications of the presence of a weak front in that region.

Magnitudes of differences for variables in the Caribbean were smaller than those in the other regions due to the small gradients of meteorological variables in that region. Differences in Canada were similar in magnitude to those for the United States regions, but different in shape due to the different air mass (polar) which covered most of the region.

7. CONCLUSIONS

Major conclusions reached in this study are:

1) Satellite-derived temperatures are not of desired accuracy for large-scale synoptic analysis although general patterns may be determined.

2) The satellite measurements of dew-point temperature are smoothed to such an extent that location of frontal zones and diagnosis of features on anything but a large scale is difficult.

3) The variables that seem to distinguish frontal structure and differences between air masses are the equivalent potential temperature, temperature, and lapse rate of temperature.

4) Differences in the accuracy with which geopotential height can be computed from satellite data do not affect the computations of geostrophic wind, so that differences in calculated winds are fairly consistent in the four regions considered.

8. RECOMMENDATIONS FOR FUTURE RESEARCH

Further research into the uses and capabilities of satellite-derived atmospheric soundings should be concerned with improving computations of wind and moisture distributions. While the temperature is sensed quite well by atmospheric sounders, as is evidenced by this as well as other studies, the moisture distribution is not measured as well, and this is an important meteorological parameter. Improvements in both the hardware on board the satellite and the software used for calculating temperature and moisture soundings from satellite-measured radiances are in the offing, and future research should be centered around the resulting data.

REFERENCES

Arnold, J. E., J. R. Scoggins, and H. E. Fuelberg, 1976: A comparison between Nimbus-5 THIR and ITPR temperatures and derived winds with rawinsonde data obtained in the AVE II experiment. NASA Contractor Report CR-2757, 76 pp.

Barnes, S. L., 1964: A technique for maximizing detail in numerical weather map analysis. J. Appl. Meteor., 3, 396-409.

Bruce, R. E., L. D. Duncan, and J. H. Pierluissi, 1977: Experimental study of the relationship between radiosonde temperatures and satellite-derived temperatures. Mon. Wea. Rev., 105, 493-496.

Hanel, R., and B. J. Conrath, 1969: Interferometer experiment on Nimbus-3: Preliminary Results. Science, 165, 1258-1260.

Horn, L. H., R. A. Peterson, and T. M. Whittaker, 1976: Intercomparisons of data derived from Nimbus 5 temperature profiles, rawinsonde observations and initialized LFM model fields. Mon. Wea. Rev., 104, 1363-1371.

Kapela, A. F., and L. H. Horn, 1975: Nimbus-5 satellite soundings in a strongly baroclinic region. Meteorological Applications of Satellite Indirect Soundings, Project Report, NOAA Grant 04-158-2, Department of Meteorology, University of Wisconsin, Madison, 1-19.

Peterson, R. A., and L. H. Horn, 1977: An evaluation of 500 mb height and geostrophic wind fields derived from Nimbus-6 soundings. B. A. M. S., 58, 1195-1201.

Rosenkranz, P. W., F. T. Barath, J. C. Blinn III, E. J. Johnston, W. B. Lenoir, D. H. Staelin, and J. W. Waters, 1972: Microwave radiometric measurements of atmospheric temperature and water from an aircraft. J. Geophys. Res., 77, 5833-5844.

Shen, W. C., W. L. Smith, and H. M. Woolf, 1974: An intercomparison of radiosonce and satellite-derived cross sections during the AMTEX. NOAA Technical Report NESS 72, 18 pp.

Shuman, F. G., 1957: Numerical methods in weather prediction: II Smoothing and filtering. Mon. Wea. Rev., 85, 357-361.

Smith, W. L., 1969: Statistical estimation of the atmosphere's geopotential height distribution from satellite radiation measurements. Environmental Science Services Administration Technical Report NESC 48, 29 pp.

REFERENCES (Continued)

_____, H. M Woolf, and H. E. Fleming, 1972: Retrieval of atmospheric temperature profiles from satellite measurements for dynamical forecasting. J. Appl. Meteor., 11, 113-122.

_____, and H. M. Woolf, 1974: An intercomparison of meteorological parameters derived from radiosonde and satellite vertical temperature cross sections. NOAA Technical Report NESS 71, 13 pp.

Snider, J. B., 1972: Ground-based sensing of temperature profiles from angular and multi-spectral microwave emission measurements. J. Appl. Meteor., 11, 958-967.

Staelin, D. H., A. H. Barrett, and J. W. Waters, 1973: Microwave spectrometer on the Nimbus 5 satellite: Meteorological and geophysical data. Science, 182, 1339.

Wark, D. Q., and D. T. Hilleary, 1969: Atmospheric temperature: Successful test of remote probing. Science, 165, 1256-1258.

Waters, J. W., K. F. Kunzi, R. L. Pettyjohn, R. K. L. Poon, and D. H. Staelin, 1975: Remote sensing of atmospheric temperature profiles with the Nimbus 5 microwave spectrometer. J. Atmos. Sci., 32, 1953-1969.

Weinreb, M. P., 1977: Sensitivity of satellite retrievals of temperature to errors in estimates of tropospheric water vapor. J. Appl. Meteor., 16, 605-613.

1. REPORT NO.	2. GOVERNMENT ACCESSION NO.	3. RECIPIENT'S CATALOG NO.
NASA RP-1071	AD-A094480	

4. TITLE AND SUBTITLE	5. REPORT DATE
Atmospheric Structure Determined From Satellite Data	January 1981
	6. PERFORMING ORGANIZATION CODE

7. AUTHOR(S)	8. PERFORMING ORGANIZATION REPORT #
Keith Shelburne Knight and James R. Scoggins	

9. PERFORMING ORGANIZATION NAME AND ADDRESS	10. WORK UNIT NO.
Department of Meteorology Texas A&M University College Station, Texas 77843	11. CONTRACT OR GRANT NO. M-328
	13. TYPE OF REPORT & PERIOD COVERED Reference Publication

12. SPONSORING AGENCY NAME AND ADDRESS	14. SPONSORING AGENCY CODE
U.S. Army Research Office Research Triangle Park, North Carolina	

15. SUPPLEMENTARY NOTES

The U. S. Army Research Office has granted permission for NASA to publish these data for use in studies using space technology for weather-related programs.

16. ABSTRACT

The capabilities of the Nimbus-6 satellite sounding data for use in synoptic analysis are considered and interpreted. An evaluation of the ability of the satellite sounding data to detect and depict structural features of the atmosphere is made on the basis of (1) vertical profiles of average difference and standard deviation of differences between satellite and rawinsonde data at nine pressure levels from 850 to 100 mb, and (2) constant-pressure charts and cross sections of satellite, rawinsonde, and difference values. Results indicate that (1) satellite measurements of temperature as well as the vertical lapse rate and horizontal gradient of temperature are accurate enough to show large-scale patterns but not to precisely define fronts or tropopauses; (2) satellite measurements of dew-point temperature are smoothed enough to severely reduce contrasts between air masses across fronts; (3) the magnitude of the standard deviation of differences between rawinsonde and satellite data for most variables increases with the synoptic activity in the region; and (4) the most reliable variables to examine from satellite data for depiction of synoptic features are the temperature, lapse rate of temperature, equivalent potential temperature, and mixing ratio.

17. KEY WORDS	18. DISTRIBUTION STATEMENT
Meteorological satellite data Satellite-derived soundings Satellite-derived winds	Unclassified - Unlimited Subject Category 47

19. SECURITY CLASSIF. (of this report)	20. SECURITY CLASSIF. (of this page)	21. NO. OF PAGES	22. PRICE
Unclassified	Unclassified	106	A06

For sale by National Technical Information Service, Springfield, Virginia 22161

NASA-Langley, 1981

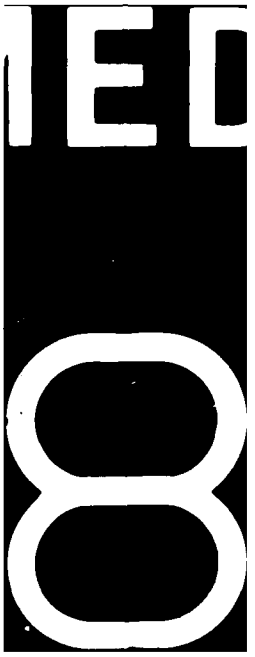
IED
8